ELECTRONIC STRUCTURES OF LIGAND BRIDGED
RUTHENIUM AND COBALT BINUCLEAR COMPLEXES

Thesis by

Irving Marvin Treitel

In Partial Fulfillment of the Requirements

for the Degree of

Doctor of Philosophy

California Institute of Technology

Pasadena, California

1971

(Submitted December 31, 1970)

To

my parents,

wife,

and

son

ACKNOWLEDGMENTS

I wish to gratefully acknowledge the guidance of Professor Harry B. Gray. His chemical acumen as well as his unmatched enthusiasm have contributed greatly to this work. I also wish to thank him for the personal considerations shown me during my graduate career.

Thanks are also due Dr. Richard Marsh for his assistance on crystallographic matters.

Professor Henry Taube and Dr. Carol Creutz of Stanford University are thanked for some of the compounds used in this research.

My colleagues in the Gray research group all are worthy of acknowledgment, both for their advice on chemical problems and for their comradeship. In particular, I wish to thank Dr. Michael Flood, both for his instruction in X-ray structural techniques and for his friendship. Messrs. J. Thibeault and V. Miskowski are thanked for helpful suggestions and invaluable discussions on many matters in this thesis.

I wish to thank Mrs. Susan Brittenham for her expert preparation of this manuscript.

My parents are thanked for their constant encouragement without which this task could never have reached fruition.

My wife, Gladys, is to be thanked for her successful contributions to the illustrations in this thesis, despite working under the most trying circumstances. More important, her constant faith and encouragement have sustained me during the inevitable gloomy periods of graduate study.

ABSTRACT

Bridged superoxo and peroxodecaamminedicobalt complexes have been investigated using electronic room and low temperature spectroscopy. Assignments for these spectra have been proposed. The most important feature in the superoxo spectra is a low energy metal ligand, $Co \rightarrow O_2^-$, charge transfer transition of moderate intensity. Both the superoxide and peroxide ions have been assigned positions in the spectrochemical series. The Dq of superoxide is very close to ammonia, while the Dq of peroxide is between NCS^- and H_2O. These results have been used to eliminate $Fe(III) - O_2^-$ as a possible model for oxyhemoglobin.

Cyano bridged dicobalt and mixed iron-cobalt dimers have been looked at, and their spectra assigned as simple superpositions of their component parts.

A series of 4+, 5+, and 6+ μ-pyrazinedecaamminediruthenium compounds have been investigated. Magnetic susceptibilities of the 5+ and 6+ compounds were measured and analyzed, assuming a tetragonally distorted d^5 ion. Values for the tetragonal field, delocalization, and spin-orbit coupling parameters have been obtained. The 5+ compound gives an ESR signal at room temperature, a result not usually obtained for d^5 Ru(III) salts.

Electronic spectra were looked at for the ruthenium pyrazine dimers. The interesting 1570 nm band was found to be temperature

independent, indicating an orbitally allowed transition. The origin
of this band is discussed. A molecular orbital description of these
compounds is suggested. The near IR transition is explained as a
b_{3u} (xz + xz) $\rightarrow$ b_{2g} (xz - xz) d-d transition. The applicability of the
Marcus Hush theory of electron transfer to the 5+ cation is discussed.

The crystal structure of μ-nitrogendecaamminediruthenium(II)
was determined. The Ru–N–N–Ru linkage is linear, and the N–N
distance was found to be 1.124 Å, — only slightly longer than that
in free nitrogen. An approximate molecular orbital scheme is
given which assumes back donation of electrons from ruthenium d
orbitals to the $\pi*N_2$ orbital.

TABLE OF CONTENTS

CHAPTER 1. SPECTRAL STUDIES OF BRIDGED PEROXO,

SUPEROXO, AND CYANO COMPLEXES

Introduction

In 1852, Fremy isolated a new complex when he oxidized ammoniacal solutions of cobalt(II) salts.[1] The species he found was formulated as a μ-peroxodecaamminedicobalt(III) cation, $(NH_3)_5CoO_2Co(NH_3)_5{}^{4+}$. Subsequently, Werner was able to oxidize Fremy's diamagnetic ion, and obtain a novel paramagnetic 5^+ species.[2] In order to explain this paramagnetism and the total charge on the cation, Werner assigned oxidation states of III and IV to the two cobalt atoms, and assumed the bridging oxygen to be a peroxo linkage.
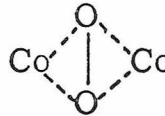
It was pointed out later by Gleu and Rehm[3] that the chemistry of this ion may be interpreted equally well by assuming both cobalt atoms are Co(III), and bridged by a superoxo $O_2{}^-$ moeity. Another alternative was proposed by Malatesta.[4] He argued from a resonance viewpoint that the two cobalt atoms may be thought to be equivalent, and possess an oxidation state intermediate between III and IV.
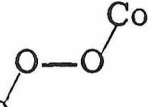
It was only with the application of electron spin resonance (ESR) techniques that a reasonably consistent formulation for these salts has been developed. The hyperfine structure in the ESR of the 5^+ ion has confirmed the equivalence of the two cobalt atoms.[5] O^{17} substitution,[6] the magnitude of the cobalt hyperfine constant,[5] as well as direct comparison with alkali superoxide ESR spectra,[7] have indicated that the unpaired electron spends most of its time on the oxygen bridge. A superoxo bridge linking two equivalent Co(III)

atoms, therefore, is the best description of this system. The corresponding diamagnetic 4+ ion is then correctly represented as a true O_2^{2-} peroxo bridge between two Co(III) metals.

The next important piece of information about these dimers which was obtained was the actual disposition of the four atom CoO_2Co unit in the 5+ cation. First, Okaya[8] obtained X-ray data suggesting a $Co\overset{O-O}{\diagup\diagdown}Co$ cis structure. Then, Brosset and Vannerberg[9] obtained data indicating a structure, $Co\underset{O}{\overset{O}{\diamondsuit}}Co$, similar to certain metal-olefin π complexes. Finally, Schaeffer and Marsh[10] found that the unit in the 5+ cation was actually $Co\diagup^{O-O\diagup^{Co}}$, with an O—O distance of 1.31 Å. This distance is very much like that found in alkali superoxides (1.28 Å), and much shorter than most peroxide bond lengths of 1.48 Å. The four atom bridging unit is nearly coplanar, while the Co—O—O angle is ~118°.

Following this, Schaeffer[11] determined the structure of the diamagnetic 4+ salt, and found the O—O distance to be 1.47 Å, a length in perfect agreement with the idea of a peroxo oxygen linkage. Furthermore, he found the CoO_2Co unit to be non-planar, with the torsion angle about the O—O bond being 146°.

In 1961, Haim and Wilmarth[12] were the first to isolate the decacyano analogs of the peroxo and superoxo decaammines. Although as yet no structural work on these cyano compounds has been reported, there is no evidence to suggest that the basic unit, the CoO_2Co linkage,

is markedly different from that reported for the ammine species. In fact, ESR work on the 5+ cyano compound suggests that the central four atom unit is essentially the same as in the 5+ ammine unit. [13]

Until we began our work, no one had satisfactorily interpreted the electronic spectra of these complexes. To be sure, attempts had been made previously, but all labored under the handicap of not knowing the true symmetry of the cations. For example, Dunitz and Orgel[14] gave a MO description of the decaammines, but they assumed a linear CoO_2Co unit. Another group attempted to interpret the electronic spectra based on the π-bonding structure of Vannerberg and Brosset. [15]

We decided to investigate these compounds primarily because of our general interest in the electronic structure of binuclear complexes. The study also fit in nicely with the work in our laboratory on biological systems or model biological compounds. The whole field of biological oxygen transport is intimately connected with the bonding properties of peroxo and superoxo oxygen. [16] More specifically, the recent revival in studies on model cobalt oxygen carriers, such as the cobalt salicylaldimines, goes hand in hand with studying the decaammine and decacyano dimers.

In studying the cobalt peroxo and superoxo dimers, we had a number of goals. In addition to giving definitive assignments for their spectra, we wished to associate characteristic metal $\rightarrow$ superoxo, superoxo $\rightarrow$ metal, and peroxo $\rightarrow$ metal transitions with similar transitions in cobalt oxygen carriers. We also wanted to position the peroxo and superoxo anions in the spectrochemical series.

One reason for choosing the decacyano and decaammine oxo dimers for these goals was that the corresponding hexacyanide and hexaammine, as well as pentaammine-X and pentacyano-X complexes, have been intensively studied.[21,25] Furthermore, most other peroxides and superoxides have structures which deviate much more substantially from simple octahedral fields.[19] Their spectra would have a correspondingly more complicated interpretation.

There was another, more general, goal we had in mind when starting out. That was to ascertain the nature of the electronic perturbations one metal center can exert on another, when linked by a single small π system. In order to see what the effect of these perturbations are with a change in π linkage, we looked at a number of cyano bridged cobalt complexes.

More specifically, we looked at those cyano bridged species which were well characterized and singly bridged. We restricted ourselves to some cyano bridged compounds first isolated by Haim and Wilmarth.[12] Again, a big factor influencing our choice of these compounds was the fact that their basic units, $Fe(II)(CN)_5X$, $Fe(III)(CN)_5X$, $Co(III)(CN)_5X$, and $Co(III)(NH_3)_5X$, had all been studied intensively.[25,21]

It was hoped originally to look at compounds with SCN^- and N_2 as π bridges. Unfortunately, all known bridged thiocyanates contain multiple linkages, and none contains cobalt as a metal center. Nitrogen linked dimers are still too rare to study extensively. Because of this, only the ruthenium nitrogen dimer described in a later chapter of this thesis has been investigated.

Experimental

$[(NH_3)_5Co-O_2-Co(NH_3)_5]SO_4(HSO_4)_3 \cdot H_2O$ was prepared by the literature procedure.[3] It was crystallized as suggested by Marsh and Schaeffer[10] from 2 M H_2SO_4. The crystals were analyzed by Schwarzkopf Microanalytical Laboratory, Woodside, New York.

Calc: Co, 16.28; S, 17.66; N, 19.31; H, 4.82.

Found: Co, 16.43; S, 17.30; N, 19.11; H, 4.90.

$[(NH_3)_5CoO_2Co(NH_3)_5](SO_4)_2$ was prepared according to Schaeffer's method.[11] No recrystallization was possible because of the compound's instability in solutions of all pH's. The compound was used within 24 hours of preparation. During the time between preparation and use, the compound was stored in a vacuum dessicator.

$K_5[(CN)_5CoO_2Co(CN)_5] \cdot H_2O$ was prepared, using the method of Mori, Weil, and Kinnaird.[13] The final precipitation step was done at 0°C. Small magenta crystals were obtained.

Attempts to oxidize an alkaline solution of $[(CN)_5CoO_2Co(CN)_5]^{6-}$, with an excess of alkaline Br_2 at 0° as described by Haim and Wilmarth,[12] failed to give any of the desired product.

Calc: Co, 17.39; C, 17.73; N, 20.67; H, 1.19.

Found: Co, 17.78; C, 17.38; N, 22.35; H, 1.65.

$K_6[(CN)_5CoO_2Co(CN)_5] \cdot H_2O$ was synthesized using the preparation of Haim and Wilmarth.[12] The compound was recrystallized by dissolving it in a minimum amount of water, and reprecipitating using an equal volume of cooled ethanol.

Calc: Co, 17.79; C, 18.13; N, 21.14; H, 0.30.

Found: Co, 16.46; C, 18.06; N, 21.00; H, 0.57.

Oxygenated bis (3-flourosalicylaldehyde)ethylenediimine cobalt(II) was obtained from Dr. B. C. Wang of Caltech.

Bis(salicylaldehyde)ethylenediimine cobalt(II) was prepared as follows. To 24.6 g of cobalt acetate in 250 ml boiling water, 32.2 ml (0.4 mole) of pyridine were added. This was followed by the addition of 6.67 ml (0.1 mole) ethylenediimine and 20.9 ml (0.2 mole) salicaldehyde. Red crystals formed, which were heated and pumped under an aspirator. The precipitate was filtered, dried under a nitrogen flush, and finally heated in a vacuum at ~170°C for one and one-half hours to drive off the pyridine. A brown solid remained.

Calc: C, 59.07; H, 4.31; N, 8.62.

Found (Galbraith): C, 58.92; H, 4.30; N, 8.51.

This compound reversibly oxygenated upon exposure to air; its color changed from brown to black upon oxygenation. The black solid was used in our spectral work here.

$Ba_3[(CN)_5CoNCFe(CN)_5]$ · 16 H_2O was made using the literature procedure.[12] A significant amount of excess $BaCl_2$ coprecipitated with the desired anion. Fractional precipitation a second time failed to eliminate the excess chloride. Infrared measurements in the CN stretch region agreed with the results reported in the literature for the anionic dimer.[22] No additional bands from excess KCN, $K_3[Fe(CN)_6]$, or $K_3[Co(CN)_6]$ were observed.

$K_5[(CN)_5CoNCFe(CN)_5]$ was prepared in situ by two different methods, both of which gave almost identical room temperature electronic spectra. The first method was a slight variant of

Wilmarth's method.[12] An excess of iodine was added to $Ba_3[(CN)_5CoCNFe(CN)_5]$. Instead of back titrating the residual iodine with thiosulfate, the unreacted I_2 was extracted with CS_2. The second method involved adding H_2O_2 to the 6- anion. Excess H_2O_2 was allowed to decompose before spectra were taken. No attempts at crystallization were made.

$[(CN)_5CoCNCo(NH_3)_5]$ was made using Haim's procedure.[23a] The heating of the 5+, 5- intermediate salt was at $\sim 120\,°C$ for 18 hours. No final chromatographic purification was used. The orange solid was checked for purity in the IR, and its CN stretch region agreed nicely with the literature.[23] No trace of excess hexacyanide was found.

Electronic Spectra

All ultraviolet, visible, and near infrared spectral measurements were made on a Cary Model 14RI spectrophotometer. Measurements of spectra at $77\,°K$ were carried out using a quartz dewar which allowed complete immersion of the sample. Bubbling of the liquid nitrogen under operating conditions was prevented by cooling to $75\,°K$ under reduced pressure. Measurements were made using quartz square cells formed by molding round quartz tubing on a square molybdenum frame.

All runs were made using a 9:10 $MgCl_2:H_2O$ mixture. All solutions were filtered before being used in order to facilitate glass formation at $77\,°K$. Cells were always washed with cleaning solution, rinsed with distilled water, and allowed to dry before low temperature spectra were taken. Without these precautions, cracks in the glass were almost always present. The $MgCl_2:H_2O$ mixture was found to be

a fairly stable glass, in that it could stand the addition of small amounts of dilute sulfuric acid as well as hydrogen peroxide without cracking. Measurements were made using commercial Suprasil square cells and water when checking a compound for purity. Quantitative agreement between the results from commercial cells and the results obtained using the homemade tubing cells was fair.

A number of room and low temperature spectra using KBr pellets were measured. The pellets were placed in a brass block, the bottom of which was immersed directly into liquid N_2.

Results and Discussion

In Table I-1, we have set out both the room and low temperature electronic spectra of the μ-superoxo and μ-peroxo compounds investigated. Figures I-1, I-2, I-3, and I-4 display these spectra. Because of the glass used ($MgCl_2$), the low temperature spectrum of μ-peroxodecacyanodicobalt(III) could only be obtained in an acidic or neutral solution (Figure I-5). These spectra contain peaks attributable to decomposition products. Because of this, they were not included in Table I-1.

Bridging Superoxo Spectra

In proceeding with the assignments of the spectra of the μ-superoxo complexes, a crucial point is reached immediately. How are we to assign the first band, i.e., the band which occurs ~ 675 nm in the decaammine, and ~ 485 nm in the decacyanide? We have chosen to assign these bands as metal $\rightarrow$ ligand, Co(III) $\rightarrow$ O_2^-, charge transfer excitations rather than to intrametal d-d transitions. This choice leads to an internally consistent formulation of the assignments of all the spectra.

Table I-1

Electronic Spectra of μ-peroxo and

μ-superoxodicobalt Complexes at 300°K and 77°K

	300°K			77°K		
	λ_{max}(nm)	ν(kK)[a]	ϵ[f]	λ_{max}(nm)	ν(kK)[a]	ϵ[f]
[(NH$_3$)$_5$Co]$_2$O$_2$(HSO$_4$)$_3$SO$_4$[b]	673	14.86	866	674	14.84	1120
				~650 (sh ?)	15.4	
	483	21.1	352	475	20.7	397
	~340 (sh ?)	29.4		346 (sh)	29.0	3600
	303	33.0	13,250	300	33.3	17,100
	~225 (w sh ?)	44.4		~225 (w sh ?)	44.4	~17,100
K$_5$[CN)$_5$Co]O$_2$[b]	812	12.3	24	812	12.3	
	486	20.6	952	485	20.6	1350
	~375 (sh)	26.7	~1700	359	27.9	1450
	311	32.2	17,100	303	33.0	14,300
	271	36.9	~5200	266	37.6	5600
	~225 (sh)	44.4	~11,100	~225	44.4	11,900

Table I-1 (Continued)

	300°K			77°K		
	λ_{max}(nm)	ν(kK)[a]	ϵ[f]	λ_{max}(nm)	ν(kK)[a]	ϵ[f]
[(NH$_3$)$_5$Co]$_2$O$_2$(SO$_4$)$_2$]^c	~525 (sh)	19.0		530	18.9	
	400	20.0		395	25.3	
K$_6$[(CN)$_5$Co]$_2$O$_2$^{d}	~370 (sh)	27.0	~5050			
	314	31.8	~10,100			
K$_3$[Co(CN)$_6$]^e	312	32.1	243			
	260	38.5	180			
	202	49.5	35,400			
K$_3$[Co(CN)$_5$SCN]^e	378	26.5	191			
	265	37.7	17,100			
	227	44.0	4300			
	200	50.0	16,700			

a 1 kK = 1000 cm^{-1}. b 9:10 MgCl$_2$:H$_2$O mixtures. c KBr pellet. d Obtained at 0°C in 3M KOH. LN$_2$ measurements could not be made because of the MgCl$_2$ glass used. At neutral pH's, spurious

Table I-1 (Continued)

bands appear, but the two real peaks both had an increase in ϵ's on going to 77°K.

[e] From reference 21. [f] A caveat concerning ϵ's: ϵ's at low temperature were calculated using an approximate contraction factor of 10%. This is probably accurate to within 2%. At both 300°K and 77°K, commercial cells were not used when a $MgCl_2:H_2O$ glass mixture was the solvent.

Figure I-1. Spectra of $[(CN)_5CoO_2Co(CN)_5]^{5-}$

in an aqueous $MgCl_2$ solvent
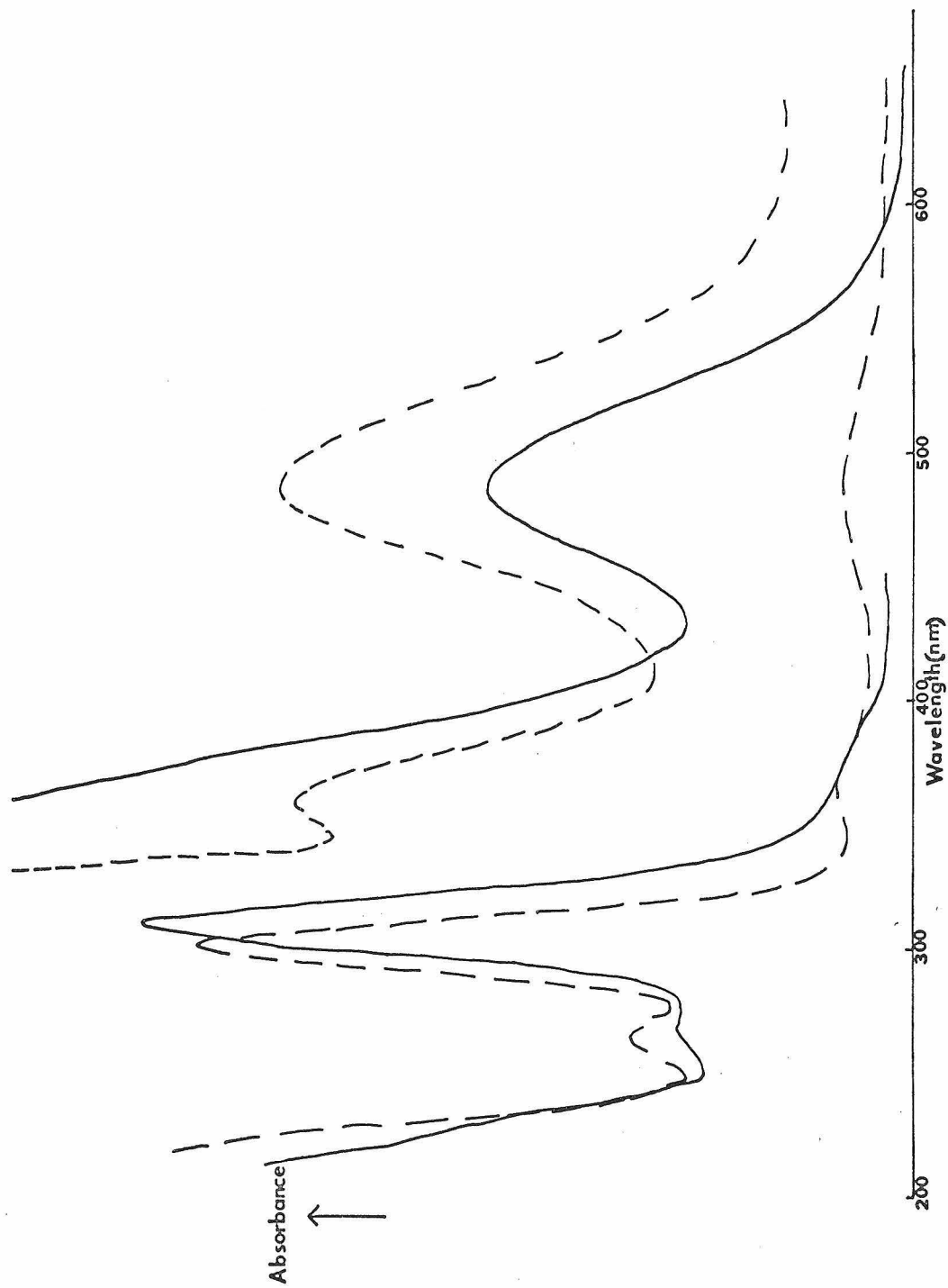
at 300°K (———) and 77°K (-----).

Figure I-2. Spectra of KBr pellets

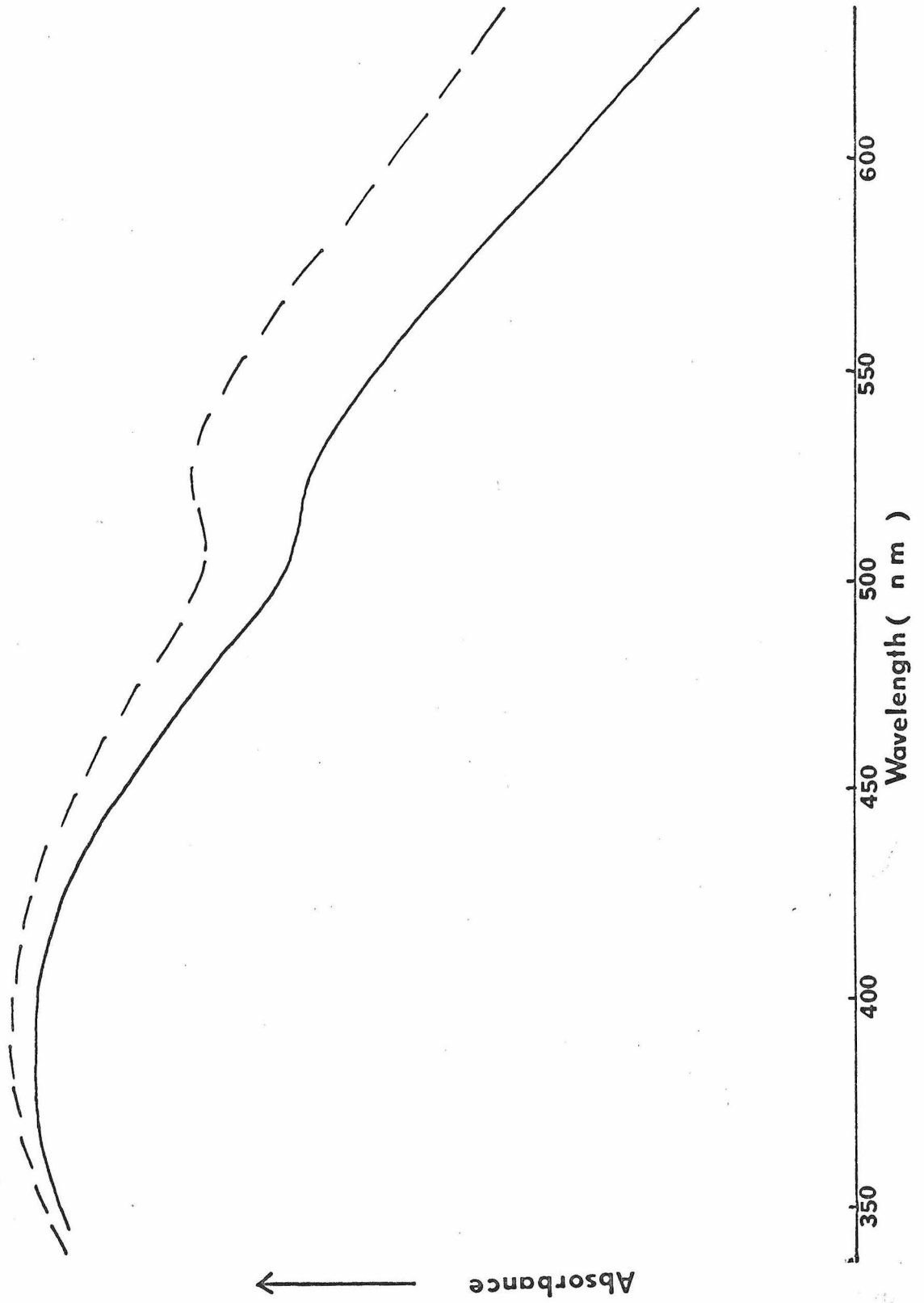of $[(NH_3)_5CoO_2Co(NH_3)_5]^{4+}$.

at 300°K (———) and 77°K (-----).

Figure I-3. Spectra of $\left[(NH_3)_5CoO_2Co(NH_3)_5\right]^{5+}$

in an aqueous $MgCl_2$ solvent at

$300\,°K$ (———) and $77\,°K$ (-----).

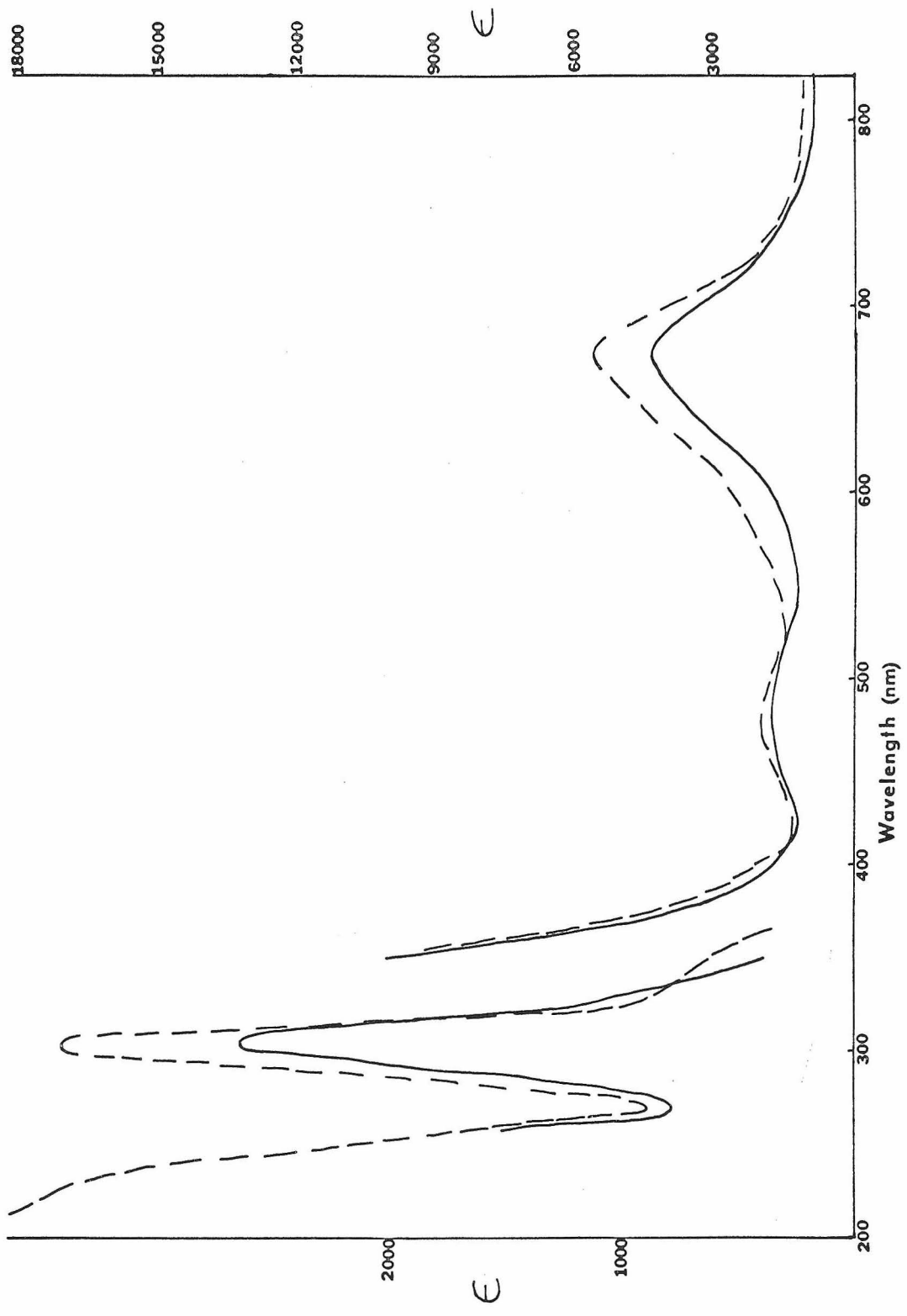Some dilute H_2SO_4 was added to

stabilize the ion in solution.

Figure I-4. Spectrum of $[(CN)_5CoO_2Co(CN)_5]^{6-}$

in a 3 M KOH solution at 0 °C.

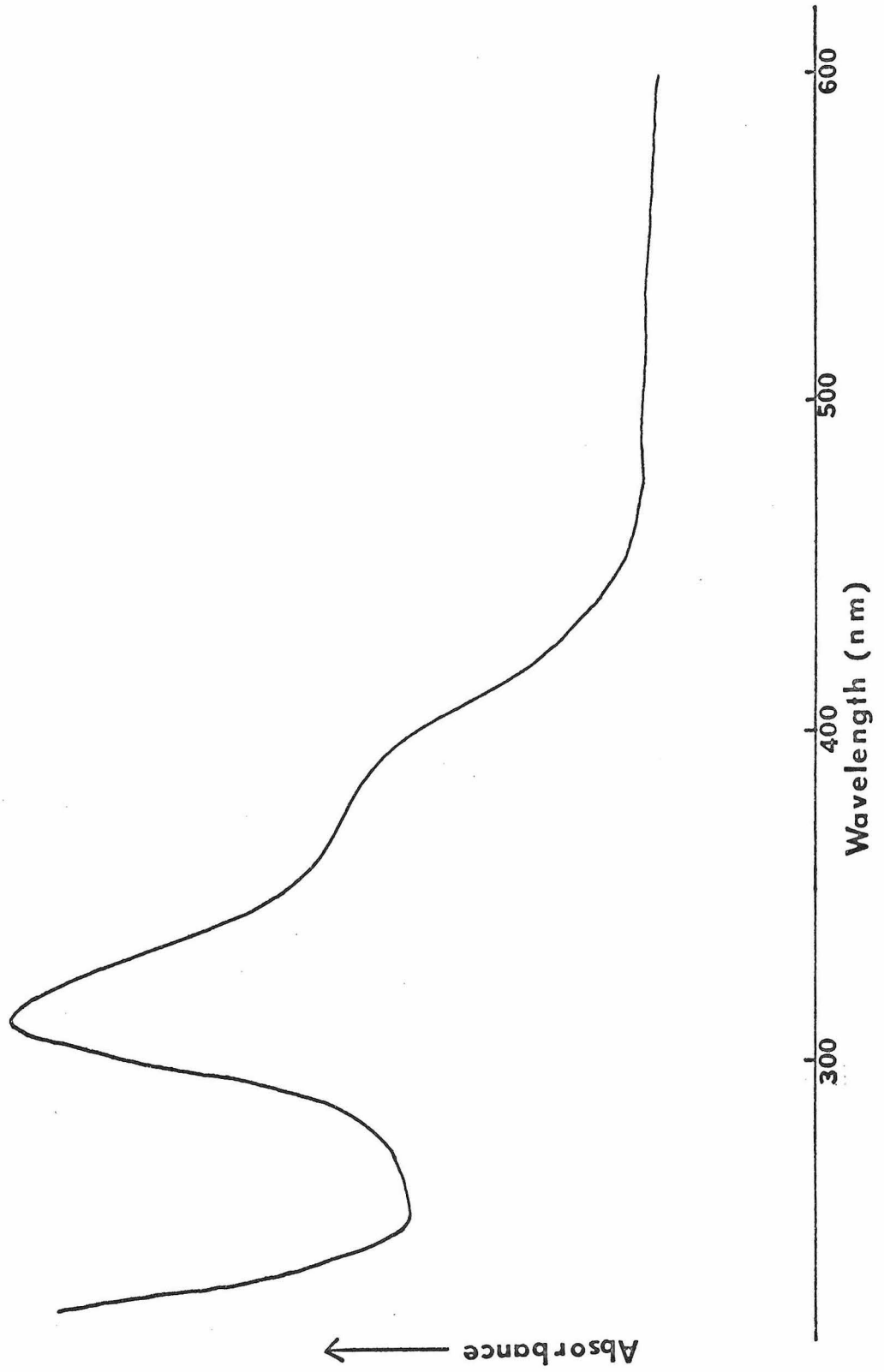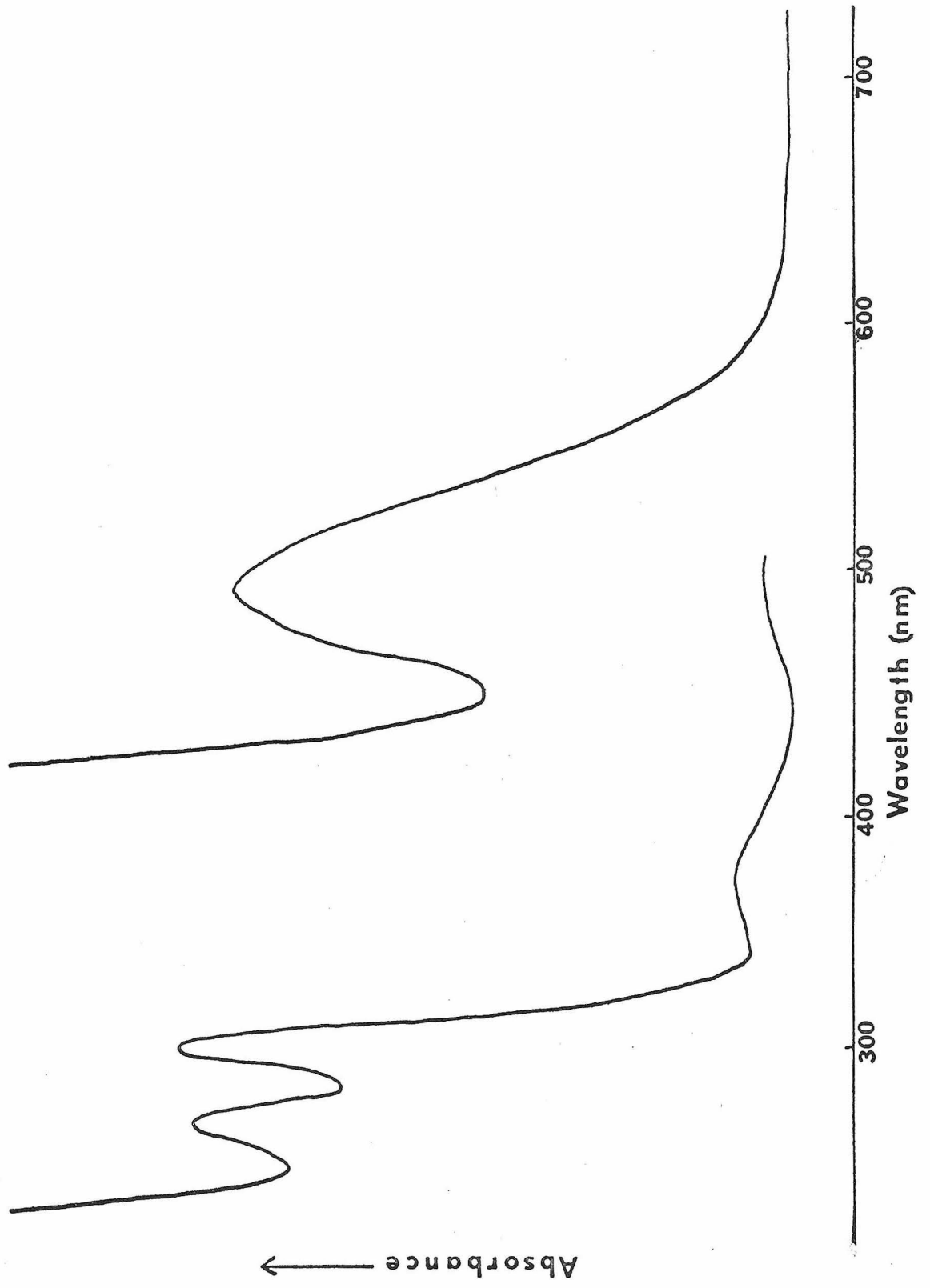Figure I-5. Spectrum of $[(CN)_5CoO_2Co(CN)_5]^{6-}$

in an aqueous $MgCl_2$ solvent at 77°K.

Absorbance

Wavelength (nm)

An octahedral complex of Co(III) is expected to possess two ligand field transitions: $^1A_1 \rightarrow {}^1T_1$ and $^1A_1 \rightarrow {}^1T_2$.[24] Lowering the symmetry to C_{4v} causes the first transition to split into $^1A_1 \rightarrow {}^1E^a$ and $^1A_1 \rightarrow {}^1A_2$, while the second octahedral transition should split into $^1A_1 \rightarrow {}^1B_2$ and $^1A_1 \rightarrow {}^1E^b$ [25]. This is shown in Figure I-6.

It has been shown by Wentworth and Piper[25] that the C_{4v} $^1A_1 \rightarrow {}^1A_2$ transition occurs at approximately the same energy as the O_h $^1A_1 \rightarrow {}^1T_1$ transition. Considering first the superoxodecaammine, we note a band at 21.05 kK, which corresponds exactly to the $^1A_1 \rightarrow {}^1T_1$ excitation in cobalt(III) hexaammine.[26] We assign the 21.05 kK band in our dimer to the $^1A_1 \rightarrow {}^1A_2$ transition.

The next problem is to locate the $^1A_1 \rightarrow {}^1E^a$ transition. Either it lies under the same band as the $^1A_1 \rightarrow {}^1A_2$ excitation at 21.05 kK, or it lies under what we have already called the $Co(III) \rightarrow O_2^-$ charge transfer at 14.85 kK. If in fact the latter supposition is true, we obtain using the relation $E(^1A_2) - E(^1E^a) = 35/4\, Dt$,[25] a value of ~ 700 cm^{-1} for the tetragonal field parameter Dt. This value is ~ 300 cm^{-1} higher than the highest observed values for Dt in other monoacidopentaammines.[25] Furthermore, using this value for Dt and assuming the usual value for $Dq(NH_3)$, we obtain the absurd result of $Dq(O_2^-) \sim 0$. Similarly, if we assume Dt is negative by taking the 29.24 kK band to be the $^1A_1 \rightarrow {}^1E^a$ transition, we obtain a Dt ~ -930 cm^{-1} and a $Dq(O_2^-) \sim 5.75$ kK, both very unreasonable values.

Figure I-6. Tetragonal splitting of the
excited states of octahedral Co(III).

$^1T_2$ ⎯⎯⎯⎯⎯ $^1E^b$

$^1B_2$

$^1T_1$ ⎯⎯⎯⎯⎯ $^1A_2$

$^1E^a$

$^1A_1$ ⎯⎯⎯⎯⎯ $^1A_1$

O_h　　　　　C_{4v}

25
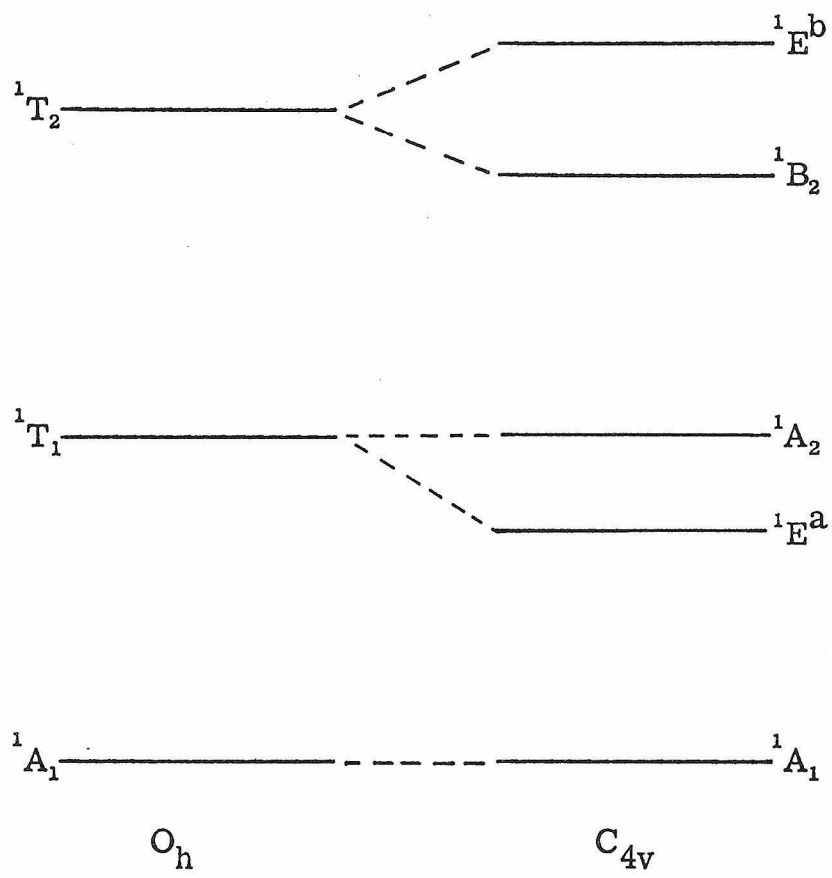
All this then intimates that the $^1A_1 \rightarrow {}^1E^a$ transition is buried under the 21.05 kK band. A final bit of evidence that this band is comprised of two transitions is the slight shift in band maximum upon going to liquid nitrogen temperatures, a shift from 20.75 to 21.05 kK. The $^1A_1 \rightarrow {}^1E^a$ transition is a symmetry allowed band, while the $^1A_1 \rightarrow {}^1A_2$ transition is only vibronically allowed. The shift itself may be interpreted as a cooling out of the $^1A_1 \rightarrow {}^1A_2$ transition. The shift to the blue can be explained by saying that O_2^- is slightly on the high side of NH_3 in the spectrochemical series. With Dt now approximately zero, $Dq(NH_3) \sim Dq(O_2^-)$.

We can assume that the splitting of the O_h $^1A_1 \rightarrow {}^1T_2$ transition in our C_{4v} species is unresolvable, a good assumption in light of the fact that in all the cobalt monoacidopentaammines this transition has never been observed to be split.[25] With this assumption, we assign the band at 29.24 kK to the $^1A_1 \rightarrow ({}^1B_2, {}^1E^b)$ transition, and we can arrive at a value for B. Wentworth and Piper[25] have shown that $E(^1B_2) - E(^1A_2) = -4\,Ds - 5\,Dt + 16\,B$. This reduces to 16 B, since we have shown Dt $\sim$0 and Ds is usually just 3 Dt. We arrive at a B $\sim$510 cm^{-1} which is compatible with the B for $Co(NH_3)_6^{3+}$, 530 cm^{-1}.[25]

It has also been shown[25] that the first singlet $\rightarrow$ triplet transition should occur at approximately 10 Dq - 3 C. Since Dq and C are almost the same as in the hexammine, a spin forbidden band should occur near 13.5 kK. In the decaammine, there is a very weak but decided tail on the red side of the low energy M $\rightarrow$ L charge

transfer transition. This occurs in the 800 - 700 nm region and could reasonably be assigned to the first forbidden transition. Finally, in the decaammine, the transition at 33.2 kK can be ascribed to a ligand → metal, O_2^- → Co(III) charge transfer excitation.

Moving to the decacyanide, we expect the $^1A_1 \to {}^1A_2$ component of the $^1A_1 \to {}^1T_1$ O_h transition to come about the same energy as the first ligand field transition in $K_3Co(CN)_6$, i.e., ~32.1 kK. [21] Since this is so close to the O_2^- → M band at 33.0 kK, the ligand field transition is very possibly obscured. The band at 27.9 kK can be assigned to the $^1A_1 \to {}^1E^a$ ligand field transition. Assuming all this, and using $Dt = -\frac{4}{35}[W - (10\ Dq - C)_{xy}]$, [25] we get a $Dq(O_2^-) =$ 1.92 kK. Even though this value for $Dq(O_2^-)$ is less than that obtained from the decaammine analog, it is well within the range of Dq for the N-donor part of the spectrochemical series. It must be noted that Dq's obtained from the pentacyano series can be at least 5-10% less than the Dq's obtained from the pentaammine series. [23b] Finally, the value of the band assigned as the $^1A_1 \to {}^1E^a$ transition at 27.9 kK is at least in the proper position with respect to the few other monoacidopentacyano complexes studied [21,12]: Cl^- (25.5) < N_3^- (26.1) < OH_2 (26.3) < SCN^- (26.5) < NCS^- (27.6) ~ $NCSe^-$ (27.6) < O_2^- (27.9) << CN^- (32.1).

We proceed by assigning the 37.6 kK band as the unsplit $^1A_1 \to {}^1T_2$ ligand field transition. Using this assignment, together with our calculated value for Dt ~0.5 kK, we obtain a value for the Racah parameter B from the relation $E(^1T_2) - E(^1E^a) =$ $16B - \frac{35}{4} Dt$. ΔE experimentally is 9.7 kK. This gives a

$B \sim 430$ cm^{-1}, in good agreement with the hexacyanide value of 420 cm^{-1}.[25]

The decacyanide peak at 33.0 kK has been assigned to a charge transfer $O_2^- \rightarrow$ Co(III) transition. Previous work on pentacyanocobaltates indicate that CN$^- \rightarrow$ Co(III) transitions occur at energies $\gtrsim 50,000$ cm^{-1}.[21]

The presence in the decacyanide of a shoulder at ~ 225 nm is reminiscent of shoulders in the 44-45 kK region found in pentacyanocobaltates possessing bent triatomic ligands.[21] The absorption may represent a transition to one of the forbidden components of the $M \rightarrow \pi^*$(CN) excitation.[21] An excitation from $e^4(xz, yz)b_2^2(xy) \rightarrow e^4 b_2 e(\pi^*CN)$ gives a ^1E excited state, while an excitation to $e^3 b_2^2 e(\pi^*CN)$ gives $^1A_1$, $^1A_2$, $^1B_1$, $^1B_2$ excited states. Only transitions to $^1A_1$ and ^1E excited states are orbitally allowed. As the axial symmetry is destroyed with a non-linear axial perturbation, the other excited states may be expected to appear. Alternatively, since in the C_{2h} symmetry of our compound the π orbitals of O_2^- are no longer exactly degenerate, it is possible that a component of the $O_2^- \rightarrow$ Co(III) charge transfer centered at 33.0 kK may be found at 10,000 - 12,000 cm^{-1} above the first band.[21]

Finally, a very weak peak at ~ 800 nm is found. On an intensity basis ($\epsilon \sim 20$) one would assign this to a spin-forbidden transition, although the first such transition is predicted from theory to come at ~ 25.0 kK in our complex. Why it appears where it does is still enigmatic. Perhaps the triplet excited state couples in some

way with the electron localized on the O_2^-, bringing the singlet-triplet energy down ~ 12.5 kK.

It is interesting to note that the $O_2 \to M$ excitation is at about the same energy in both the decacyano and decaammine compounds. This could arise from an accidental cancellation of effects. The larger 10 Dq of CN^- is probably just matched by smaller electron repulsion effects in CN^-.

The decacyanide exhibits a 1.4 kK red shift of its $M \to O_2^-$ band when its spectrum is taken in the solid state. (The decaammine also exhibits this shift, but to a much lesser extent.) A solid state hydrogen bonding mechanism may stabilize the π^* orbital O_2^- to an extent impossible in solution.

Finally, it should be pointed out that attempts to find a near IR band failed. Unlike the ruthenium-pyrazine dimer discussed later in this thesis, the electron in the cobalt compound is localized primarily on the π bridge. This is in accord with ESR results reported.[5]

Now that a set of plausible assignments for the superoxo species has been advanced, we will proceed to show why other assignments are not as satisfactory. Assume, in the case of the decacyanide, that the 20.6 kK transition is not the $M \to O_2^-$ charge transfer transition, but an unsplit $^1A_1 \to {}^1T_1$ ligand field excitation. Assume also that the 27.85 kK transition is the second unsplit ligand field transition $^1A_1 \to {}^1T_2$. Under these assumptions, we arrive at Dq =

1.7 for the complex as a whole. When using $Dq(CN^-) = 3.6$ kK with the calculated Dq (μ-superoxodecacyanide) $= 1.7$ kK, we obtain a $Dq(O_2^-) < 0$, certainly an absurd result. We arrive at the same result in the decaammine if we make the following assignments: $^1A_1 \rightarrow {}^1T_1$ (14.85 kK), $^1A_1 \rightarrow {}^1T_2$ (21.05 kK).

Another possible assignment which must be considered is one already proposed by Barrett and his coworkers.[29] They assigned the ligand-field transitions in the decaammine in the following fashion: $^1A_1 \rightarrow {}^1E$, 14.85 kK, $^1A_1 \rightarrow {}^1A_2$, 21.05 kK, $^1A_1 \rightarrow ({}^1E^b, {}^1B_2)$, 29.29 kK. In the decacyanide, they made the following assignments: $^1A_1 \rightarrow {}^1E^a$, 20.6 kK, $^1A_1 \rightarrow {}^1A_2$, 27.85 kK, $^1A_1 \rightarrow ({}^1B_2, {}^1E^b)$, 37.6 kK. Their assignments are based on the fact that photolysis at 14.84 kK in the decaammine fails to produce decomposition products as may be expected from irradiating a charge transfer band. In reality, this line of reasoning is fallacious since irradiation at a charge transfer transition does not necessarily lead to photochemistry. If the energy of irradiation fails to put the molecule into a "dissociative state", no reaction need be expected. In any event, using these assignments leads to a Dt = 700 cm^{-1}, which in turn gives a $Dq(O_2^-) \sim 5$ cm^{-1}. Similarly, Barrett's assignments for the decacyanide lead to the untenable values of Dt ~ 830 cm^{-1} and $Dq(O_2^-) \sim 700$ cm^{-1}. Finally, Barrett does not seem to recognize the possibility that a $M \rightarrow O_2^-$ transition may exist.
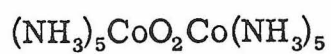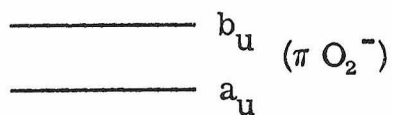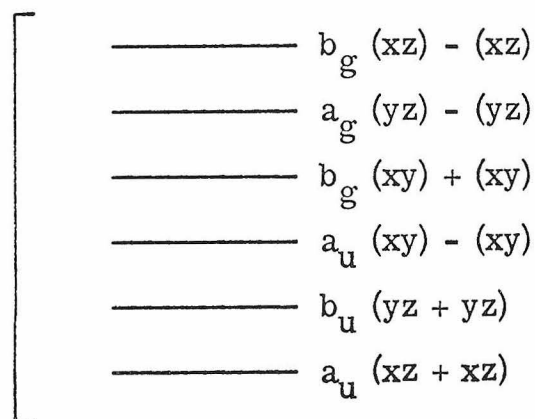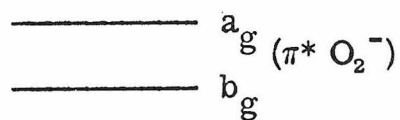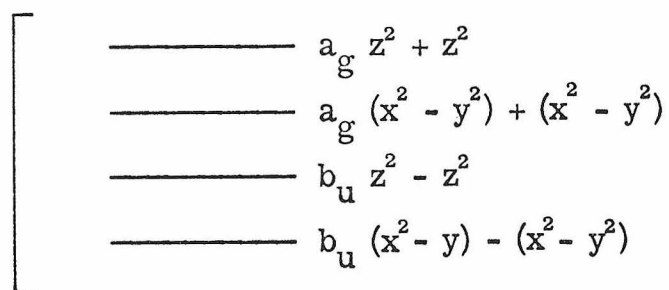
In addition to the internal consistency of the Dq's, Dt's, and B's calculated, there is other experimental evidence for assigning the

675 nm band in the decaammine as a M → O_2^- transfer. In the symmetry of our molecule, the π^* orbitals of oxygen must be split into A_g and B_g orbitals. In the low temperature spectrum, we see this splitting of the 675 nm band as a shoulder on the high energy side. Second, the oscillator strength of this band is the same at 77°K and 300°K to within 1%-2%.
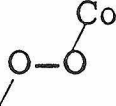
It will be admitted that these two facts constitute evidence for a $^1A_1 → {}^1E^a$ ligand field transition as well as for a M → O_2^- charge transfer. This d-d transition, assuming C_{4v} symmetry around cobalt, is orbitally allowed. It should also be ever so slightly split because of the lower than C_{4v} symmetry of the whole molecule. However, if the transition is really a ligand field transition $^1A_1 → {}^1E^a$, it should be polarized ⊥ to the long axis of the molecule, provided that C_{4v} symmetry suffices in describing an intrametallic d-d transition. Experimentally, the first band is actually polarized ‖ to the O-O bond.

If we assume C_{2h} symmetry, we can obtain a molecular orbital scheme as in Figure I-7. The exact ordering of the t_{2g} d orbital combinations is not important. They should all be about the same energy. Assuming we have a ^2A_g ground state, only excitations to a non-centrosymmetric state are allowed. We have a 2:1 ratio of $a_u:b_u$ orbitals in which to place a hole in the excited state. If this is so, we should have twice the number of $^2A_g → {}^2A_u$ ‖ polarized transitions than $^2A_g → {}^2B_u$ ⊥ polarized transitions. Hence, the band for our M → O_2^- excitation should be polarized ‖ to the z-axis, and be of essentially $^2A_g → {}^2A_u$ character.

Figure I-7. Approximate MO scheme for

μ-superoxodecaamminedicobalt(III).

———————— a_g $z^2 + z^2$

———————— a_g $(x^2 - y^2) + (x^2 - y^2)$

———————— b_u $z^2 - z^2$

———————— b_u $(x^2 - y) - (x^2 - y^2)$

———————— a_g $(\pi^* O_2^-)$

———————— b_g

———————— b_g $(xz) - (xz)$

———————— a_g $(yz) - (yz)$

———————— b_g $(xy) + (xy)$

———————— a_u $(xy) - (xy)$

———————— b_u $(yz + yz)$

———————— a_u $(xz + xz)$

———————— b_u (πO_2^-)

———————— a_u

———————— a_g (σO_2^-)

$(NH_3)_5 CoO_2 Co(NH_3)_5$

The only assumption that requires elaboration is the ^2A_g ground state. The $a_g(\pi^*O_2^-)$ orbital can be thought of as being in the plane of the paper in the $C\overset{\displaystyle Co}{\underset{\displaystyle O-O}{}}$ unit, while the $b_g(\pi^*O_2^-)$ orbital is $\perp$ to the plane of the paper. It is probably reasonable to suspect that in-plane π bonding remains fairly constant upon going from linear overlap to bent overlap. Out-of-plane π bonding probably decreases upon going from head-on overlap to tangential overlap. This is a plausible reason for the $a_g(\pi^*O_2^-)$ orbital being destabilized relative to the $b_g(\pi^*O_2^-)$ orbital producing an A_g ground state.

Our assignment for the decaammine 485 nm band is $^1A_1 \rightarrow (^1E^a, ^1A_2)$ in C_{4v} notation. In C_{2h} notation, this corresponds to $^1A_g \rightarrow (2\,^1B_g + ^1A_g)$, a transition which should show no appreciable polarization. This prediction has been experimentally observed by ourselves and Yamada.[30]

One last possible assignment for the 675 band must be ruled out. Garbett[31] has suggested, on the basis of his circular dichroism work on ethylenediamine analogs of our dimer, that this band is due to a $\pi \rightarrow \pi^*$ intraoxygen transition. He fails to note that the $\pi \rightarrow \pi^*$ transition in free O_2^- is known to appear at $\sim$240 nm.[32] Furthermore, a $\pi \rightarrow \pi^*$ band should be unpolarized in C_{2h}, and experimentally the 675 band is polarized.

Bridging Peroxo Spectra

Prior to looking at our μ-peroxo compounds, let us examine another well characterized series of binuclear μ-peroxo complexes. Examining the spectra of the binuclear $[\text{Co(cyclam)X}]_2\text{O}_2^{n+}$ species and the spectra of $[\text{Co(cyclam)X}_2]^{n+}$, where $X = \text{Cl}^-$, OH_2, NO_2^-, N_3^-, NCS^-, and where cyclam is a cyclical tetradentate amine ligand,[33] we can abstract a value of Dq $(\text{O}_2^{2-}) \sim 2.1$ kK. When compared with other values for Dq obtained in other ammino Co(III) series, this places O_2^{2-} slightly below NCS^- in the spectrochemical ranking,[25] i. e., H_2O $(1.9) < \text{O}_2^{2-}$ $(2.1) < \text{NCS}^-$ $(2.2) < \text{NH}_3$ (2.5).

Turning to our μ-peroxo decacyano species, we see in Figure I-4 that we have a relatively uninformative spectrum. We expect the μ-superoxo $M \rightarrow \text{O}_2^-$ band to disappear, because such a transition is impossible in peroxide with a filled π^* level. However, let us assign the shoulder at ~ 370 nm to the $^1A_1 \rightarrow {}^1E^a$ transition. At the same time, let us assume the second band, the $^1A_1 \rightarrow {}^1A_2$ transition, to occur near the $^1A_1 \rightarrow {}^1T_1$ excitation of the hexacyanide. This would require $^1A_1 \rightarrow {}^1A_2$ to be buried under the 31.3 kK $\text{O}_2^{2-} \rightarrow$ M charge transfer band. Dt then comes out ~ 490 cm^{-1}, and Dq $(\text{O}_2^{2-}) \sim 1.95$ kK. This certainly is compatible with a Dq (O_2^{2-}) of 2.1 kK from the cyclam series, especially when both of our decacyanide transitions are only approximately known. The fact that the shoulder in the decacyanide appears at ~ 370 nm while the first band in $\text{Co(CN)}_5\text{H}_2\text{O}^{2-}$ appears at ~ 380 nm[12] indicates that O_2^{2-} exerts a stronger crystal field than H_2O. Similarly, the fact that the

same transition appears at 359 nm in the μ-superoxodecacyano
species again indicates that Dq $(O_2^-) >$ Dq $(O_2^{2-}) >$ Dq (H_2O).

When we proceed to the μ-peroxodecaammine complex, we
run into problems. This compound is highly unstable in solution,
and only marginally stable as a solid. KBr pellets were the only
means of investigating this compound. They gave a very poorly
resolved spectrum which is displayed in Figure I-2. Again, one
wouldn't expect to see the low energy M $\rightarrow$ O_2^- transfer, and no
such transition is seen. What one expects to see, however, are
vestiges of the octahedral $^1A_1 \rightarrow {}^1T_1$ and $\rightarrow {}^1T_2$ transitions. Due to
scattering, only two transitions are observed; a shoulder at $\sim$19.0 kK
and a peak at $\sim$ 25.3 kK. Since the shoulder sharpens to a peak at
19.0 kK at 77°K, one may assume a vibrationally allowed transition
is present, adjacent to and slightly to the blue of 525 nm. This may
very well be the orbitally forbidden $^1A_1 \rightarrow {}^1A_2$ excitation. This
transition should again be close to the 485 nm hexaammine $^1A_1 \rightarrow {}^1T_1$
band. Let us arbitrarily set this obscured transition at 20 kK, while
assuming the $^1A_1 \rightarrow {}^1E^a$ excitation to be the band at 19.0 kK. We will
then call the 25.3 kK band an unsplit $^1A_1 \rightarrow ({}^1B_2, {}^1E^b)$ excitation.
These assumptions lead to a Dt $\sim$170 cm^{-1}, and a Dq $(O_2^{2-}) \sim$1.7 kK,
a result very much like that for water. Considering the poor
resolution of the bands and our somewhat arbitrary positioning of
$^1A_1 \rightarrow {}^1A_2$, this is well within the range of our previous results for
O_2^{2-} (1.95 - 2.1 kK). All this, then, is consistent with O_2^{2-} being
between H_2O and NCS$^-$ in the spectrochemical ranking. That O_2^{2-} is
below O_2^- in the series may have been predicted qualitatively. Both

ions are probably equal in σ bonding ability, but O_2^- is a better π acceptor and hence should be higher in the spectral ordering.

Decomposition of μ-peroxodecacyanodicobalt(III)

As already noted, the peroxo bridged decaammine species is so unstable in aqueous solutions at all pH's that one must turn to solid techniques to obtain any spectra at all. Similarly, the μ-peroxodecacyano compound is unstable, although not as unstable as its ammine analog. This instability has led various authors to include in the spectrum of the decacyanide peaks which, in our opinion, are spurious.

In order to sort out the spectrum of the decacyanide, we looked at it at various pH's. Bayston, et al.,[34] made the only previous attempt to investigate this problem. We arrived at almost identical conclusions.

At anything less than very basic solutions, > 1 M KOH, the decacyanide has a tendency to protonate (pK ~ 11.3),[35] as do other peroxides and superoxides. Like Bayston, we believe the 272 nm peak often ascribed to the parent dimer is, in reality, a pentacyano hydroperoxide $O_2H^- \rightarrow$ M charge transfer. In addition there may be a relatively long lived dimer bridged by a hydroperoxide group

$$Co \underset{\displaystyle O}{\overset{\displaystyle \overset{\textstyle H}{\underset{\textstyle |}{O}}}{\diagdown}} Co$$

Co, with a characteristic absorption ~ 300 nm. The bridged hydroperoxide, over a period of time, goes to the hydroperoxide monomer and aquopentacyanide.

Unlike Bayston, who seemed uncertain, we believe that our failure to get the parent dimer to obey Beer's law at ~ 485 nm proves that this peak arises because of an initial presence and/or a subsequent generation of μ-superoxodecacyanide. One other slight variation in our results is that we were never able to get the parent decacyanide $O_2^- \rightarrow M$ peak down to 327 nm. The best we were able to do was ~ 320 nm.

Before departing from the pentacyanohydroperoxide, let us examine the ordering of the $L \rightarrow M$ charge transfer energies in O_2^-, O_2^{2-}, and OOH^-. This band comes at 272 nm in OOH^-, at 303 nm in O_2^-, and at ~ 320 nm in O_2^{2-}. In all these species, the $L \rightarrow M$ excitation is one from a $\pi^* O_2$ orbital to a d_{z^2} cobalt orbital. When a proton is added to O_2^{2-} on a pentacyanocobaltate, the relevant O_2H^- (π^*) orbital is stabilized vis-à-vis the O_2^{2-} (π^*) orbital when a second cobalt group is added. This can crudely be thought of as arising from the repulsion of a filled d_{xz} orbital on the second cobalt with the filled π^* orbitals in O_2^{2-}. When, instead of a second cobalt nucleus, a proton with its positive charge is added, no such repulsion is possible. By a similar crude argument, the repulsion of filled cobalt d_{xz} orbitals with a filled O_2^{2-} (π^*) orbital should be greater than the repulsion between filled d_{xz} cobalt orbitals and filled O_2^- (π^*) orbitals.

Some Biological Implications

With the recent interest in synthetic oxygen carriers as models for oxygen transport in biological systems, our assignments of the bridged superoxo and peroxo compounds assume added importance.

The most extensive series of reversible carriers in the literature is the cobalt(II) salicylaldimino (salen) series.[36] Work on these compounds has shown that the cobalt atom is oxidized to the III state, with the oxygen carried as a superoxo ion.[36, 37, 7] In both the salen complexes that we looked at, we were able to discern a shoulder at $\sim$700 nm - 725 nm arising in the oxygenated species. Although this shoulder has been observed elsewhere for a solution spectrum of the parent salen complex,[38] its interpretation was never discussed. It is quite plausible, we believe, that this band arises from the very same $Co \rightarrow O_2^-$ transition as the 14.85 kK band in the μ-superoxo-decaammine. Considering that the transition is centered in the same bridging unit as in the decaammine, and also considering that the other ligands in the Schiff base are of comparable ligand field strength to ammonia, one would expect a relatively small shift in the $Co \rightarrow O_2^-$ transition.

Now this interpretation has serious consequences for oxyhemo-globin. Oxyhemoglobin is known to be diamagnetic while deoxyhemo-globin has a $\mu_{eff} \sim 5$ B.M.[39] Among the various models of hemo-globin that have been proferred is one that relies on its analogy to the cobalt salen oxygen carriers.[40] As pointed out already, it has been established that these compounds consist of Co(III) and a superoxide anion, a triatomic unit which has been found to be non-linear.[37] Weiss[40, 27] has proposed that oxyhemoglobin is nothing more than $Fe(III)\text{-}O_2^-$ with its diamagnetism being explained by a large anti-ferromagnetic coupling between low spin Fe(III) and O_2^-.

If, however, our conclusion is correct that the Co(III) → O_2^- charge transfer comes characteristically at ~700 nm (with an ϵ ~ 1000), when the cobalt has around it 4 or 5 other nitrogen and/or oxygen ligands, one would predict that in a similar iron environment such as oxyhemoglobin, the corresponding Fe(III) → O_2^- transition would be red shifted. The only band in oxyhemoglobin found to the red of 700 nm is at ~915 nm with an ϵ ~ 200. This ϵ makes a charge transfer assignment unlikely, although this is far from conclusive. If we are correct in assigning the 915 nm band to a d-d transition, then a Fe(III) → O_2^- structure for oxyhemoglobin must be ruled out.

We have, in addition, another even stronger piece of evidence against a "metsuperoxide" formulation for oxyhemoglobin. Perhaps the most important result of our ligand field analysis of the peroxo and superoxo spectra is the positioning of O_2^- near NH_3 in the spectrochemical series. Using this information, we can deduce that Weiss' formulation is extremely unlikely.

It is known that Fe(III)-NCS hemoglobin has considerable high-spin (S = 5/2) character at 300°K.[41] It seems unlikely upon going to the superoxide that O_2^-, with a crystal field about the same as NCS$^-$, can force spin pairing in Fe(III). This pairing is necessary for antiferromagnetic coupling between ferric ion and superoxide to occur in order to produce the required diamagnetic species at room temperature.

Cyano Bridged Spectra

Our results on μ-cyano compounds are summarized in Table I-2 and displayed in Figures I-8, I-9, and I-10. When compared

Table I-2

Electronic Spectra of Cyano Bridged Complexes

and Some Related Species

	300°K			77°K		
	λ_{max}(nm)	ν (kK)[a]	ϵ[b]	λ_{max}(nm)	ν (kK)[a]	ϵ[b]
$(NH_3)_5CoNCCo(CN)_5$[c]	475	21.1	69	466	21.5	174
	313	31.9	230	303	33.0	306
$Ba_3[(CN)_5FeCNCo(CN)_5]$[c]	392.5	25.5	606	380	26.3	481
				320 (sh)	31.3	511
	324	30.9	890	305	32.8	555
$K_5[(CN)_5FeCNCo(CN)_5]$[c]	420 (sh)	23.8		417	24.0	1145
	400	25.0	688	400	25.0	1130
	~320 (sh)	31.3		322	31.1	1249
	303	33.0	1055	303	33.0	1759
	~280 (sh?)	35.7		~285 (sh)	35.1	~1200
				~260 (sh)	38.4	

Table I-2 (Continued)

	300°K			77°K	
λ_{max}(nm)	ν (kK)[a]	ϵ[b]	λ_{max}(nm)	ν (kK)[a]	ϵ[b]
$K_3[Co(CN)_6]$[d]					
312	32.1	243			
260	38.5	180			
202	49.5	35400			
$[n\text{-}Bu_4N]_3[Fe(CN)_6]$[e]					
	23.5	493			
	25.3	395			
	30.7	876			
	33.0	1338			
	35.0	864			
	38.5	1157			
	44	5480			
$K_4[Fe(CN)_6]$[e]					
	23.7	7			
	31.0	73			
	32.8				
	37.0	47			

Table I-2 (Continued)

	300°K			77°K	
λ_{max}(nm)	ν (kK)[a]	ϵ[b]	λ_{max}(nm)	ν (kK)[a]	ϵ[b]
	45.8	6600			
	29.5				

$Co(NH_3)_6^{3+}$ [f]

a 1 kK = 1000 cm^{-1}. b See note f Table I-1. c 9:10 MgCl$_2$:H$_2$O. d From reference 42.

e From reference 42. f From reference 26.

Figure I-8. Spectra of $[(CN)_5FeCNCo(CN)_5]^{6-}$
in an aqueous $MgCl_2$ solvent at $300\,°K$ (———) and $77\,°K$ (-----).
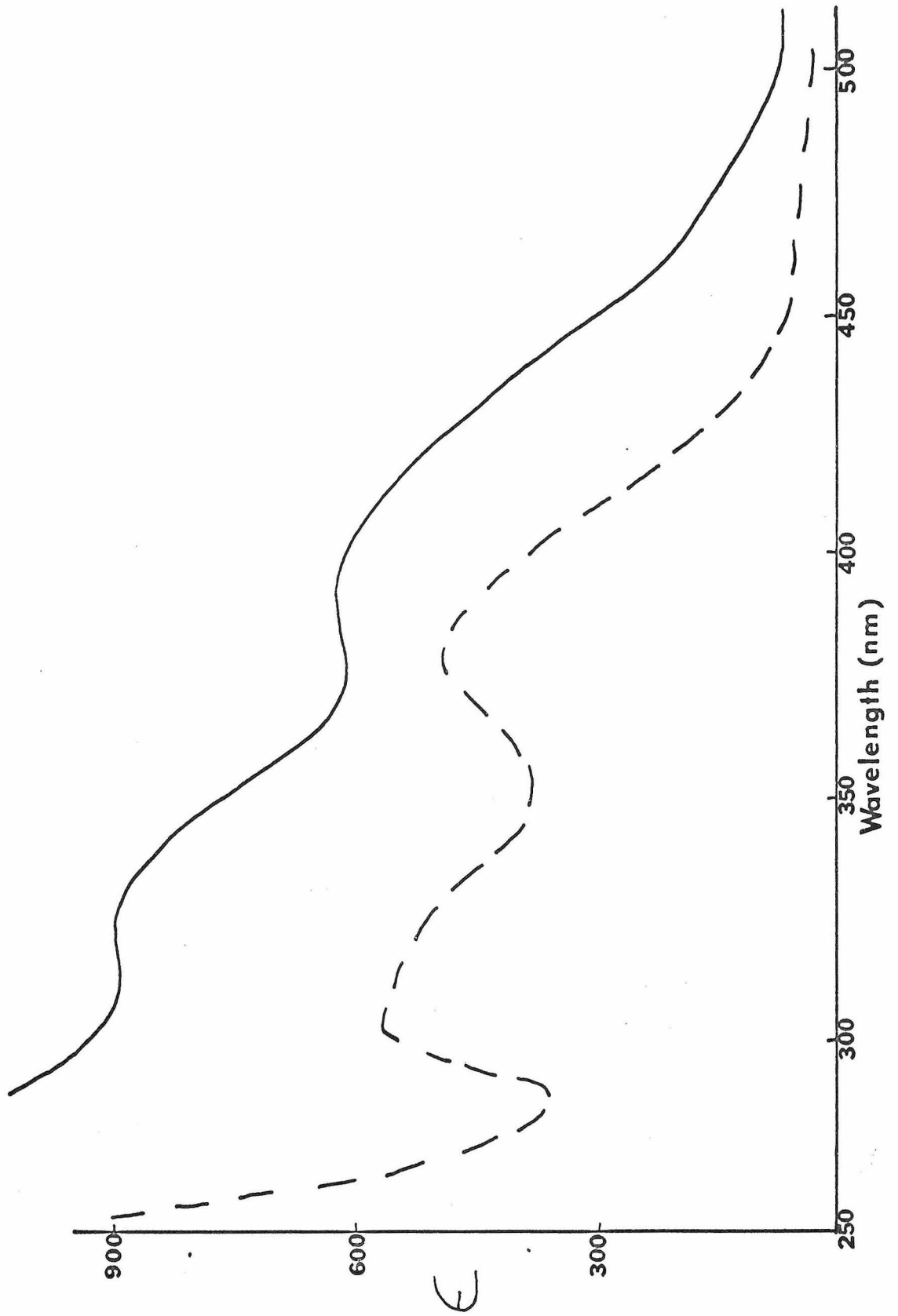
Figure I-9. Spectra of $(CN)_5CoCNCo(NH_3)_5$
in an aqueous $MgCl_2$ solvent at 300°K (———) and 77°K (-----).

46
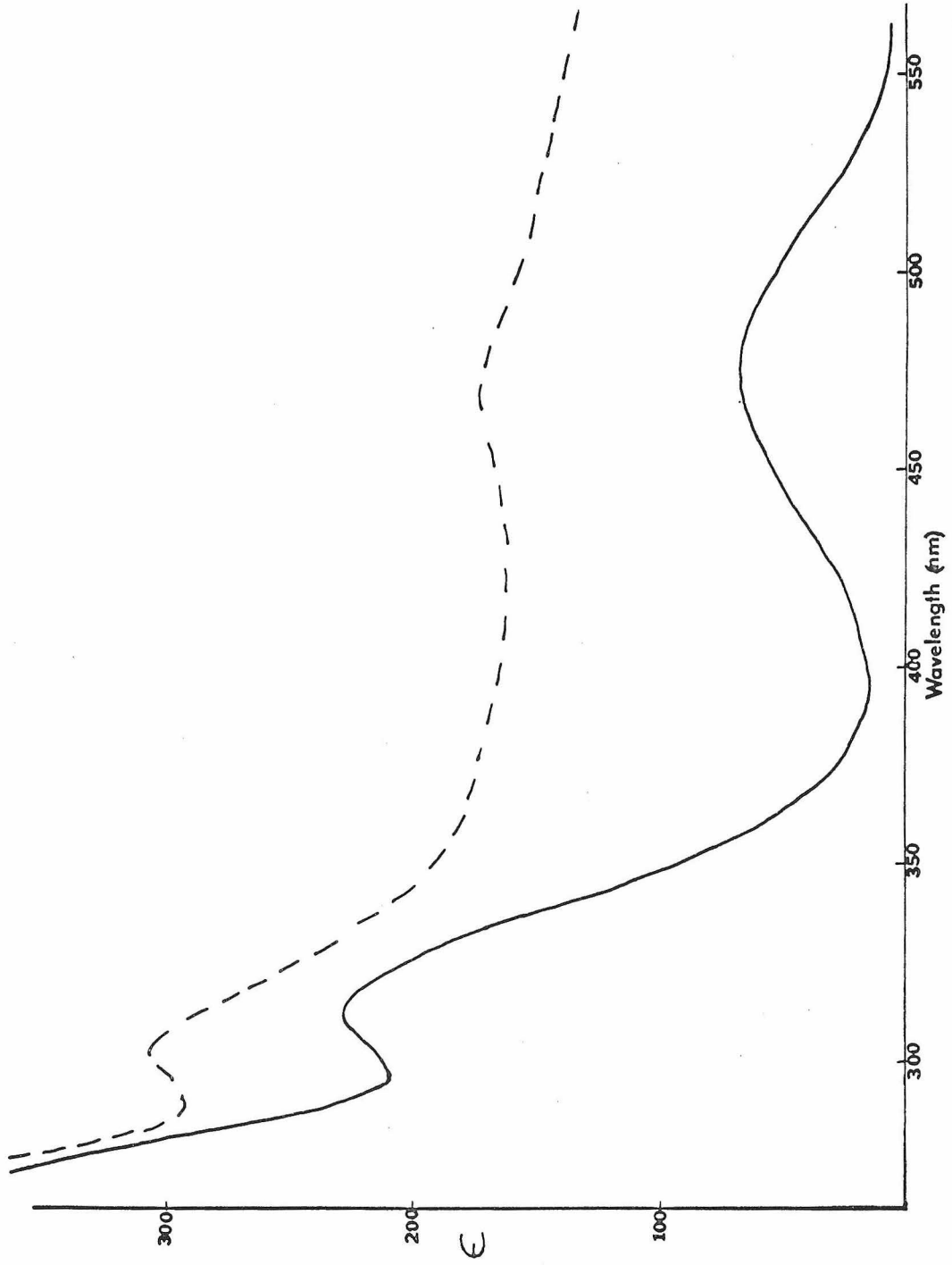
Figure I-10. Spectra of $[(CN)_5CoNCFe(CN)_5]^{5-}$

in an aqueous $MgCl_2$ solvent at 300°K (———) and 77°K (-----).
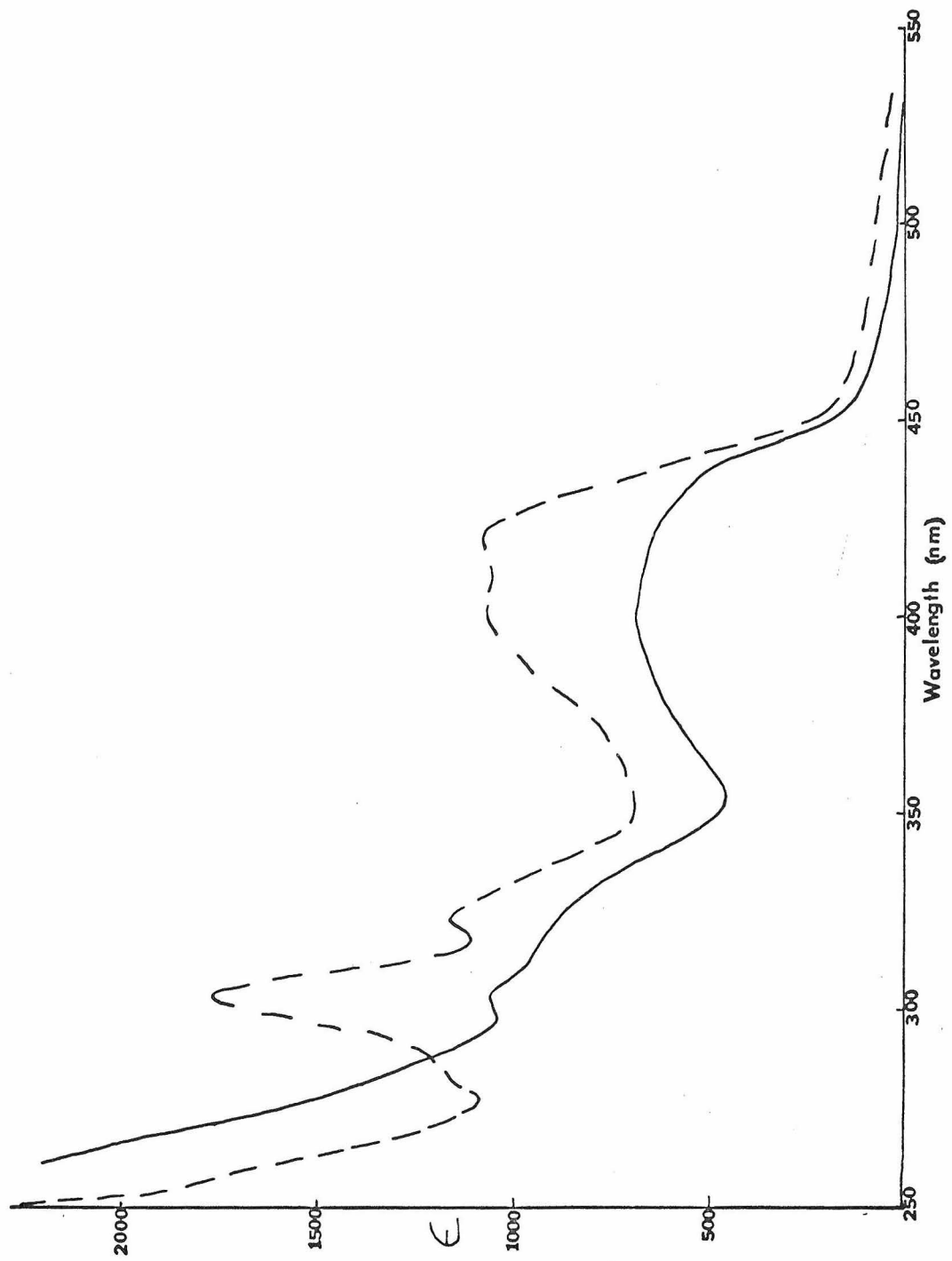
with the parent hexacyanides and hexammines the corresponding
bridged species have remarkably similar spectra. This similarity
makes their assignments relatively straightforward.

$Co(NH_3)_6^{3+}$ and $Co(CN)_6^{3-}$ have their first ligand field bands
at 21.05 and 32.1 kK, respectively.[25, 42] The bands at 21.1 and
31.9 kK in $(NH_3)_5CoNCCo(CN)_5$ can be assigned to the corresponding
first ligand field transition, $^1A_1 \rightarrow {}^1T_1$ $(^1A_2, {}^1E^a)$. The first d-d
transition in the pentacyano moiety would not be expected to show
tetragonal splitting. The presence of a cobalt ammine substituent
on a cyanide should only be a relatively minor perturbation. The first
d-d transition originating in the pentaammine moiety also would not
need to show the effects of a tetragonal distortion. The Dq of isocyanide
is known to be very similar to that of ammonia ($\lesssim 300$ cm^{-1}).[25] The
second ligand field transition from the ammonia group, $^1A_1 \rightarrow {}^1T_2$,
would be expected to be buried under the 31.9 kK cyano band. Charge
transfer transitions into the bridge itself can be expected to occur at
much higher energies.[21]

In the cyano bridged Fe(III) - Co(III) decacyanide, one sees
almost the identical spectrum as one sees in $Fe(CN)_6^{3-}$, especially at
low temperatures. That this spectrum is in fact the spectrum of the
dimer, and not the ferricyanide monomer, was established by reduction
of the dimer back to Fe(II)-CN-Co(III). All the bands expected to
arise from the Co(III) portion of the dimer should be buried under the
more intense Fe(III) peaks. All the bands of $Fe(CN)_6^{3-}$ have been
assigned by Alexander and Gray,[28] and their assignments are

applicable to our spectrum with little, if any, modification.

When one goes to the Fe(II)-CN-Co(III) dimer, one sees a 31.3 kK shoulder which may be assignable to the $^1A_1 \rightarrow {}^1T_1$ ligand field transition of the pentacyanoferrate. This should be compared to the corresponding transition at 31.0 kK in $Fe(CN)_6^{4-}$. Alternatively, the 31.3 kK transition may be the $^1A_1 \rightarrow {}^1A_2$ excitation in the pentacyano-cobaltate, a transition found at 32.1 kK in the hexacyanide. The peak at 32.8 kK comes exactly at an energy where ferrocyanide shows an additional band. If, however, we assign the 31.3 kK band to the ferrate unit, the cobalt $^1A_1 \rightarrow {}^1A_2$ transition can be assigned to the 32.8 kK peak. A clear distinction of these alternatives can not be made. One may assign both bands to the ferrate unit because of its expected larger intensities. In $Fe(CN)_6^{4-}$ we find the intensities larger than in $Co(CN)_6^{3-}$.

The band at 26.3 kK is probably the $^1A_1 \rightarrow {}^1E^a$ transition in the axially distorted pentacyanocobaltate. This assignment, together with our acceptance of the 31.3 kK shoulder (or a band buried somewhere in that region) as the $^1A_1 \rightarrow {}^1A_2$ transition, gives a Dq for metal substituted isocyanide of ~1.8 kK. This value is very similar to water. That Dq is reduced from ~2.2 - 2.5 kK in the ammine end of $(NH_3)_5CoCNCo(CN)_5$ to ~1.8 kK in the cobaltcyano end of Fe(II)-CN-Co(III) is not disturbing Similar occurrences have been noted elsewhere upon going from an ammine series to a cyano series. [23b]

Conclusion

The rather straightforward way in which the μ-cyano compounds are assignable as superpositions of their component parts seems to indicate only very minor interaction between metal centers via the π

bridge. The same can be said of the superoxo and peroxo compounds. It should be noted that even the superoxo complexes, with unpaired spin density on the bridging π system, fail to perturb the ligand field transitions of the metals.

We will now proceed to look at the μ-pyrazine ruthenium system, a system also possessing an unpaired spin. Here, apparently, the unpaired electron is no longer located exclusively on the bridge. It will be shown that delocalization present in this binuclear ruthenium species has important effects on its ESR and electronic spectrum. Only its magnetic susceptibility will be interpretable by treating the dimer as a normal tetragonally distorted d^5 monomer.

CHAPTER 2. ELECTRONIC STRUCTURAL STUDIES OF PYRAZINE BRIDGED RUTHENIUM DIMERS

Introduction

In 1969, Creutz and Taube[43] synthesized the 4+, 5+, and 6+ salts of μ-pyrazinedecaamminediruthenium. The 5+ cation in this series was found to exhibit an unusually intense band in the near IR region at ~1570 nm. The intensity of this band was suggestive of a charge transfer transition. Ruthenium, however, is known to have metal → ligand and ligand → metal charge transfer excitations at much higher energies.[88, 58] Similarly, all the intraligand transitions of pyrazine occur $\gtrsim 30,000$ cm^{-1}.[45] The only remaining type of charge transfer transition which could occur at low energies would be the Ru(II)Ru(III) → Ru(III)Ru(II) excitation. This last possibility was, in fact, the way Taube and Creutz[43] assigned the 6400 cm^{-1} band.

Although this assignment postulated ruthenium atoms in two distinct oxidation states, there was no a priori certainty that such was actually the case. For the 5+ cation, a number of other formulations are possible. First, one could consider the dimeric cation to be made up of an anionic pyrazine bridging two identical Ru(III) metal atoms. This would be analogous to the current description of the μ-superoxodecaamminedicobalt(III) ion.[10] This anionic bridge formulation itself could be considered to consist of two different subformulations. The three unpaired electrons could either be an extensively coupled system, or an essentially non-interacting system. The cation may also be described as consisting of two equivalent

$Ru(II\frac{1}{2})$ metals. This equivalence would easily come about if electron transfer between metals is very rapid.

Subsequent to the appearance in the literature of the ruthenium pyrazine dimer, a second case of a near IR transition in a stable mixed valent dimer was reported. This time, biferrocene picrate, a salt containing Fe(II) and Fe(III) bridged by a bicyclopentadiene moiety, was found to have a transition at 1900 nm.[46] Again, the near IR transition was interpreted in terms of an intermetallic transition, i.e., Fe(II)Fe(III) → Fe(III)Fe(II). Alternative formulations, analogous to those postulated above for the ruthenium dimer, could also be proposed for the biferrocene dimer.

Because the low energy transitions in both the iron and ruthenium dimers have been interpreted as an electron transfer from one metal center to another, one can calculate rates of electron transfer using the theory developed by Marcus and Hush.[47, 63] Intervalence transfer absorptions found in mixed valence solid lattices and in mixed valence dimers formed in solution have already been treated in this manner.[48] The ruthenium-pyrazine dimer, as well as the biferrocene dimer, however, are unique systems for testing this theory. They alone are known to be stable dimeric units in both the solid state and in solution. They alone should be unencumbered with extended lattice effects and solution equilibria complications.

With all this in mind, we set out to determine the electronic structure of the ruthenium dimers especially the 5+ ion. In particular, we wanted to verify the charge transfer nature of the low energy transition. We also wanted to determine which of the above formulations

for the 5+ species was correct. And finally, in keeping with our general objective, we wanted to see if there were any discernible metal-metal interactions via the π bridge.

Experimental

Compounds and Electronic Spectral Measurements

All the complexes under investigation here were analyzed samples kindly furnished by Professor Henry Taube and Dr. Carol Creutz of Stanford University. Electronic spectral measurements were made on KBr pellets, and in 9:10 $MgCl_2$:H_2O glass forming mixtures. The $MgCl_2 \cdot 6H_2O$ used was Baker reagent grade. Mallinckrodt reagent grade often contained impurities which inhibited glass formation. Measurements were carried out as described elsewhere in this thesis.

ESR Measurements

ESR measurements at X-band (~ 10 GHz) were carried out on a Varian 4502 spectrometer employing 100 Kc field modulation, and a nine inch Varian electromagnet with Fieldial. This system was equipped with a V-4532 Dual Sample Cavity. Microwave frequencies were measured using a wave meter attached to one arm of the "Magic Tee" detection system. The field was calibrated using a standard sample of solid diphenylpicrylhydrazine (K and K Chemical Comp.) placed in the rear compartment of the dual cavity assembly. The DPPH signal was detected using a low frequency (20-400 cps) modulation detector system. This measurement was carried out simultaneously on all spectra. Cooling samples to obtain LN_2 temperatures was achieved by passing a stream of pure nitrogen gas

through a liquid nitrogen heat exchanger, and then leading it through a small quartz dewar which sat in the ESR cavity and held the sample tube.

Magnetic Measurements

Magnetic susceptibilities were determined using a Princeton Applied Research FM-1 vibrating sample magnetometer fitted with a liquid helium dewar obtained from Andonian Associates, Inc. Liquid nitrogen from a reservoir above the instrument is allowed to drop slowly through a capillary tube onto the floor of the sample compartment, where it vaporizes to produce a stream of cold gas, which in turn flows past the sample. The temperature is regulated by the nitrogen flow rate and by heating coils located in the compartment walls. Temperature is monitored by a copper-constantan thermocouple, located in the compartment wall near the sample. If sufficient time is allowed for equilibrium to be established, temperatures can be read to within less than 3°K over the temperature range measured. Measurements were not made at lower temperatures, because the age of the thermocouple prevented accurate measurements at these lower °K. The diamagnetism of the nylon sample holder was corrected for by using diamagnetic readings obtained on the holder alone. Calibration constants for the instrument were obtained using $CuSO_4 \cdot 5H_2O$ as a calibrant. The magnetic field used during these measurements was 10,000 Oersteds.

Infrared Measurements

Infrared spectra were taken using potassium bromide and cesium iodide pellets on a Perkin-Elmer 225 grating infrared spectro-

meter. When KBr discs were used, blanks were used in the reference beam. When CsI was used, measurements were made versus air. Low temperature measurements were made using a VLT-2 variable temperature unit manufactured by Research Industrial Instruments Company of London, England, and purchasable from Beckman Instruments, Inc. This unit was equipped with KBr windows which precluded scans below 400 cm^{-1}.

Results and Discussion

Magnetic Susceptibilities and Electron Spin Resonance

The magnetic susceptibilities for the 5+ tosylate and 6+ perchlorate salts are listed in Table II-1. The μ_{eff} versus temperature curves of both salts together with some reference Ru(III) compounds are shown in Figures II-1 and II-2. As expected, χ for both dimeric ions varies little with temperature because of the large spin-orbit coupling constant of trivalent ruthenium.[50] The $Ru(NH_3)_6{}^{3+}$ curve in Figure II-1 was taken from measurements made here. It agrees well with the reported literature values.[50] Both bridged cations fail to follow the Curie-Weiss law. More unsatisfactory, however, is the sharp deviation from linearity below 150°K exhibited by the 5+ cation. This last fact can be explained by attributing the increased paramagnetism at lower temperature to the presence of 6+ impurity. Another possible cause of the observed deviation is the large diamagnetic correction for the tosylate anion. At lower temperatures, this correction becomes a very large fraction of the total paramagnetism observed in the one spin II-III system. In a two spin system like the III-III case, this correction is proportionately smaller.

Table II-1

χ_g vs. T for $[\![Ru(NH_3)_5]\!]_2\ \underset{\hexagon}{N\bigcirc N}{}^{5+,\,6+}$

Temperature (°K)	5+ Tosylate	6+ Perchlorate
299	1.000×10^{-6} cgs	3.208×10^{-6} cgs
288.4	1.036	3.271
278.3	1.065	3.360
268	1.010	3.431
257.4	1.142	3.505
246.5	1.514	3.625
235.2	1.255	3.747
223.6	1.326	3.886
211.6	1.420	4.061
199.1	1.503	4.249
186	1.616	4.503
172.2	1.770	4.798
157.6	1.952	5.176
149	2.062	5.415
142	2.198	5.677
133.8	2.355	6.009
125.1	2.563	6.400
115	2.694	6.935
106.4	3.148	7.614
101	3.394	7.988
96	3.648	8.532
Diamagnetic correction (cgs/mole)	699×10^{-6}	398×10^{-6}

Figure II-1. $\mu_{eff/metal}$ vs. temperature
curves for the 5+ tosylate salt and some reference compounds.

OOOO - 5+ tosylate

●●●● - $Ru(NH_3)_6 \cdot Cl_3$
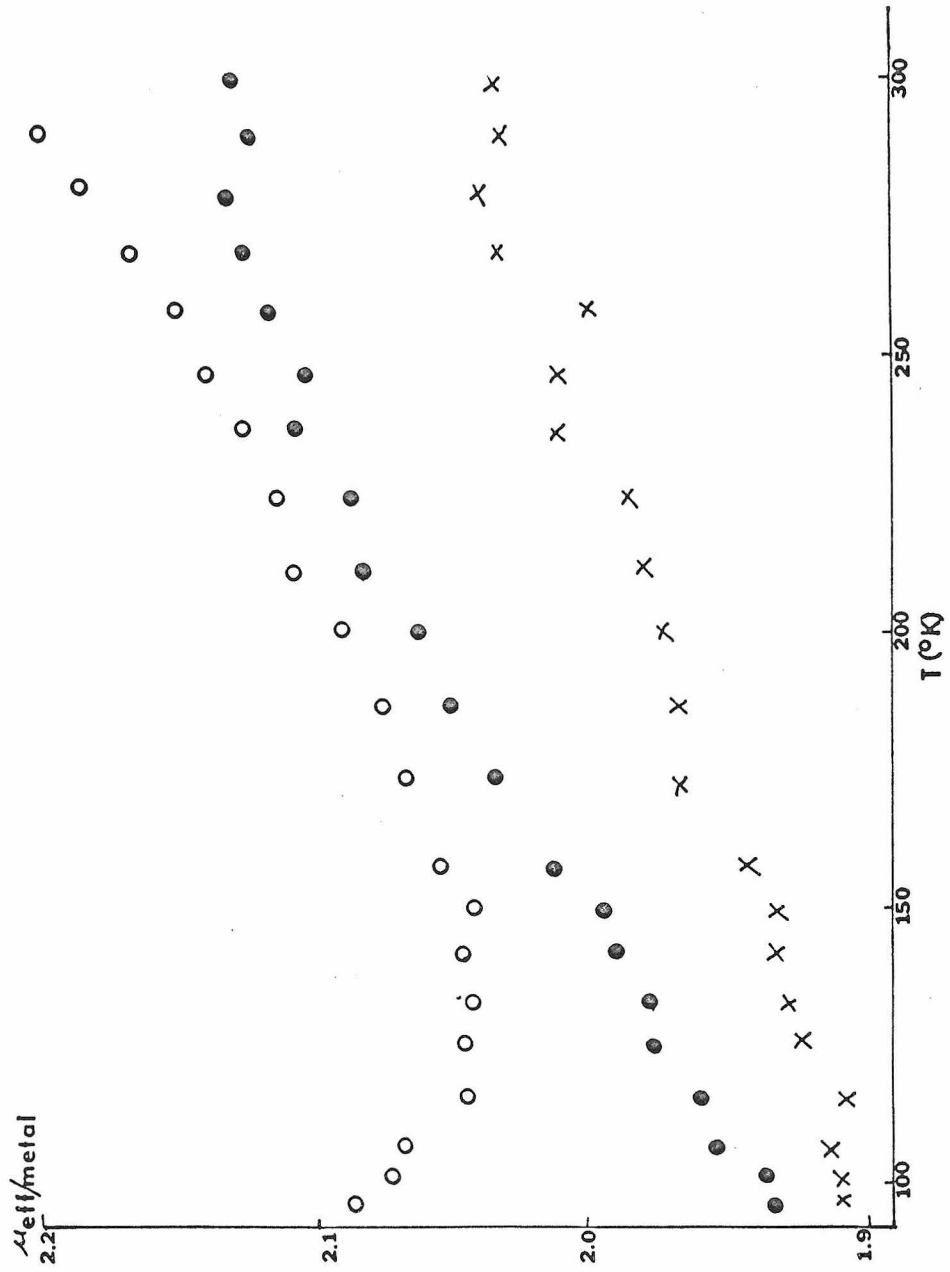
×××× - $K(RuH_2EDTACl_2)$

Figure II-2. $\mu_{eff/metal}$ vs. temperature
curves for the 6+ perchlorate salt and some reference compounds.

OOOO - 6+ perchlorate

●●●● - $Ru(NH_3)_6 \cdot Cl_3$

×××× - $K[RuH_2EDTACl_2]$
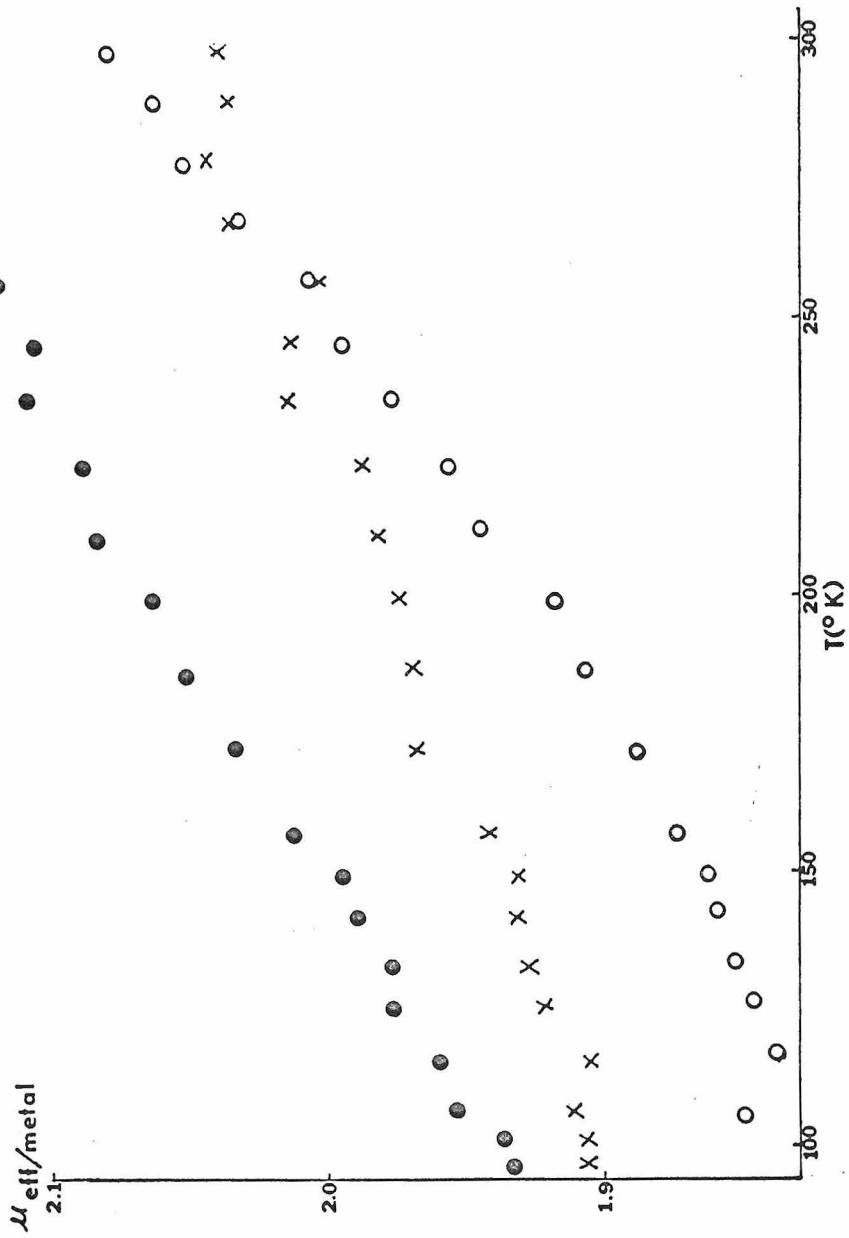
From the curves in Figure II-1, a description of the 5+ species as anionic pyrazine bridging two Ru(III) ions is untenable. Such a formulation reasonably can be expected to give a room temperature moment in the range of 3.5 - 5.0 B.M. The room temperature value of 2.23 B.M. is, however, in excellent agreement with that reported for other Ru(III)(NH$_3$)$_5$X complexes.[50] The simplest interpretation of the magnetic data involves a mixed valence structure Ru(II)-Ru(III) for the compound. Our results are in agreement with magnetic measurements on the Fe(II)-Fe(III) biferrocene system.[51] There, too, the magnetism indicates a relatively normal Fe(III) ion. The possibility of a formulation containing two Fe(III) ions, bridged by a bicyclopentadiene holding the odd electron, is correspondingly reduced. Similarly, the room temperature moment of our 6+ dimer, 2.92 B.M., supports a species made up of two equivalent Ru(III) ions.

An ESR signal from the 5+ cation was observed at room temperature and is presented in Figure II-3. Going to 77°K failed to significantly increase resolution. All spectra were taken using polycrystalline samples. The 5+ (as well as 6+) cation was found to be sufficiently insoluble in ethanol or acetonitrile ($< 10^{-4}$ M) to make observation of a solution spectrum impossible.

As seen from Figure II-3, the 5+ spectrum looks very much like an ordinary two g value spectrum.[52] If this is true, we have here a g$_\perp$ = 2.32, and a g$_{||}$ = 2.04. The fact that a signal can be seen at room temperature is, in itself, unusual. Most, if not all, Ru(III) species studied to date do not show any ESR signal until the temperature is 80°K or lower. Even at 77°K, most signals are broad unless the

Figure II-3. 77°K ESR spectrum of a
polycrystalline sample of the 5+ tosylate salt.

2895G

3182G

3269G

3344G
DPPH
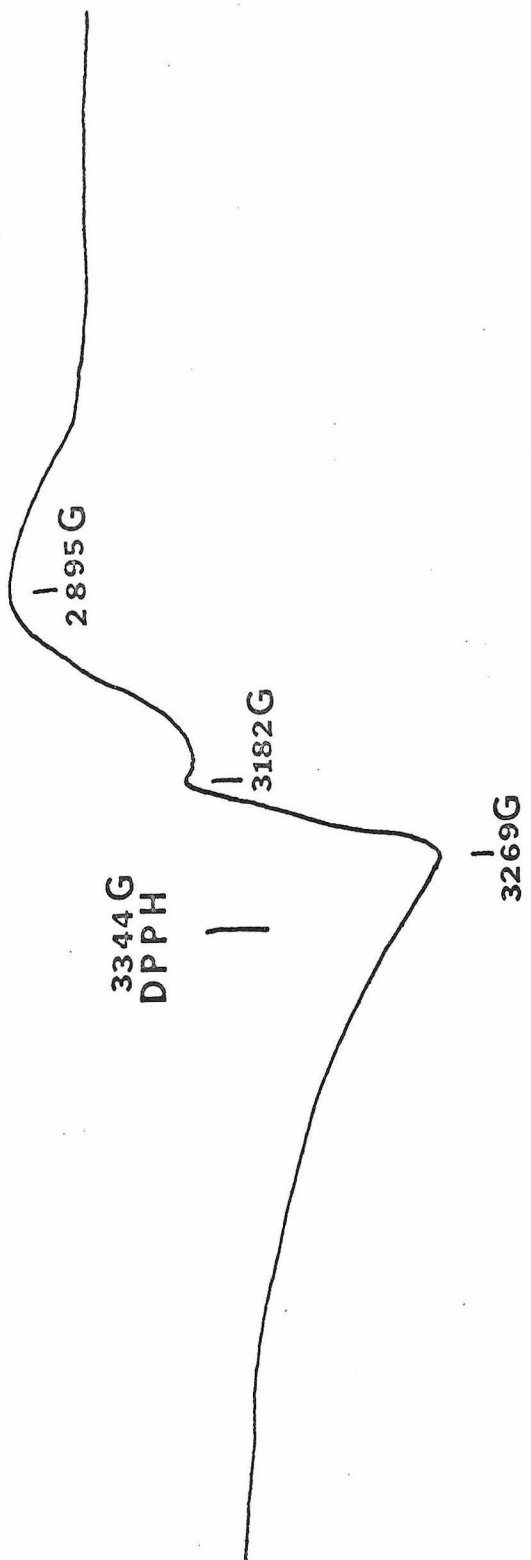
Ru(III) ion is doped in a diamagnetic lattice. Undiluted $Ru(NH_3)_6Cl_3$

powder has a $\langle g \rangle \sim 1.94$, while $Ru(NH_3)_6^{3+}$ doped in $Co(NH_3)_6Cl_3$ has

$g_{\parallel} = 1.72$, $g_{\perp} = 2.04$.[53] The only other Ru(III) ESR spectra reported

are doped crystals of K_3RuCl_6[49] and $Ru(acac)_3$,[54] as well as Ru(III)

diluted in Al_2O_3.[18] All give signals only at low temperatures. The

hexachloride has a $g_z = 3.2$, $g_x = 1.0$, $g_y = 1.2$. The trisacac has a

$g_{\parallel} = 2.82$, $g_{\perp} = 1.52$. The fact that a signal from the 5+ cation can be

observed at room temperature implies that the ground state may not

be simply described as a normal Ru(III) system. The signal observed

could indicate an important contribution to the ground state from the

structure $Ru(II)$-pyrazine$^+$-$Ru(II)$.

The 6+ cation shows no signal at room temperature. Looking at

polycrystalline samples at LN_2 temperatures reveals a narrower, but

still broad, signal centered at $g \sim 2.51$ (Figure II-4). The fact that

one needs to go to lower temperatures upon going from the 5+ to 6+

ion could possibly be interpretable as arising from a small spin-spin

interaction between d^5 metal centers.

In both the III-III and III-II spectra, no evidence of hyperfine

structure was noted even at low temperatures. In the 5+ salt, one

could reasonably expect hyperfine structure at least from the pyrazine

nitrogens. The ESR signal is so broad, however, that a moderate

hyperfine interaction would escape detection.

<u>Theoretical Treatment of the Magnetism and g-values</u>

Both the 5+ and 6+ cations can be considered to be tetragonally

distorted Ru(III)(d^5) species, and can be analyzed accordingly.[50]

Figure II-4. 77°K ESR spectrum of a polycrystalline sample of the 6+ perchlorate salt.

2506 G

2625G
g = 2.50₄

2780 G
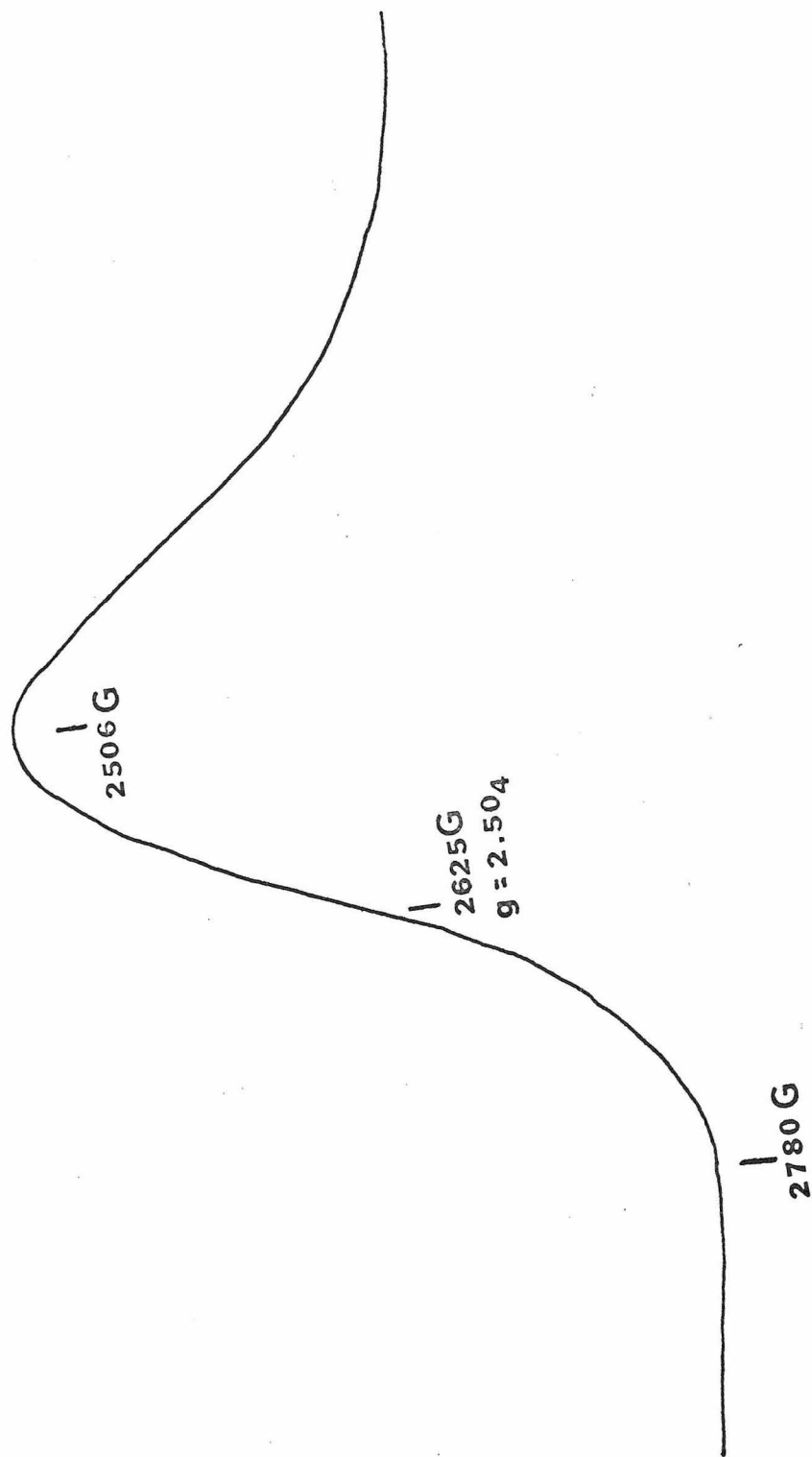
If an axial ligand field is applied to a $^2T_{2g}$ term (neglecting spin-orbit coupling), two components, ^2E and $^2B_2$, are generated. These are separated by an energy δ, which is considered positive when $^2B_2$ is lower. If both the axial field and spin-orbit coupling, $H_{s.o.} = \lambda L \cdot S$, are applied together, the $^2T_{2g}$ term splits into three Kramer's doublets with energies [55]:

$$\epsilon_1 = \frac{1}{2}(\delta + \frac{\lambda}{2} + \zeta),$$

$$\epsilon_2 = \frac{1}{2}(\delta + \frac{\lambda}{2} - \zeta),$$

$$\epsilon_3 = (\delta - \frac{\lambda}{2}),$$

$$\text{where } \zeta^2 = \delta^2 + \lambda\delta + (\frac{9}{4})\lambda^2.$$

The corresponding eigenfunctions are

$$\phi_1 = \{\cos\theta_1 [\frac{1}{\sqrt{2}}(|2, \frac{1}{2}\rangle - |-2, \frac{1}{2}\rangle)] + \sin\theta_1 |-1, -\frac{1}{2}\rangle\}$$

$$\phi_2 = \{\cos\theta_2 [\frac{1}{\sqrt{2}}(|2, -\frac{1}{2}\rangle - |-2, -\frac{1}{2}\rangle)] + \sin\theta_2 |1, \frac{1}{2}\rangle\}$$

both with energy ϵ_2

$$\phi_3 = |1, -\frac{1}{2}\rangle$$

$$\phi_4 = |-1, \frac{1}{2}\rangle$$

both with energy ϵ_3

$$\phi_5 = \{\sin\theta_1 [\frac{1}{\sqrt{2}}(|2, \frac{1}{2}\rangle - |-2, \frac{1}{2}\rangle)] - \cos\theta_1 |-1, -\frac{1}{2}\rangle\}$$

$$\phi_6 = \{\sin\theta_2 [\frac{1}{\sqrt{2}}(|2, -\frac{1}{2}\rangle - |-2, -\frac{1}{2}\rangle)] - \cos\theta_2 |1, \frac{1}{2}\rangle\}$$

both with energy ϵ_1

and where $\tan 2\theta_1 = (2\sqrt{2}\,\lambda)/(2\delta + \lambda)$

$$\tan 2\theta_2 = (-2\sqrt{2}\,\lambda)/(2\delta + \lambda)$$

The magnetic susceptibility is then found by applying the Van Vleck formula for a Boltzmann distribution over closely spaced energy levels.[56] The Zeeman perturbation used is given in the form $H = (kL + 2S)\beta$, as suggested by Figgis,[50] where k is a measure of the electron delocalization.[20] In our case, the Van Vleck equation was not solved explicitly for λ, δ, and k. Instead, a program written by Dr. D. F. Gutterman at Caltech was used, in which various values for the three parameters were selected on a trial and error basis.[21] Calculated values of μ_{eff} were then compared with the experimental values. The set of parameters which minimized

$$\Sigma = \sum_{i=1}^{n} \left(\frac{\mu_i^{expertl} - \mu_i^{calc}}{\mu_i^{expertl}} \right)^2$$

was taken as the best fit.[21]

The best fit for the 5+ tosylate occurred when $\delta = 500$ cm^{-1}, $\lambda = -425$ cm^{-1}, k = 0.85. For these parameters, $\frac{1}{n}\Sigma = 5.77 \times 10^{-4}$ where n = 21, which includes readings down to 96°K. To give an idea of the sensitivity of the curves, the data were fit nearly as well with curves calculated with δ between 500 and -500 cm^{-1}, λ between -375 and -450 cm^{-1}, and k between 0.85 and 0.9. Interestingly, curves which were fit to our data down to 150°K (n = 14) gave almost the same best fit parameters ($\delta = 500$ cm^{-1}, $\lambda = -500$ cm^{-1}, k = 0.85, $\frac{1}{n}\Sigma = 3.5 \times 10^{-5}$) as the data down to 96°K, n = 21. In both fits, all points

down to 125°K are within 2% of experimental, and, in most instances, within 1%.

Unfortunately, a second very good minimization occurs at $\delta = -5000$ cm^{-1}, $\lambda = -1100$ cm^{-1}, k = 1.0. Although the residual is actually smaller with these parameters, the unusually large value of δ, as well as a large unreduced λ, makes this choice of parameters much less likely.

That a $\delta = -5000$ cm^{-1} is too large may be argued as follows. It has been shown that $Dq = f_{lig} \cdot g_{metal}$, where f and g are constants determined for a given ligand and metal respectively.[58] In RuCl$_6^{3-}$, $Dq = 2400$ cm^{-1}.[59] Using the $f(Cl^-) = 0.8$ of Jorgensen,[58] we get a $g(Ru(III)) = 3000$ cm^{-1}. Now assume a very large tetragonal distortion, much larger than in our pyrazine ammonia case, a case like the hypothetical Ru(NH$_3$)$_5$CN^{2+} species. We obtain

$$Dq^{z+} = Dq(CN^-) = f(CN^-)g(Ru(III)) = 1.7\,(3000)$$
$$= 5100 \text{ cm}^{-1}$$

$$Dq^{xy} = Dq(NH_3) = f(NH_3)g(Ru(III)) = 1.25\,(3000)$$
$$= 3750 \text{ cm}^{-1}$$

Now,

$$Dt = \frac{2}{7}(Dq^{xy} - Dq^{z+}) = \sim420 \text{ cm}^{-1}$$

Since $Ds \sim 3Dt$, we have $Ds \sim 1300$ cm^{-1}. It has been shown[25] that in a tetragonally distorted d^5 system

$$\delta(^2E - {}^2B) = 3Ds - 5Dt,$$

which here gives a $\delta \sim 1700$ cm^{-1}. In our case of an ammonia

octahedron distorted by the substitution of pyrazine, δ should not be anywhere near this large. Hence $\delta = 500$ cm^{-1} is a much better choice than $\delta = -5000$ cm^{-1}.

For the 6+ perchlorate salt, a best fit is obtained at about $\delta = 0$ cm^{-1}, $\lambda = -850$ cm^{-1}, $k = 0.9$. Here, $\frac{1}{n}\sum = 1.8 \times 10^{-3}$ for $n = 21$. Almost as good a minimization can be achieved with a δ from 250 to -250 cm^{-1}, a λ from -900 to -700 cm^{-1}, and a k from 0.85 to 0.9. Again, the curve fits each data point down to 115°K to within 1%. The calculated curves are shown in Figures II-5 and II-6.

The best parameters are listed in Table II-3, along with similar parameters from the literature[50] for comparison with other low spin Ru(III) compounds. When we examine this table, we see that assuming a choice of $\delta = 500$ cm^{-1} for the III-II salt, we have quite reasonable results. A k = 0.85 indicates greater delocalization in this mixed valence salt than in either the hexaammine, chloropenta-ammine, or chlorobipyridyl complexes, a result which may have been qualitatively predicted. Similarly, $\lambda = -425$ cm^{-1}, while very much reduced from λ_0, is also lower than bipyridyl. Since λ/λ_0 should decrease as k decreases, according to Figgis,[50] our results move in the right direction upon going to pyrazine as a ligand. Figgis[50] points out that δ can at best be obtained to ± 250 cm^{-1} from experimental measurements. Therefore, nothing of real import can be concluded for the III-II ion having a $\delta = 500$ cm^{-1}.

Table II-2

Calculated χ_g vs. T for $[Ru(NH_3)_5]_2$ ⬡ $^{5+, 6+}$

Temperature (°K)	5+ tosylate[a]	6+ perchlorate[b]
299	2103×10^{-6} cgs	1808×10^{-6} cgs
288	2163	1849
278	2223	1892
268	2288	1938
257	2359	1989
247	2437	2046
235	2524	2110
224	2621	2183
212	2730	2266
199	2856	2363
186	3004	2479
172	3182	2620
158	3402	2795
149	3550	2915
142	3684	3023
134	3858	3164
125	4067	3334
115	4348	3564
106	4630	3793
101	4831	3957
96	5037	4126

[a]Parameters used: $\delta = 500$ cm^{-1}, $\lambda = -425$ cm^{-1}, k = 0.85.

[b]Parameters used: $\delta = 0$ cm^{-1}, $\lambda = -900$ cm^{-1}, k = 0.9.

Figure II-5. A plot of $\mu_{eff}^{(calc)}$ (xxx) and $\mu_{eff}^{(exper)}$ (OOO) vs. temperature for the 5+ cation.
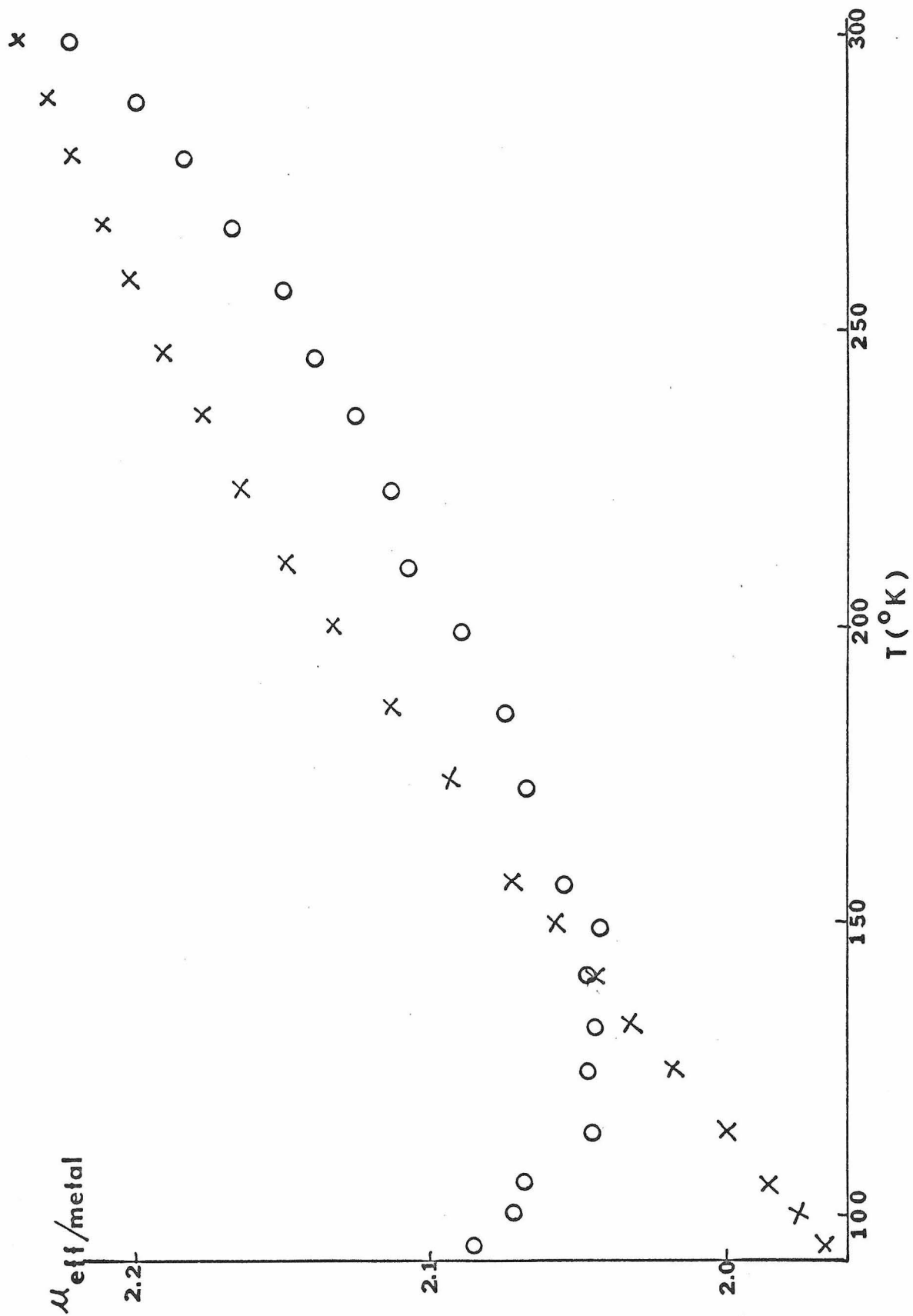
Figure II-6. A plot of $\mu_{\text{eff}}^{(\text{calc})}$ ($\times\times\times$) and $\mu_{\text{eff}}^{(\text{exper})}$ ($\bigcirc\bigcirc\bigcirc$) vs. temperature for the 6+ cation.
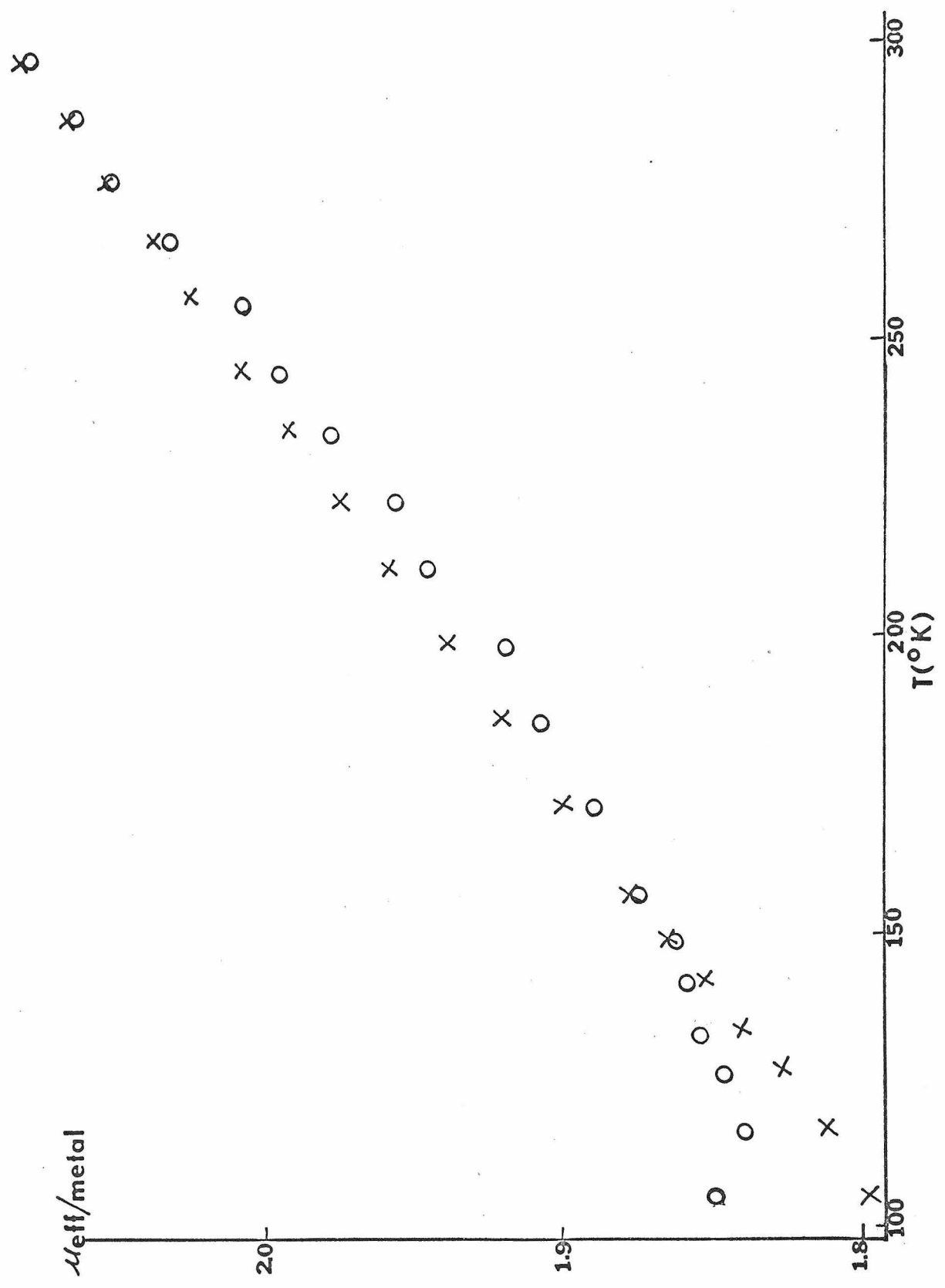
Table II-3

Values of the Parameters Used to Describe the

Magnetic Behavior of Some Low Spin Ru(III) Compounds

	k	δ/λ	λ (cm^{-1})	λ/λ_0[b]	δ (cm^{-1})	$\mu_{eff}(300\,^\circ K)$
$[Ru(NH_3)_5]_2NON^{5+}$	$\Big\{\begin{array}{l}0.85\\1.0\end{array}$	$\begin{array}{l}1.17\\4.54\end{array}$	$\begin{array}{l}-425\\-1100\end{array}$	$\begin{array}{l}0.36\\0.93\end{array}$	$\begin{array}{l}500\\-5000\end{array}$	2.23
$[Ru(NH_3)_5]_2NON^{6+}$	0.9	0.0	-850	0.72	0	2.08[c]
$Ru(NH_3)_6^{3+}$ [a]	1.0	0.0	-1000	0.85	0	2.14
$Ru(NH_3)_5Cl^{2+}$ [a]	0.9	0.0	-600	0.50	0	2.24
$Ru(bipy)Cl_4^-$ [a]	0.9	0.0	-550	0.50	0	2.31
$Ru(acac)_3$ [a]	0.7	+5.0	-1000	0.85	-5000	1.91

[a]From reference 50. [b]λ_0, the free ion value of λ for Ru^{3+} is taken as -1180 cm^{-1}; see reference 50.

[c]μ_{eff}/metal.

Moving to the III–III salt, we see that delocalization has decreased relative to the III–II cation. λ/λ_0, however, moves in the correct direction, in that it increases from 0.36 to 0.72. Why this should happen at all is not clear. Perhaps it indicates the crudeness of the calculation itself, in that it neglects spin-spin interaction in a $d^5 - d^5$ system. Alternatively, the results may be rationalized as follows. Delocalization actually decreases in the 6+ salt because the first electronic excitation causes Ru(III)Ru(III) $\rightarrow$ Ru(IV)Ru(II) to take place. These two states, being very different electronically, do not mix to any appreciable extent. Consequently, delocalization will be reduced.

From the matrix elements $\langle \phi_i | kL + 2S | \phi_j \rangle$ calculated in our program, one can directly abstract approximate g-values.[55] The g-values for the wavefunctions used can be shown to be

$$g_z = 2[1 - \sin^2 \theta (k + 2)] \qquad \phi_{1,2}$$

$$g_z = 2[k - 1] \qquad \phi_{3,4}$$

$$g_z = 2[(k + 2) \sin^2 \theta - (k + 1)] \qquad \phi_{5,6}$$

$$g_{x,y} = 2[\cos \theta_1 \cos \theta_2 + \frac{k}{\sqrt{2}} (\cos \theta_1 \sin \theta_2 - \sin \theta_1 \cos \theta_2)] \phi_{1,2}$$

$$g_{x,y} = 0 \qquad \phi_{3,4}$$

$$g_{xy} = 2[\sin \theta_1 \sin \theta_2 + \frac{k}{\sqrt{2}} (\cos \theta_1 \sin \theta_2 - \sin \theta_1 \cos \theta_2)] \phi_{5,6}$$

Using the following three sets of parameters

A, $\delta = 500$ cm^{-1}, $\lambda = -425$ cm^{-1}, $k = 0.85$,

B, $\delta = -500$ cm^{-1}, $\lambda = -375$ cm^{-1}, $k = 0.85$,

C, $\delta = -5000$ cm^{-1}, $\lambda = -1100$ cm^{-1}, $k = 1.0$,

it was found that only set A gave anywhere near a reasonable $\langle g \rangle$, a

$\langle g \rangle$ of 2.07. It did, however, predict another component of the g-tensor at a field near 6000 G, a region which we failed to scan. But, a second component of the g tensor at ~ 2.5 is well within a reasonable range, considering the crudeness of the calculation. Set C also gave a $\langle g \rangle > 2$, but it predicted a g_z of ~ 4. In this region (~ 1600 G), we found no evidence of a signal. For this reason, choosing the $\delta = 500$ cm^{-1} parameters is again probably more correct than the $\delta = -500$ cm^{-1} or $\delta = -5000$ cm^{-1} sets.

In addition to verifying that the axial splitting is best represented by a fit of $\delta = 500$ cm^{-1}, the g components arising from this parameter imply a ground state with the unpaired electron in the $\phi_{1,2}$ orbital. Using this set of parameters, we obtain a $\theta_1 = 328°$, and $\theta_2 = 32°$. This makes our ground state $\phi_{1,2}$ contain $\sim 67\%$ d_{xy} character, with the remaining 33% consisting of d_{xz}, d_{yz} character.

Electronic Spectra

The most interesting feature of the III-II ion's spectrum, as mentioned previously, is the unusually intense band found in the near IR, the band which Taube[43] assigned to the Ru(III)Ru(II) → Ru(II)Ru(III) electron transfer. To verify this assignment and eliminate any possibility of this band being a vibrationally augmented d-d excitation, we looked at the compound's spectrum at low temperature. KBr pellets were used because no suitable non-aqueous glass could be made. The oscillator strengths[60] found at 298°K and 77°K gave a ratio $\frac{f(298°K)}{f(77°K)} \sim 1.05 \pm 0.05$, implying that this is an orbitally allowed transition. The $\epsilon \sim 6500$ also suggests that the band is fully allowed.

Table II-4

Electronic Absorptions of Pyrazine

Bridged Decaamminediruthenium Compounds

(λ given in nm; ϵ in parentheses)

+4	+5	+6
	1570 ($\sim$6300)	
	sh $\sim$775 ($\sim$1200)	
550 (37500)	562 ($\sim$20000)	
		350 (2700)
		290 (3200)
$\sim$260 (16000)	$\sim$260 (14000)	$\sim$260

The other bands in the spectra of the 4+, 5+, and 6+ ions were found to be as reported previously (see Table II-3). All three species show the characteristic $\pi \rightarrow \pi^*$ pyrazine transition at 250 - 260 nm.[45] Reasoning from other diazine and triazine Ru(II) compounds, it has been shown[61] that the ~ 560 nm transition found in the 4+ and 5+ species arises from a $t_{2g} \rightarrow \pi^*$ (pyrazine) excitation. From our measurements, this band has an oscillator strength ratio of $\frac{f(298°K)}{f(77°K)} \approx 0.9 \pm 0.15$ in the 5+ system.

The shoulder at ~ 775 nm at 300°K in the 5+ cation sharpens at 77°K, becoming almost a peak with $\lambda_{max} \sim 775$ nm. At present, the assignment of this shoulder is uncertain. Since it is absent in both the II-II and III-III salts, it could be argued that it arises from the mixed valence nature of the 5+ cation.

The spectrum of the III-III cation can not be assigned definitively. Information, in general, on Ru(III) spectra is sparse. The bands in the 6+ dimer at 290 and 350 nm are very much like those found in $RuCl_6^{3-}$.[58] The bands in the hexachloride occur at 350 nm ($\epsilon \sim 2200$), and 310 nm ($\epsilon \sim 1700$). When ϵ/Ru is calculated for our complex, the 290 nm transition has an $\epsilon/Ru \sim 1600$, and the 350 nm transition has an $\epsilon/Ru \sim 1400$. The hexachloride transitions have been assigned to $\pi(Cl) \rightarrow t_{2g}^*$, and $\pi(Cl) \rightarrow e_g^*$ excitations.[58] An analogous assignment in our case does not fit as well.

A final problem remains in the spectrum of the 6+ salt. No evidence of a $t_{2g}^* \rightarrow \pi^*$(pyrazine) excitation exists, an excitation which theoretically should be observed. In the Ru(III) pyrazine monomer,[61]

this transition also appears to be absent, although there is a possibility of its being buried under the $\pi \rightarrow \pi^*$ intrapyrazine band. This $\pi \rightarrow \pi^*$ excitation shows an increased broadness when compared with the Ru(II) monomer, and may indicate the presence of the $t_{2g}^* \rightarrow \pi^*$ transition underneath. In the dimeric case, however, there does not appear to be any trace at all of this transition. Perhaps the 290 nm peak can be ascribed to the $t_{2g}^* \rightarrow \pi^*$ excitation.

Stability of the Dimers

In view of the literature's silence on the stability of these bridged complexes, we will summarize our findings on this point. First, the 5+ species is highly unstable in aqueous solution, a result not entirely·unexpected. After a period of two or three days, a deep violet solution was found to turn reddish-pink. The absorption maxima characteristic of the III-II ion steadily disappear, and the 360 nm and 290 nm absorptions of the 6+ complex grow. In fact, the appearance of the 360 nm peak begins only a short while after dissolution. No sign of the II-II ion is present in the final solution, as would be expected from a disproportionation mechanism.

More unsatisfactory is the fact that even when the solid phase is kept under N_2, one sees evidence of decomposition in the III-II compound over extended periods. For example, examining the ESR signal of the III-II compound over a long period, one sees a marked change in signal position and shape. The center of the signal moves to a g $\sim$ 2.5, and the shape broadens considerably, revealing a signal very much like, if not identical to, that exhibited by the III-III salt.

A sample of the 5+ ion reputedly analyzed at Stanford was examined using Weissenberg X-ray techniques immediately upon arrival here. Two different crystallographic space group patterns were discernible. One type of crystal possessed a triclinic space group; the second type showed a pattern with at least one mirror plane, indicating a space group belonging to the monoclinic class or higher. No determination of the exact group was possible because of extraneous reflections arising from imperfections in the crystal. Despite this irregularity, this sample of mixed crystals was used in our other studies because it possessed the electronic spectrum reported in the literature for the III-II system.

One can conclude from this that either, (1) the 5+ species can not be isolated in pure crystallographic form, or (2) that ceric nitrate potentiometric titrations fail to produce a clean product, or (3) that decomposition of a pure product begins almost immediately after isolation. This last interpretation is attractive when one remembers the ESR results.

After allowing the solid sample to stand for a few months, electronic spectra were retaken. This time, all three compounds showed peaks in the near IR (~1600 nm) in their pellet spectra. The 6+ ion showed the characteristic 560 - 570 nm peak of the 5+ (and/or 4+) salt. In the III-III case, decomposition was not complete; the III-III's 360 nm peak was still present long after the corresponding 5+ peaks first appeared. Only the 5+ species appeared to have the same spectrum over an extended period of time. Apparently, and

quite unexpectedly, when one considers these results vis-a-vis the results in aqueous solution, the 6+ ion is less stable than the 5+ ion. Perhaps the III-III dimer disproportionates into Ru(II) and Ru(IV) salts. This last possibility, however, could not be verified by electronic spectroscopy.

Rate of Electron Transfer

Creutz and Taube[43] estimated the rate of electron transfer between metal centers in the 5+ cation, using Marcus-Hush (MH) theory.[47] This theory predicts that the potential energy of an ion can be represented as a quadratic function in λ, the coordination sphere distortion. From this, it is easy to show that the Franck-Condon barrier of electron transfer from one metal to another is approximately 4 times the energy barrier between the ground state and that of the thermally activated complex for electron transfer (Figure II-7). By assuming the near IR band to be the Franck-Condon transition, a $\Delta G^{\ddagger}$ of 1600 cm^{-1} was obtained. Proceeding further, Creutz and Taube calculated a rate constant of 3×10^9 sec^{-1} when their $\Delta G^{\ddagger}$ was inserted into the classical Arrhenius rate expression.

Unfortunately, from our experimental results, it is apparent that this calculated rate of transfer is many orders of magnitude below the actual rate. This is not all that surprising once one remembers that MH theory was developed for outer-sphere mechanisms only,[63] and our mechanism is much closer to inner-sphere. Our ESR results, specifically the appearance of a signal at 300°K for the

5+ salt, suggests that the electron is either transfering at a rate $< 10^8$ sec^{-1}, or $> 10^{12}$ sec^{-1}. Any intermediate rate can be expected to give exchange broadening, and all evidence of a signal at room temperature will be eliminated. It should be noted that MH theory uses a classical rate expression with a pre-exponential factor $\propto \frac{kT}{h} \sim 10^{13}$ sec^{-1}.[57] This, then, is the upper bound to the rate calculable.

It is easy to theoretically justify the breakdown in MH theory. This theory assumes no metal-metal interactions. In our 5+ case, however, there is definite interaction. This has the effect of causing the potential energy curves in Figure II-7 to become more like those in Figure II-8. This energy gap between the curves, shown in Figure II-8, can be very crudely thought to arise from the non-crossing rule for states of the same symmetry.[65] It is this gap, with its concomitant lowering of $\Delta G^{\ddagger}$, which causes the rate to be much greater than that calculated from MH theory. The actual mechanism of electron transfer is still unclear. It may be due to an extra large increase in the rate of tunnelling because of the smaller barrier in Figure II-8, or to some "photocatalyzed" type of mechanism as yet poorly understood. Finally, the possibility exists that the barrier is non-existent and the 5+ ion has a symmetrical $(II\frac{1}{2}-II\frac{1}{2})$ ground state.

Experimental evidence is available for the existence of a rate of transfer $> 10^{13}$ sec^{-1}, possibly even $\sim 10^{15}$ sec^{-1}. ESCA experiments,[66] for example, have failed to discern two different Ru atoms, as would be expected if there are really distinct Ru(II) and Ru(III) metals present.[64]

Figure II-7. Potential energy vs. atomic configuration (λ) curves for an electron transfer between states with identical potential minima. Note $4\Delta G^{\ddagger} = \Delta E(\text{vertical})$. No interaction between states is assumed to be present.

$E_{3,2} = b(\lambda - 2_a)^2$

$E_{3,2}$

$E_{2,3} = b\lambda^2$

$E_{2,3}$

Potential energy

λ

$-\frac{1}{2a}$

$-\frac{1}{a}$

O
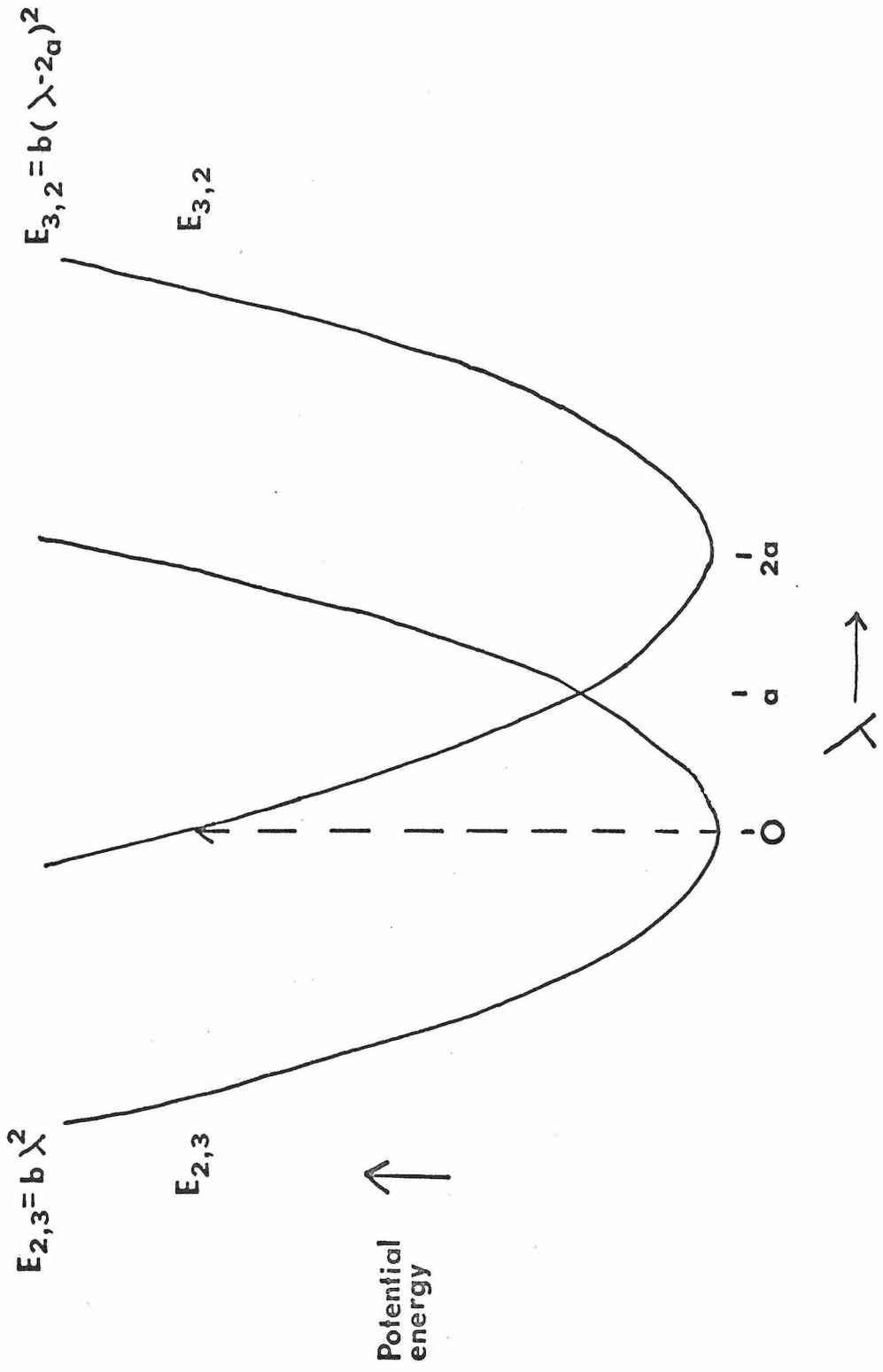
Figure II-8. Potential energy vs. atomic configuration (λ) curves for an electron transfer between states with identical potential minima. Weak interaction between states is assumed to be present.
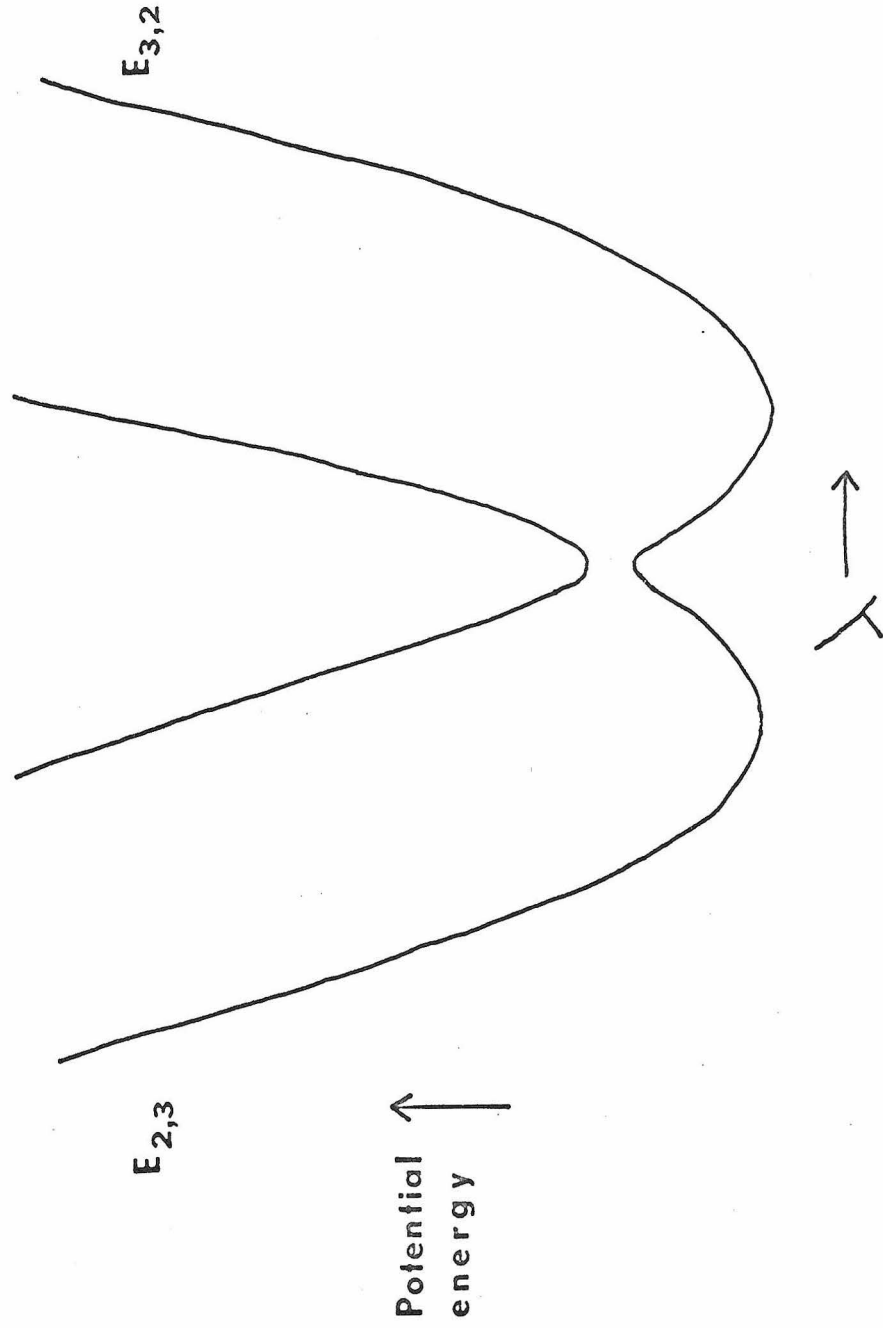
An infrared investigation of the asymmetric stretching mode of NH_3 also failed to reveal two different stretches, as would be expected from ammonia molecules attached to metal atoms with different oxidation states. In the asymmetric stretch region of Ru(III) hexaammine,[67] we find bands at 1362, 1338, 1316 cm^{-1}, while in the same region for Ru(II) hexaammine,[67] we find only a single band at 1220 cm^{-1}. In our mixed valence salt, there is a stretch located at 1280 cm^{-1}. This indicates very strongly that an electron transfer faster than the IR time scale of 10^{12} - 10^{13} sec^{-1} is taking place. Effectively, again a $II\frac{1}{2}$ - $II\frac{1}{2}$ formulation is suggested.

Although it is currently impossible to give the rate of electron exchange a definitive value (or even to say that an electron transfer "rate" exists), it may perhaps be instructive to examine complexes with various substituents on the rutheniums. This procedure should generate more asymmetric ground and excited states, and make it possible to define a II-III system experimentally.

An Alternative to the Taube-Creutz Formulation: A Delocalized Molecular Orbital Model for the 5+ Dimer

The molecular orbitals of pyrazine have been shown by Innes, et al. [93] to have the following order: $b_{3u}(\pi^b) < b_{2g}(\pi^b) < b_{1g}(\pi^b) < a_g(n) < b_{1u}(n^*) < b_{3u}(\pi^*) < a_u(\pi^*) < b_{2g}(\pi^*)$. The energies of excitation for the $a_g \rightarrow b_{3u}$, $b_{1g} \rightarrow b_{3u}$ and $b_{1g} \rightarrow a_u$ transitions are known to be 33.7, 38.2, and 51.6 kK, respectively. [93]

Using this sequence for pyrazine, the following approximate molecular orbital scheme for the 5+ complex can be derived:

π^b(pyrazine) $\gtrsim$ n $\sim$ n*(pyrazine) $<$ b_{3g}(yz-yz) $\sim$ b_{2u}(yz + yz) $\sim a_u$(xy - xy) $\sim$ b_{1g}(xy + xy) $<$ b_{3u}(xz + xz) $<$ b_{2g}(xz - xz) $<$ $a_u(\pi^*)$ $[b_{3u}(\pi^*)?]$.

The splitting of the b_{3u}(xz + xz) and b_{2g}(xz - xz) levels results from their interaction with the $b_{2g}(\pi^b)$ and $b_{3u}(\pi^*)$ pyrazine levels. Both of the heterocyclic levels are orbitals centered primarily on the ring nitrogens. In addition, the two xz ruthenium orbitals may mutually interact and destabilize the b_{2g}(xz - xz) antibonding combination even further. All levels up to and including b_{3u}(xz - xz) are completely filled. The b_{2g}(xz - xz) level contains a single electron. The ground state is $^2B_{2g}$. With the unpaired electron spread over a molecular orbital centered on both metal xz orbitals the best description of the dimer is one where the rutheniums possess identical oxidation states of $II\frac{1}{2}$.

The observed near IR band can now be explained as a b_{3u}(xz + xz) $\rightarrow$ b_{2g}(xz - xz) excitation. The large intensity observed for this excitation may arise from the self-overlap of metal xz orbitals.[94] This excitation should not be observable in the 4+ and 6+ species. In the 4+ cation, the b_{3u} and b_{2g} levels are both filled. In the 6+ complex, this transition would correspond to a spin-forbidden $(b_{3u})^1(b_{2g})^1 \rightarrow (b_{3u})^0(b_{2g})^2$ excitation.

The 560 nm transition could arise from a b_{2g}(xz - xz) $\rightarrow$ $a_u(\pi^*)[b_{3u}(\pi^*)?]$ excitation. The shoulder at $\sim$775 nm may be due to an orbitally forbidden charge transfer transition, b_{2g}, b_{1g} $(\pi^b$pyrazine) $\rightarrow$ b_{2g}(xz - xz). This is conjectural, however. Finally, the 260 nm band is the result of an excitation from b_{2g}, $b_{1u}(\pi^b) \rightarrow a_u[b_{3u}?](\pi^*)$ pyrazine levels.

The presence of only one kind of ruthenium atom in the ESCA experiments, as well as a single NH_3 stretch in the IR experiments, is now explicable in terms of the postulated $Ru(II\frac{1}{2})$-$Ru(II\frac{1}{2})$ ground state. From the accumulated data, it appears that a barrier such as depicted in Figure II-8 is virtually non-existent. Finally, the magnetic measurements indicate that a delocalized t_{2g} hole in the $Ru(II\frac{1}{2})$-$Ru(II\frac{1}{2})$ formulation is similar to a localized hole in a single $Ru(III)$ center.

A final piece of evidence exists for the 5+ dimer having similarly symmetrical ground and first excited states such as those we have postulated. The 1570 nm band has been found to show no solvent dependence.[66] This indicates that ligand reorganization is not extensive following the "transfer" (excitation) of the electron. This is contrary to what would be expected if states with only discrete $II(A)$-$III(B)$ and $III(A)$-$II(B)$ formulations were involved. A ground state with a symmetrical $II\frac{1}{2}$-$II\frac{1}{2}$ delocalized structure, together with a similar symmetric delocalized excited state like $^2B_{3u}$, could account for the failure to observe a solvent effect.

CHAPTER 3. THE CRYSTAL, MOLECULAR, AND ELECTRONIC STRUCTURE OF μ-NITROGEN-DECAAMMINEDIRUTHENIUM(II)

Introduction

Ten years ago, molecular nitrogen was described as an inert gas. In 1960, only the reaction of $N_2(g)$ with metallic lithium giving the nitride, Li_3N, was known to proceed under mild conditions. There were, however, intimations of a dormant reactivity in N_2. The well publicized, but hardly understood, fixation of atmospheric nitrogen by plants served as a constant source of speculation for chemists. Even then, it was thought that this facile conversion of N_2 into NH_3 was being effected by enzymes containing transition metal centers.[68]

In the subsequent ten years molybdenum and iron have definitely been identified as metals present at the active sites of plant enzymes used in the fixation process.[68] Equally important, the synthesis of transition metal compounds which bind molecular nitrogen has been achieved in the last five years. Currently, there are about 20 well characterized transition metal compounds which contain molecular N_2 as a ligand. These compounds contain a variety of transition metals, Ir, Co, Rh, Ru, Fe, Os, Ni, almost all in lower oxidation states.[69,70] As of yet, most of these synthetic compounds do not permit reduction of their molecular N_2 to NH_3 by common reducing agents. So far, only the titanium alkoxide/sodium napthalide/alcohol systems of van Tamelen,[71] and the titanocenyl dichloride/ethylmagnesium bromide

system of Vol'pin[72] have been found to abstract atmospheric nitrogen, which is reducible to ammonia. Nevertheless, the transition metal compounds having N_2 as ligands are still of major import. Even if reduction to NH_3 is unattainable at present, these compounds serve as models for the first step of the proposed fixation-reduction-protonation cycle for $N_2(g) \rightarrow NH_3(g)$ conversion.[68]

Of these compounds, $Ru(NH_3)_5N_2^{2+}$ is perhaps the most important, not only because it was the first one prepared, but also because it alone is made up of extremely simple auxiliary ligands, i.e., NH_3 rather than more complex ligands like phosphines. This compound was first prepared in 1965 by refluxing an aqueous solution of $RuCl_3$ and $N_2H_4 \cdot HCl$, and has subsequently been prepared in a number of different ways. It has been found to possess a $\nu(N-N)$ of $\sim 2100\text{-}2170$ cm^{-1} with variations ascribable to the anion present.[73]

In 1967, Harrison and Taube[74] found that equimolar amounts of $Ru(NH_3)_5N_2^{2+}$ and $Ru(NH_3)_5H_2O^{2+}$ condense quantitatively to give the dimer $(NH_3)_5RuN_2Ru(NH_3)_5^{4+}$. This was the first nitrogen dimer made. These two cations are easily distinguishable by their electronic absorptions; the monomer has a $\lambda_{max} = 221$ nm and the dimer a $\lambda_{max} = 263$ nm.

Itzkovich and Page[75] studied the monomeric and dimeric compounds, and found that both were very much more resistant to oxidation than normal Ru(II) pentaammine-X salts. Also perplexing was the fact that $Ru(NH_3)_5N_2^{2+}$ had such an unusually strong affinity for Ru(II)-H_2O, almost completely replacing the aquo group via nucleophilic attack, despite a 500 fold excess of water over Ru(II)-N_2.

This compound was not only perplexing, but important when viewed with the biological nitrogen fixation process in mind. It is thought that in plants, initial nitrogen binding is a result of entrapment between two metal centers (perhaps even atoms of different metals).[69] This fact makes the ruthenium dimer extremely important, and an understanding of its bonding necessary.

Because nitrogen has two π bonds, a number of alternate modes of bonding in the dimer are possible[69]:

$$M{-}N{\equiv}N{-}M$$

(A)

$$\begin{array}{c} M{-}N \\ \quad\quad\diagdown\diagdown \\ \quad\quad N{-}M \end{array}$$

(B)

$$\begin{array}{c} N{=}N \\ \diagup \quad\quad \diagdown \\ M \quad\quad\quad M \end{array}$$

(C)

$$M{-}{-}{-}\overset{\displaystyle N}{\underset{\displaystyle N}{\|\|\|}}{-}{-}{-}M$$

(D)

$$M'\diagup\,\overset{\displaystyle N}{\underset{\displaystyle N}{\|\|\|}}{-}{-}{-}M$$

(E)

$$\begin{array}{c} \overset{\displaystyle N}{\underset{\displaystyle N}{\|\|\|}} \\ \diagup \quad\quad \diagdown \\ M \quad\quad\quad M \end{array}$$

(F)
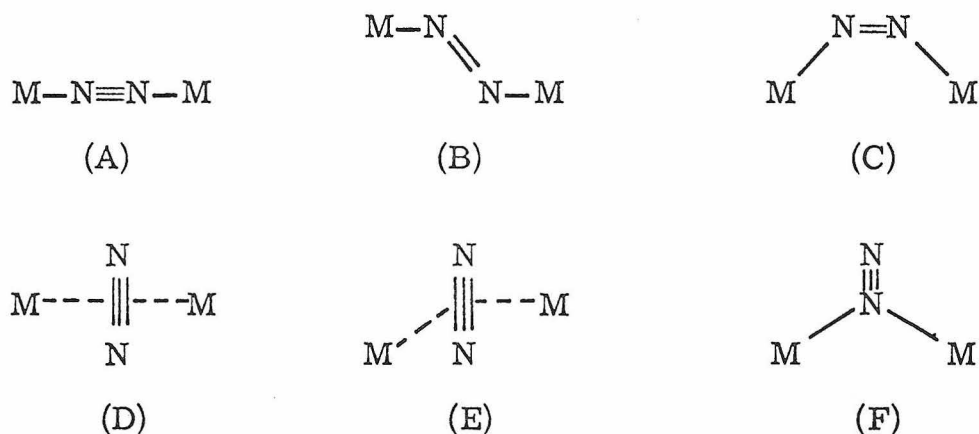
The dimer N—N stretch was known to be inactive in the infrared[74]; a structure without a center of symmetry such as (C), (E), and (F) could therefore be eliminated. Determination of the structure of the ruthenium monomer had already been attempted,[76] but because of disorder in the crystal, exact bond lengths could not be gotten. However, from the limited data obtained, the $M{-}N_2$ unit appeared to be linear. This information could not be used to extrapolate to the dimer. In the dimer, it could be argued, additional electronic density would be transferred from the second metal to the

bridging N_2 to produce a trans-azo structure (B). Such a structure, with rutheniums in a formal oxidation state of three, conceivably could explain the difficulty in oxidizing a supposedly Ru(II) dimer.

In addition to the question of the RuNNRu angle, the question of the N—N length in the dimer was important. It was reasoned that the back bonding from Ru d orbitals to the empty π^* orbital of N_2 was not very extensive, at least in the monomer, because the ν(N—N) in the monomer was reduced only about 150-200 cm^{-1} from the free N_2(g) value of 2331 cm^{-1}. The bond order here has to be almost three as in free N_2. Azo compounds with a formal bond order of two have N—N stretches in the 1500-1600 cm^{-1} region. Again, it could be argued that with an additional Ru atom, enough electronic density could be placed in the π^* orbital to reduce the bond order significantly and produce a structure like (B).

To answer the questions of bond angle and bond order, an X-ray structural determination of the ruthenium dimer was undertaken. In addition to its importance as a model for the intermediates in plant fixation of atmospheric N_2, the structure would aid in understanding the electronic absorptions of the dimer and monomer. These spectra are in themselves of interest because they would help in understanding the interactions of metals and π-acceptor ligands. The dimer is an important link in the class of binuclear compounds containing simple diatomic bridging ligands such as O_2^- and CN^-.

Experimental Section

The crystals used in our study were prepared by the procedure described in the literature.[74] A 0.05 M solution of $Ru(NH_3)_5Cl \cdot Cl_2$ (0.1 M in H_2SO_4) was reduced with Zn(Hg) under argon. After 50 min., the solution was separated from excess Zn. Nitrogen was bubbled in for 10 hrs., and the solution was then allowed to sit in a nitrogen-filled glove bag for another four days. The color changed from an initial dark blue to green and then finally to golden yellow. Following this, the solution was filtered in the absence of air into an excess of KBF_4. A few days later, small golden yellow octahedral crystals were found buried under an excess of fluoroborate. A number of these crystals were separated, washed with ethanol, mounted on glass fibers, and used for X-ray studies. These crystals exhibited an absorption at 262 nm, with an extinction coefficient of $\sim 4.8 \times 10^4$, a value which agrees with that found in the literature.[74]

Weissenberg photographs (CuKα radiation) of the hk0, hk1, and hk2 layers showed the systematic absences of the 0kℓ reflections with k = 2n + 1, h0ℓ reflections with ℓ = 2n + 1, and hk0 reflections with h = 2n + 1, confirming the space group as orthorhombic D_{2h}^{15} - P_{bca}. Unit cell constants were gotten by a least-squares fit of seven reflections, measured on an automated diffractometer. The dimensions obtained were a = 12.777(5), b = 15.531(6), c = 13.342(4)Å. The observed density obtained by flotation in a carbontetrachloride-1,2-dibromoethane mixture was 1.96 g/cm^3. This is in excellent agreement with the value of 1.97 g/cm^3 calculated for four dimeric cations, sixteen BF_4^- anions, and eight water molecules per unit cell.

In the P_{bca} space group, each dimeric cation must lie on a center of symmetry.

Intensity data were collected, using zirconium-filtered MoKα radiation. The crystal used was mounted with its body diagonal approximately parallel to the Φ axis of a Datex-automated General Electric XRD-6 diffractometer. Measurements were made using a θ-2θ scanning rate of 4° per minute. Background was counted for 30 seconds at the end of the scan. The scan range was 2° at low angles, and 4° at higher angles. An intense reflection, 408, was chosen as a check reflection, and measured every 20 reflections. During the period of data collection, about 8 days, this reflection remained constant to within 2 percent, indicating the lack of serious decomposition.

Of 3040 independent reflections, 2645 were calculated as greater than zero, and were used in the refinement of the structure. The 1490 reflection was deleted in the refinement because of an obviously false scintillation count.

Treatment of the Data

The value of the observed intensities, I_{obsvd}, were derived from the formula $I_{obsvd} = S - \frac{B_1 + B_2}{2} \left(\frac{t}{30}\right)$, where S is the scan count, B_1 and B_2 the two background counts, and t the scan time in seconds. Negative values of I_{obsvd}, calculated from the formula, were set equal to zero.

The standard deviation for each reflection was calculated using

$$\sigma_2(I_{obsvd}) = S + \frac{B_1 + B_2}{2} \left(\frac{t}{30}\right)^2 + (0.02S)^2.$$ The intensities and their

standard deviations were corrected for Lorentz and polarization

factors, but not for absorption. The standard deviations calculated

in this way were the basis for the weights used in the least squares

refinement.

Determination and Refinement of the Structure

The approximate coordinates of the ruthenium atoms were

easily found from a three-dimensional sharpened Patterson map.

A structure-factor calculation using these coordinates gave an

R index of 0.42 $\left(R = \frac{\Sigma \left| F_o \right| - \left| F_c \right|}{\Sigma \left| F_o \right|}\right)$. An electron density map quickly

revealed all the other non-hydrogenic atoms. After four cycles of

full matrix least-squares, varying in a single matrix the scale factor,

the positional parameters for all non-hydrogen atoms, anisotropic

temperature factors for the ruthenium atoms, and isotropic temperature

factors for all the other atoms, the R index was reduced to 0.17.

Introducing anisotropic temperature factors for all non-hydrogenic

atoms into a subsequent least-squares calculation (163 parameters)

brought R down to 0.099.

At this point in the refinement, difference maps were

calculated in the planes where the ammine hydrogens were expected.

No distinct peaks appeared; rather smeared out rings of electron

density were present. A number of different choices for each hydrogen

were tried. The one giving the most satisfactory distances and angles

was used. Computations showed that a preferential orientation, due

to hydrogen bonding between the ammino hydrogens and the BF_4^- fluorines, was not present, and therefore the smeared out rings on the difference maps were reasonable. The water hydrogens were placed on lines connecting the oxygen with their nearest fluorine neighbors, at what is the usual OH distance. The hydrogen coordinates, together with their isotropic temperature factors, were varied in a least-squares cycle. Together with the previously refined coordinates and anisotropic factors of the non-hydrogen atoms, they produced a final R of 0.090. In this least-squares cycle, 154 parameters were refined. The final weighted R index was 0.013. The goodness of fit, $[\Sigma w(F_0^2 - F_c^2/k^2)^2/(m - s)]^{\frac{1}{2}}$, where m is the number of reflections, s the number of refineable parameters, and k the scale factor, was 1.63.

Calculations were carried out on IBM 360-75 and IBM 7094 computers at the California Institute of Technology, using subprograms operating under the CRYM and CRYRM crystallographic computing system. The quantity minimized in the least-squares calculations was $\Sigma w(F_0^2 - F_c^2)$ where $w = 1/\sigma^2(F_0)^2$. Atomic form factors for ruthenium, nitrogen, oxygen, fluorine, and boron were taken from the "International Tables."[77] The form factor for hydrogen was that calculated by Stewart, Davidson, and Simpson.[78] Correction for the real part of anamolous dispersion was applied to the ruthenium atom.

Table III-1 contains the observed and calculated structure factors. The final parameters and their standard deviations for the

non-hydrogen atoms are listed in Table III-2. Positional parameters for the hydrogen atoms are contained in Table III-3. Interatomic distances and bond angles can be found in Tables III-4 and III-5, respectively.

The estimated standard deviations (e.s.d.) for the positional parameters are about 0.0005Å for the ruthenium atoms, 0.005Å for the ammino nitrogens, 0.005Å for the nitrogeno nitrogens, 0.007Å for oxygen, 0.01Å for the boron, and 0.006Å for fluorine. These latter two numbers apply only to the well-behaved BF_4^- group. These e.s.d.'s lead to an e.s.d. of 0.006Å for the Ru-NH$_3$ bond, 0.006Å for the Ru-N$_2$ bond, 0.015Å for the N—N bond, 0.002Å for the Ru—Ru distance, and $0.5°$ for the Ru—N—N angle.

Description and Discussion of the Structure

The Cation

Of primary interest in this investigation was the configuration of the Ru—N$_2$—Ru unit. The bridging group was found to be very nearly linear with a Ru—N—N angle of $178.3(5)°$. The N—N distance was found to be $1.124(15)\text{Å}$, only slightly larger than free N$_2$ (1.0976Å)[79] or N$_2^+$ (1.118Å).[80] It is well below the N—N distance in hydrazine (1.46Å).[81] Our N—N length is almost equal to that found in N$_2$O (1.126Å),[81] and the unprotonated N—N distance in HN$_3$ (1.128Å).[81] Five ammonia groups complete the octahedral coordination about each ruthenium with the two equatorial sets of ammonias in an eclipsed conformation, as required by symmetry.

Table III-1

Observed and Calculated Structure Factors

for $[(NH_3)_5RuN_2Ru(NH_3)_5](BF_4)_4 \cdot 2H_2O$

Table III-2

Positional Parameters for Non-hydrogen Atoms^{c,d}

Atom	x	y	z
Ru(1)	12930 (4)	10712 (3)	6271 (4)
N(3)^a	3011 (41)	2370 (36)	1352 (43)
N(5)^b	22077 (46)	856 (38)	13010 (46)
N(6)^b	21955 (44)	9742 (39)	-7060 (46)
N(7)^b	4163 (47)	12183 (37)	19683 (47)
N(8)^b	4293 (49)	20844 (39)	-480 (51)
N(9)^b	23773 (50)	20001 (41)	11966 (45)
B(10)	25254 (97)	14066 (75)	39733 (74)
F(11)	30621 (45)	9278 (37)	32851 (43)
F(12)	17474 (57)	9166 (52)	43151 (75)
F(13)	31444 (52)	16150 (56)	47278 (51)
F(14)	20577 (54)	20892 (37)	35425 (45)
B(15)	49033 (160)	10939 (197)	-21762 (110)
F(16)	54603 (125)	6385 (76)	-26313 (125)
F(17)	44238 (114)	15220 (100)	-28818 (105)
F(18)	44947 (94)	12222 (144)	-14721 (95)
F(19)	57288 (90)	16907 (77)	-20438 (130)
O(20)	43803 (57)	8329 (54)	6475 (64)

Atom	b_{11}	b_{22}	b_{33}
Ru(1)	443 (3)	271 (2)	418 (3)
N(3)^a	461 (45)	311 (30)	402 (36)
N(5)^b	664 (48)	363 (33)	709 (49)

Table III-2 (Continued)

Atom	b_{11}	b_{22}	b_{33}
N(6)[b]	604 (42)	462 (33)	610 (41)
N(7)[b]	797 (46)	404 (32)	535 (44)
N(8)[b]	709 (49)	361 (32)	756 (53)
N(9)[b]	734 (50)	435 (34)	621 (48)
B(10)	754 (67)	492 (50)	580 (58)
F(11)	1283 (51)	908 (39)	993 (43)
F(12)	1109 (57)	1412 (64)	2843 (114)
F(13)	1356 (61)	1850 (71)	1320 (59)
F(14)	2109 (75)	630 (32)	1054 (49)
B(15)	1966 (179)	3089 (226)	514 (77)
F(16)	3792 (190)	1781 (95)	3406 (201)
F(17)	3184 (172)	3001 (165)	2302 (134)
F(18)	2304 (132)	6416 (315)	1656 (91)
F(19)	2416 (123)	1915 (105)	5015 (249)
O(20)	1018 (59)	1256 (64)	1490 (71)

Atom	b_{12}	b_{13}	b_{23}
Ru(1)	-88 (6)	26 (7)	-1 (6)
N(3)[a]	-72 (52)	7 (66)	63 (55)
N(5)[b]	-26 (61)	-301 (82)	164 (63)
N(6)[b]	-152 (63)	382 (74)	-42 (73)
N(7)[b]	-329 (65)	348 (77)	-169 (61)
N(8)[b]	93 (67)	2 (84)	65 (65)
N(9)[b]	-421 (65)	-75 (85)	-37 (65)

Table III-2 (Continued)

Atom	b_{12}	b_{13}	b_{23}
B(10)	226 (97)	-33 (146)	-95 (110)
F(11)	688 (76)	-38 (81)	-762 (71)
F(12)	-429 (102)	777 (138)	1748 (143)
F(13)	830 (115)	-1326 (105)	-1659 (109)
F(14)	1195 (83)	-83 (104)	98 (67)
B(15)	3093 (354)	-1009 (209)	-2277 (239)
F(16)	-83 (234)	717 (349)	-2485 (239)
F(17)	842 (295)	-730 (274)	1804 (246)
F(18)	712 (330)	2143 (186)	1290 (284)
F(19)	-1602 (187)	-1411 (309)	-2858 (273)
O(20)	153 (103)	158 (116)	63 (118)

[a] Nitrogeno nitrogen.

[b] Ammino nitrogen.

[c] Labelling of ruthenium and nitrogens corresponds to Fig. III-1. The other atoms in this figure can be generated by an inversion through the origin.

[d] Positional and thermal parameters are multiplied by 10^5. Positional parameters are expressed in fractional coordinates; anisotropic temperature factors are given in the form
$[\exp - (b_{11}h^2 + b_{22}k^2 + b_{33}\ell^2 + b_{12}hk + b_{13}h\ell + b_{23}k\ell)]$.

Table III-3

Positional Parameters for Hydrogen Atoms

Atom[b]	x	y	z	B
H(51)	2778 (69)	180 (55)	1305 (63)	6.42 (2.34)
H(52)	2043 (73)	-113 (54)	1757 (73)	6.43 (2.57)
H(53)	2137 (72)	-334 (62)	999 (71)	8.60 (2.49)
H(61)	1733 (82)	1310 (62)	-997 (73)	6.81 (2.80)
H(62)	2640 (75)	1159 (60)	-794 (68)	5.98 (2.52)
H(63)	2126 (74)	552 (65)	1126 (64)	7.26 (2.68)
H(71)	579 (59)	1654 (48)	2358 (54)	5.30 (1.92)
H(72)	-157 (75)	1157 (57)	1843 (72)	9.77 (2.49)
H(73)	567 (66)	898 (50)	2361 (57)	5.81 (2.06)
H(81)	269 (68)	2309 (55)	269 (68)	6.56 (2.35)
H(82)	761 (62)	2358 (52)	-441 (66)	8.36 (2.23)
H(83)	-163 (70)	1902 (58)	-260 (66)	10.12 (2.47)
H(91)	2118 (76)	2494 (64)	1044 (75)	11.88 (2.82)
H(92)	2906 (74)	2007 (63)	968 (76)	8.18 (2.69)
H(93)	2580 (66)	1931 (57)	1781 (67)	7.72 (2.23)
H(201)	4540 (67)	918 (55)	-77 (72)	11.55 (2.48)
H(202)	5439 (99)	1146 (73)	1254 (95)	12.92 (2.34)

[a] Positional parameters $\times 10^4$ expressed in fractional coordinates.

[b] First digit in hydrogen number indicates nitrogen or oxygen it is attached to.

Table III-4

Interatomic Distances Within the Ions

Ru(1)—Ru(2)	4.979Å	
—N(3)	1.928	
—N(4)	3.052	
—N(5)	2.125	
—N(6)	2.125	
—N(7)	2.123	
—N(8)	2.123	
—N(9)	2.140	
N(3)—N(4)	1.124	
—N(5)	2.900	
—N(6)	2.904	
—N(7)	2.885	
—N(8)	2.884	
B(10)—F(11)	1.366	
—F(12)	1.333	
—F(13)	1.321	
—F(14)	1.346	
B(15)—F(16)	1.173	
—F(17)	1.305	
—F(18)	1.093	
—F(19)	1.415	

Table III-5

The Hydrogen Bonding[a]

From	To	Dist, Å
N(5)	F(11)	3.15
	O(20)	3.13
	F(20)[b]	3.43
N(6)	F(18)	3.13
	O(20)	3.33
N(7)	F(14)	3.26
	F(16)[b]	3.14
	F(22)[c]	3.27
N(8)	F(22)[c]	3.40
N(9)	F(11)	3.36
	F(14)	3.16
	O(20)	3.22
	F(22)[c]	3.14
F(18)	O(20)	2.90
O(20)	F(12)[d]	3.03

---

[a] The atom listed in column 1 has coordinates as given in Table III-2. The symmetry transformation given after the atom listed in column 2 applies to the second atom's coordinates. These coordinates are:

[b] $\frac{1}{2} - x$, $\bar{y}$, $\frac{1}{2} + z$.

[c] $\frac{1}{2} + x$, $\frac{1}{2} - y$, $\bar{z}$.

[d] $\frac{1}{2} + x$, y, $\frac{1}{2} - z$.

Table III-6

Bond Angles

Angle	Deg	Angle	Deg
Ru(1)-N(3)-N(4)	178.3	N(9)-Ru(1)-N(7)	88.3
N(5)-Ru(1)-N(3)	91.2	N(9)-Ru(1)-N(8)	89.3
N(6)-Ru(1)-N(3)	91.4	F(12)-B(10)-F(11)	107.0
N(7)-Ru(1)-N(3)	90.7	F(13)-B(10)-F(11)	110.1
N(8)-Ru(1)-N(3)	90.7	F(14)-B(10)-F(11)	111.4
N(9)-Ru(1)-N(3)	179.0	F(13)-B(10)-F(12)	109.0
N(6)-Ru(1)-N(5)	90.3	F(14)-B(10)-F(12)	105.3
N(7)-Ru(1)-N(5)	90.7	F(14)-B(10)-F(13)	113.5
N(8)-Ru(1)-N(5)	177.9	F(17)-B(15)-F(16)	102.6
N(9)-Ru(1)-N(5)	88.8	F(18)-B(15)-F(16)	147.7
N(7)-Ru(1)-N(6)	177.7	F(19)-B(15)-F(16)	90.4
N(8)-Ru(1)-N(6)	88.8	F(18)-B(15)-F(17)	107.6
N(9)-Ru(1)-N(6)	89.6	F(19)-B(15)-F(17)	96.1
N(8)-Ru(1)-N(7)	90.2	F(19)-B(15)-F(18)	97.4

Figure III-1. A view of the dimeric cation.
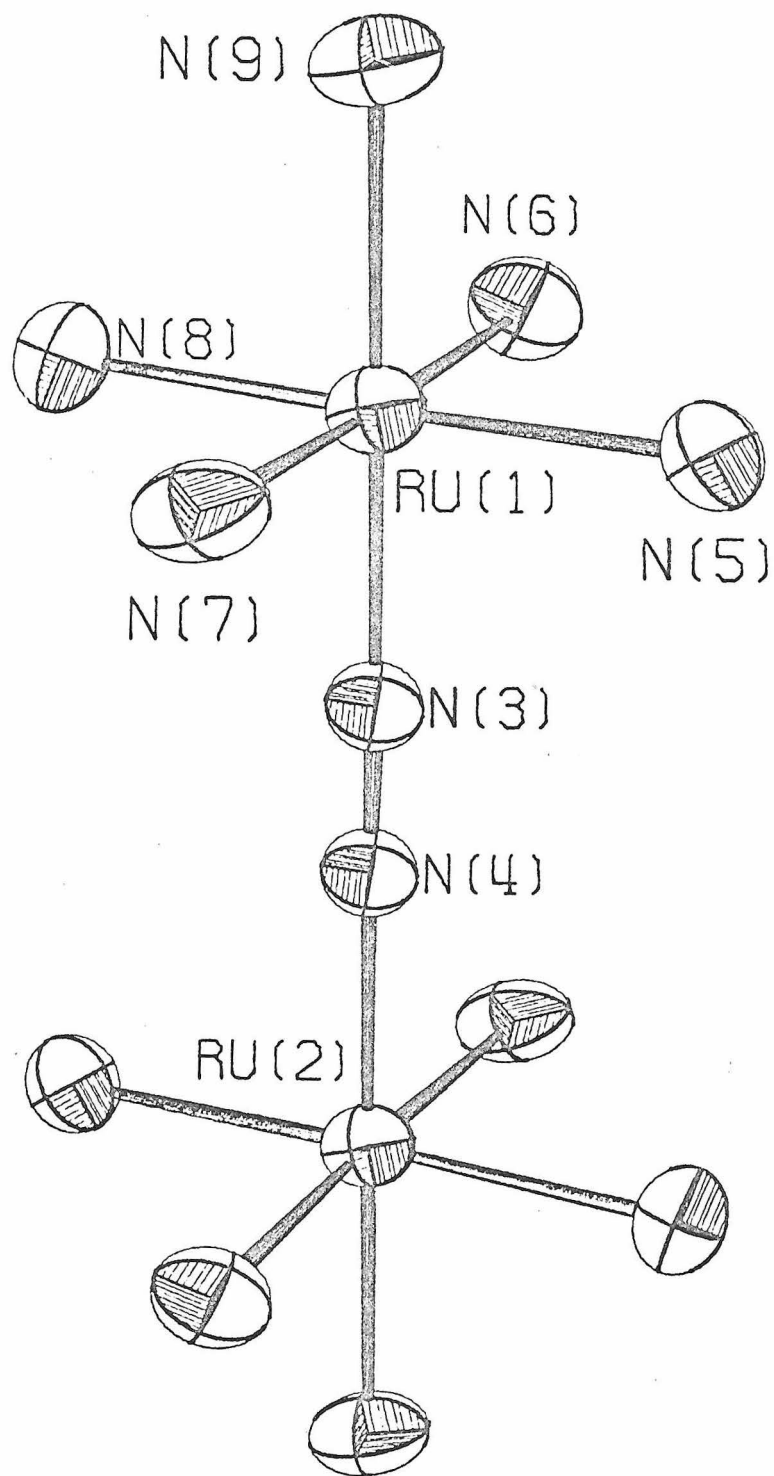
These equatorial Ru—NH_3 bonds have an average distance of 2.124(1)Å, whereas the apical N(9)—Ru(1) distance of 2.140Å indicates a slight π induced "trans effect."[44] The distances agree well with the normal Ru—NH_3 distance of 2.10-2.15Å.[82] The Ru—N_2 bond is noticeably shortened at 1.928(6)Å, lending further support to the idea of $d\pi \rightarrow \pi^*$ back bonding. As in the case of carbonyls, the metal ligand bond shortening may be more indicative of a decrease in ligand bond order than decreases in the intraligand distance itself.[83] It is interesting to note that the Ru—N_2 distance here is quite close to Ru—CO distances.[83]

The linear structure of the RuN_2Ru unit is in accord with the infrared results, which show only a very weak band in the 2050-2100 cm^{-1} region.[74] Recent Raman measurements have corroborated the linear structure by revealing a strong stretch at 2100 cm^{-1}.[85]

The only other N_2 compound on which accurate structural parameters have been obtained is $Co(H)(N_2)(PPh_3)_3$.[86] The Co—N_2 bond has been found to be 1.8Å, and is comparable to known Co—CO distances. The N—N distance is 1.11Å, only slightly shorter than our N—N value (1.124Å). This may indicate that a second metal center adds little to the total electronic density transferred into the N_2 π^* orbitals. In our dimer, therefore, each Ru transfers only half the density that the Co transfers in the nitrogen-hydride. In the trigonal bipyramidal cobalt complex, the Co—N≡N moiety has been determined to be almost linear (178°).

As mentioned previously, the $Ru(NH_3)_5N_2^{2+}$ cation was found to be disordered,[76] and this precluded the accurate determination of bond lengths. From the data collected, it was ascertained that the $Ru-N\equiv N$ unit was almost linear. The distance of the $Ru-N-N$ group was 3.22(6)Å. This triatomic distance could only be crudely partitioned. A distance of 1.12(8)Å was ascribed to the N—N bond, and 2.10(1)Å to the Ru—N linkage. It is unfortunate that these distances are only estimates and no really meaningful comparison between ruthenium monomer and dimer is possible. Comparisons between the cobalt compound and the ruthenium dimer can be made up to a point, but these comparisons must be tempered with the knowledge that we are dealing with different metals and different d configurations.

The Anions

The first tetrafluoroborate group is a well behaved tetrahedral unit having a mean B—F distance of 1.341Å, with individual values ranging from 1.321 to 1.366Å. It has a mean F—B—F angle of 109.4°, with individual values ranging from 105.3° to 113.5°. These values are in excellent agreement with those reported in the literature.[87]

The second BF_4^- in the asymmetric unit behaves more intractably, either because of disorder, or because its flourines are undergoing large thermal motions. Accurate atomic positions were unattainable. The final bond lengths varied from 1.093 to 1.415Å. Similarly, the bond angles varied from 90.4° to 147.7°. All attempts at localizing the fluorine atoms in the unit, by looking for a preferred

orientation induced by hydrogen bonding, failed. In fact, as can be seen from the distances in Table III-5, hydrogen bonding, while present to a slight degree, is not an important factor in the bonding and stabilization of the crystal.

Electronic Spectra of $Ru(NH_3)_5N_2^{2+}$ and $[Ru(NH_3)_5]_2N_2^{4+}$

Experimental

In conjunction with our work on other π bridged binuclear systems, we examined the electronic spectra of both the ruthenium monomer and dimer. The preparation of the dimer has already been described in the crystallographic experimental section. The monomer, on the other hand, was prepared by a variety of different methods.[84]

First, $RuCl_3 \cdot xH_2O$ was reacted directly with $N_2H_4 \cdot H_2O$. Following a vigorous reaction, the resulting brown-black residue was filtered and a solution of the appropriate anion added. The second procedure consisted of adding $N_2H_4 \cdot H_2O$ to a solution of $RuCl_5H_2O^{2-}$, which itself had been obtained by evaporating to dryness a concentrated solution of HCl and $RuCl_3 \cdot xH_2O$. After standing overnight, the solution was filtered, and a precipitating anion added. The third method consisted of bubbling N_2 through a solution of $Ru(NH_3)_5H_2O^{2+}$ for ten hours. This pentaammineaquo complex had been obtained by Zn(Hg) reduction of $Ru(NH_3)_5Cl^{2+}$ under argon. Subsequently, BF_4^- or Br^- was added. The final procedure consisted of aquating $Ru(NH_3)_5Cl^{2+}$ in air, bringing it to pH 7, and adding a solution of sodium azide. This solution was kept in a lukewarm bath for twenty minutes, after which the desired anion was added. It was found, as others have also noted,

that none of these procedures gave a particularly pure product. Almost without exception, at least one of the following impurities was present[95]: $Ru(NH_3)_5H_2O^{3+}$ (268 nm), $Ru(NH_3)_5Cl^{2+}$ (328 nm), $Ru(NH_3)_5OH^{2+}$ (290 nm), $Ru(NH_3)_6^{3+}$ (276 nm).

After a significant number of attempts, a good preparation of the monomer was achieved using the azide synthesis. At room temperature, only an intense charge transfer absorption, $\lambda_{max} = 221$, $\epsilon = 1.6 \times 10^4$, was noted. Hoping to see the weaker ligand field transition on the low energy side of this band, we looked at the liquid nitrogen spectrum of the monomer in a 1:1 saturated solution $LiCl:H_2O$ glass. Nothing additional was noted.

Similarly, the dimer was investigated at low temperatures in the same solvent. It, too, revealed no additional structure. The only band present was at 263 nm. In both the monomer and dimer, impurities were picked up at low temperatures, due to the starting materials or intermediates of the preparation.

Molecular Orbital Treatment

Simplified molecular orbital schemes for the monomer and dimer can be used to explain their spectra. In the monomer, assuming idealized C_{4v} symmetry, we have an ordering of : $b_2(xy) < e(xz, yz) < e(\pi^* N_2)$, with a ground state of $(b_2)^2 e^4 \equiv {}^1A_{1g}$. In the dimer we have an ordering of: $e_g(xz_1 + xz_2, yz_1 + yz_2) < b_{2g}(xy_1 + yz_2) \sim b_{1u}(xy_1 - xy_2) < e_u(xz_1 - xz_2, yz_1 - yz_2) < e_g(\pi^* N_2)$, where the ground state is $(e_g)^4(b_{2g})^2(b_{1u})^2(e_u)^4 \equiv {}^1A_{1g}$. The 221 nm charge transfer band in the monomer can be ascribed to a

$e \rightarrow e(\pi^* \ N_2)$ transition; similarly, the 262 nm band in the dimer can be assigned to the $e_u \rightarrow e_g(\pi^* \ N_2)$ excitation.

The red shift found upon going to the dimer can be explained by the fact that the withdrawal of a total of four d_π electrons leaves a monomeric ruthenium with a larger effective positive charge than in the case of the dimeric species. There, this same total of four withdrawn electrons is divided among two metal centers. This interpretation is in possible agreement with the structural work on the monomer. The $2.10(1)\text{Å}$ Ru–N distance apportioned by Bottomley and Nyburg[76] can easily be obtained by averaging five normal 2.15Å Ru–NH_3 bonds and a single $\sim 1.85\text{Å}$ Ru–N_2 bond. This decreased Ru–N_2 distance in the monomer, when compared to the dimer, would be in accord with a larger positive charge on the metal of the monomer.

The blue shift of the $e \rightarrow e(\pi^*)$ transition, upon going from the nitrogen monomer to $Ru(NH_3)_5CO^{2+}$ (where the corresponding excitation $> 50,000 \ cm^{-1}$),[89] is an indication of greater π interactions between Ru and CO than between Ru and N_2. CO, having a greater p character in its bonding σ orbital, can transfer more electronic density into a metal than the more s-like σ bonding orbital of N_2.[62] This leads to an increased synergistic effect.[83] Increased π bonding in the CO compound results, and this leads to a transition at higher energies.

It seems unlikely that the monomer transition can be ascribed to a N_2 intraligand $\pi_u \rightarrow \pi_g^*$ transition, as has been suggested.[89] In uncoordinated N_2 or in a weakly interacting N_2, the $\pi(N_2) \rightarrow \pi^*(N_2)$ transition would be $\sim 80,000 \ cm^{-1}$.[90] Even if more interaction is

present, the Ru $\rightarrow$ N$_2$ charge transfer transition would still have to be at lower energies than the intraligand excitation.

A few trivial variants of Taube's dimer have been synthesized.[91] [Ru trien H$_2$O]$_2$N$_2^{4+}$ has a λ_{max} = 268 nm, while [Ru trien OH]$_2$N$_2^{2+}$ has a λ_{max} = 273 nm. These red shifts are understandable if we assume similar σ metal-ligand interactions for NH$_3$, H$_2$O, and OH$^-$. The π donating ability of these ligands, however, is NH$_3$ < H$_2$O < OH$^-$.[92] This gives an ordering of NH$_3$ > H$_2$O > OH$^-$ for the positive charge on the metals, just the order needed to explain the observed charge transfer shifts.

References

1. E. Fremy, Ann. Chim. Phys., (3), 35, 271(1852).

2. A. Werner, Ann. Chem., 375, 9, 15, 61 (1910).

3. K. Gleu, K. Rehm, Z. Anorg. Chem., 237, 79 (1938).

4. L. Malatesta, Gazz. Chim. Ital., 72, 287 (1942).

5. E. Ebsworth, J. Weil, J. Phys. Chem., 63, 1890 (1959).

6. J. Weil, J. Kinnaird, J. Phys. Chem., 71, 3341 (1967).

7. H. Kon, N. Sharpless, Spect. Letts., 1, 49 (1968).

8. G. Goodman, H. Hecht, J. Weil in "Free Radicals in Inorganic Chemistry," Advances in Chemistry Series, No. 36, American Chemical Society, Washington, D.C., 1962, p. 93.

9. C. Brosset, N. Vannerberg, Nature, 190, 714 (1961).

10. W. Schaeffer, R. E. Marsh, Acta Cryst., 21, 735 (1966).

11. W. Schaeffer, Inorg. Chem., 7, 725 (1968).

12. A. Haim, W. K. Wilmarth, J. Amer. Chem. Soc., 83, 509 (1961).

13. M. Mori, J. Weil, J. Kinnaird, J. Phys. Chem., 71, 103 (1967).

14. J. Dunitz, L. E. Orgel, J. Chem. Soc., 1953, 2594.

15. B. Jezonska-Trzebiatowski, J. Mrozinski, M. Wojchiechowski, J. Prakt. Chim., 34, 97 (1966).

16. E. Bayer, Structure and Bonding, 2, 181 (1967).

17. M. Bersohn, J. Baird, "An Introduction to Electron Paramagnetic Resonance, W. A. Benjamin, Inc., New York, 1966, pp. 69, 77.

18. S. Geschwind, J. Remeika, J. Appl. Phys., 33, 370 (1962).

19. J. A. Connor, E. Ebsworth, <u>Advances in Inorganic Chemistry and Radiochemistry</u>, 6, 279 (1964).

20. B. Bleaney, M. O'Brien, <u>Proc. Phys. Soc.</u>, 69B, 1216 (1956).

21. D. F. Gutterman, Ph.D. Thesis, Columbia University, 1969.

22. D. Dows, A. Haim, W. Wilmarth, <u>J. Inorg. Nucl. Chem.</u>, 21, 33 (1961).

23. (a) R. de Castello, C. M^{ac}Coll, N. Egen, A. Haim., <u>Inorg. Chem.</u>, 8, 699 (1969);

    (b) B. Grossman, A. Haim, <u>J. Amer. Chem. Soc.</u>, 92, 4835 (1970).

24. B. N. Figgis, "Introduction to Ligand Fields," Interscience, New York, 1966, p. 232.

25. R. A. D. Wentworth, T. S. Piper, <u>Inorg. Chem.</u>, 4, 709 (1962).

26. M. Linhard, M. Weigel, <u>Z. Anorg. Allgem. Chem.</u>, 264, 321 (1951).

27. J. Piesach, W. Blumberg, B. Wittenberg, J. Wittenberg, <u>J. Biol. Chem.</u>, 243, 1871 (1968).

28. J. Alexander, H. B. Gray, <u>J. Amer. Chem. Soc.</u>, 90, 4260 (1968).

29. J. Barnes, J. Barrett, R. Brett, J. Brown, <u>J. Inorg. Nucl. Chem.</u>, 30, 2207 (1968).

30. S. Yamada, Y. Shimura, R. Tsuchida, <u>Bull. Chem. Soc. Japan</u>, 26, 72, 533 (1953).

31. K. Garbett, R. D. Gillard, <u>J. Chem. Soc. (A)</u>, 1968, 1725.

32. G. Czapski, B. Halperin, Israel J. Chem., 5, 185 (1967).

33. B. Bosnich, C. K. Poon, M. L. Tobe, Inorg. Chem., 5, 1514 (1966).

34. J. H. Bayston, R. Beale, N. King, M. Winfield, Aust. J. Chem., 16, 954 (1963).

35. L. C. Smith, J. Kleinberg, E. Griswold, J. Amer. Chem. Soc., 75, 449 (1953).

36. C. Floriani, F. Calderazzo, J. Chem. Soc. (A), 1969, 946, and references cited therein.

37. B. Hoffman, D. Diemente, F. Basolo, J. Amer. Chem. Soc., 92, 61 (1970), and references cited therein.

38. S. Yamada, E. Yoshida, Proc. Japan Academy, 40, 211 (1964).

39. L. Pauling, C. Coryell, Proc. U. S. Natl. Acad. Sci., 22, 210 (1936).

40. J. Weiss, Nature, 202, 83 (1964).

41. G. Schoffa, Advances in Chemical Physics, 7, 182 (1964).

42. J. Alexander, Ph.D. Thesis, Columbia University, 1967.

43. C. Creutz, H. Taube, J. Amer. Chem. Soc., 91, 3988 (1969).

44. D. Bright, J. A. Ibers, Inorg. Chem., 8, 709 (1969).

45. H. Jaffe, M. Orchin, "Theory and Application of Ultraviolet Spectroscopy," J. Wiley, New York, 1962.

46. D. Cowan, F. Kaufman, J. Amer. Chem. Soc., 92, 220 (1970).

47. N. S. Hush, Progress in Inorganic Chemistry, 8, 391 (1967).

48. N. S. Hush, Progress in Inorganic Chemistry, 8, 347 (1967).

49. B. N. Figgis, op. cit., p. 310.

50. B. Figgis, J. Lewis, F. Mabbs, G. Webb, J. Chem. Soc. (A), 1966, 422.

51. D. Cowan, private communication.

52. E. Koneg in "Physical Methods in Advanced Inorganic Chemistry," Interscience, New York, 1968, p. 311.

53. J. H. Griffiths, J. Owen, I. Ward, Proc. Roy. Soc. (London), A219, 526 (1953).

54. H. Jarrett, J. Chem. Phys., 27, 1298 (1957).

55. A. Abragam, B. Bleaney, "Electron Paramagnetic Resonance Transition Ions," Clarendon Press, Oxford, 1970, pp. 418, 419, and 481.

56. J. H. Van Vleck, "Theory of Electric and Magnetic Susceptibilities," Oxford University Press, London, 1932, p. 182.

57. W. Moore, "Physical Chemistry," Prentice-Hall, Englewood Cliffs, New Jersey, 1962, p. 297.

58. C. K. Jorgensen, "Absorption Spectra and Chemical Bonding in Complexes," Pergamon Press, Oxford, 1962, p. 113.

59. C. Ballhausen, "Introduction to Ligand Field Theory," McGraw-Hill, New York, 1962, p. 275.

60. C. Ballhausen, H. B. Gray, "Molecular Orbital Theory," W. A. Benjamin, New York, 1964, p. 55.

61. P. Ford, D. Rudd, R. Gaunder, H. Taube, J. Amer. Chem. Soc., 1187 (1968).

62. H. Jaffe, M. Orchin, Tetrahedron, 10, 212 (1960).

63. F. Basolo, R. G. Pearson, "Mechanics of Inorganic Reactions," J. Wiley, New York, 1967, p. 461.

64. J. Hollander, W. Jolly, Accts. of Chem. Res., 6, 193 (1970).

65. W. Kauzman, "Quantum Chemistry," Academic Press, New York, 1957, p. 141.

66. C. Creutz, private communication.

67. P. Ford, Coordin. Chem. Revs., 5, 75 (1970).

68. R. Murray, D. Smith, Coordin. Chem. Revs., 3, 429 (1968).

69. Y. Borod'ko, A. Shilov, Russian Chem. Revs., 38, 355 (1969).

70. A. Allan, F. Bottomley, Accts. of Chem. Res., 1, 360 (1968).

71. E. van Tamelen, G. Boche, R. Greeley, J. Amer. Chem. Soc., 91, 1551 (1969), and references cited therein.

72. M. E. Vol'pin, V. B. Shur, Nature, 209, 1236 (1966).

73. A. Allan, C. Senoff, Chem. Commun., 1965, 621.

74. D. Harrison, H. Taube, E. Weissberger, Science, 159, 320 (1968).

75. I. Itzkovich, J. Page, Can. J. Chem., 46, 2743 (1968).

76. F. Bottomley, S. Nyburg, Acta Cryst., B24, 1289 (1968).

77. "International Tables for X-Ray Crystallography," The Kynock Press, Birmingham, England, 1962.

78. R. F. Stewart, E. Davidson, W. Simpson, J. Chem. Phys., 42, 3175 (1965).

79. P. Wilkinson, N. Houk, J. Chem. Phys., 24, 528 (1956).

80. P. Wilkinson, Can. J. Phys., 34, 250 (1956).

81. "Interatomic Distances," The Chemical Society, London, 1958.

82. B. Davis, J. Ibers, Inorg. Chem., 9, 2772 (1970).

83. F. A. Cotton, G. Wilkinson, "Advanced Inorganic Chemistry," Interscience, New York, 1966, p. 723-734.

84. A. D. Allen, F. Bottomley, R. Harris, V. Reinsalu, C. Senoff, J. Amer. Chem. Soc., 89, 5595 (1967).

85. J. Chatt, A. Nikolsky, R. Richards, J. Sanders, J. Chem. Soc. (D), 1969, 155.

86. B. Davis, N. Payne, J. A. Ibers, J. Amer. Chem. Soc., 91, 1241 (1969).

87. G. Brunton, Acta Cryst., B24, 1703 (1968).

88. W. Griffith, "The Chemistry of the Rarer Platinum Metals," Interscience, London, 1967.

89. J. Stanko, T. Starinshank, Inorg. Chem., 8, 2156 (1969).

90. G. Herzberg, "Spectra of Diatomic Molecules," Van Nostrand, New York, 1950, p. 552.

91. R. O. Harris, B. Wright, Can. J. Chem., 48, 1815 (1970).

92. F. Basolo, R. G. Pearson, op. cit., p. 171.

93. K. Innes, J. Byrne, I. Ross, J. Mol. Spect., 22, 125 (1967).

94. R. A. Levenson, Ph.D. Thesis, Columbia University, 1970.

95. C. Sigwert, J. Spence, J. Amer. Chem. Soc., 91, 3991, (1969).

Proposition I

Experiments are proposed to verify the presence of D_{3h} penta-coordinate intermediates upon irradiation of metal hexacarbonyls.

Ten years ago, pentacoordinate species were generally limited to compounds of the Group V elements.[1] Only in the last decade have five coordinate transition metal complexes appeared. These compounds, involving a wide variety of ligands and metals, have added much to our understanding of trigonal bipyramidal and square pyramidal geometries. It has been found that the trigonal bipyramidal geometry is stabilized by good π donating metals and by good π accepting ligands.[1]

As a rule, the ligands found stabilizing a trigonal bipyramidal structure have been highly complex, e.g., phosphines or arsines. In most cases, true D_{3h} symmetry is not present because of the nonequivalence of all five ligands. It is this point which makes D_{3h} $Fe(CO)_5$ so important. Besides the equivalency of its ligands, iron pentacarbonyl is attractive because CO is a comparatively simple molecule which has been well characterized.

To supplement the sparse amount of data on five-coordinate transition metal complexes with five identical ligands, we propose studying the $M(CO)_5$ (M = Cr, Mo, W) analogs of iron pentacarbonyl. The pentacoordinate intermediates of Cr, Mo, and W are known to form when their corresponding hexacarbonyls are subjected to UV irradiation. Sheline and coworkers[2] have hypothesized from

infrared evidence that upon photolyzing the hexacarbonyl in a rigid glass matrix at low temperatures, one obtains a C_{4v} square-pyramidal intermediate. When this glass is melted, the IR spectrum changes. Sheline has proposed that the species into which the pentacarbonyl changes is a D_{3h} trigonal bipyramidal species.[2]

We propose verifying Sheline's idea of a $C_{4v} \rightarrow D_{3h}$ conversion by using electronic spectroscopy. A D_{3h} species with six d electrons should have a $e''(xz, yz)^4$, $e'(xy, x^2 - y^2)^2$, $a_1(z^2)^0$ ground configuration which, theoretically, should lead to two d-d transitions.[3] A d^6 C_{4v} species should possess a $e(xz, yz)^4$, $b_2(xy)^2$, $a_1(z^2)^0$, $b_1(x^2 - y^2)^0$ ground configuration which should give rise to four d-d excitations.[3]

If the temperature of an irradiated sample of hexacarbonyl is well controlled, one should be able to slowly warm up the hydrocarbon glass (e.g., isopentane:methylcyclohexane) and see the spectrum of the C_{4v} species trapped in the matrix go over to a D_{3h} spectrum. Sheline[2] says this transition occurs at ~ -155°C, about 5 - 10°C above the fluid point of the hydrocarbon glass. At this temperature, the recombination of the pentacarbonyl to the hexacarbonyl will probably be slow enough for a spectrum of the D_{3h} species to be observable (if it is present). If the spectrum is scanned rapidly and in parts, the absorptions of the D_{3h} molecule should be obtainable. At present, instruments have been designed which will maintain control of the temperature in the Cary sample cells to within the required degree of accuracy. If evidence for a D_{3h} species is found, its spectrum can be compared with that of $Fe(CO)_5$ in the literature.[4]

Another series of experiments which could be done to verify the actual presence of a D_{3h} intermediate would be to use Evans' NMR method[5] to determine the magnetic susceptibility of the species in solution. Evans' procedure consists of measuring the chemical shift of a reference proton from a solvent in which paramagnetic ions have been introduced. Simultaneously, a second sample containing just the solvent is placed in the NMR probe coaxially with the paramagnetic sample. This second sample also has its reference proton resonance measured. The susceptibility, χ_g, is given by $\chi_g \sim \frac{3\Delta f}{2\pi f m}$, where m is the mass of the paramagnetic species per ml, f the operating frequency of the instrument used, and Δf the frequency separation of the two reference proton resonances. Both the initial C_{4v} intermediate and the final O_h species are diamagnetic. They should show a $\Delta f = 0$. The D_{3h} species, however, should have two unpaired electrons in the e' $(xy, x^2 - y^2)$ orbitals. A $\Delta f > 0$ should be observed. This Δf should give a χ_g near that expected for a two-spin system, i.e., $\sim 3300 \times 10^{-6}$ cgs.

One final experiment may be tried in efforts to verify the postulated D_{3h} intermediate of $M(CO)_5$. We propose the study of the vapor phase flash photolysis of the hexacarbonyls. Provided that the hexacarbonyl loses only a single carbonyl group and is not completely photolyzed (a point which can only be determined experimentally), the spectroscopic flash coming $\sim 10^{-6}$ sec after the photolytic flash should allow time for the $C_{4v} \rightarrow D_{3h}$ conversion. In the vapor phase, no cage effect is possible. The rate of $D_{3h} + CO$ recombination should

be reduced considerably. Obtaining a D_{3h} spectrum should, therefore, be much easier than observation in a rigid matrix. By allowing the spectroscopic flash time to vary, one may also obtain kinetic data on the rate of D_{3h} + CO recombination. It should be reiterated that this last series of experiments is predicated on our ability to find conditions both photolytic and thermal, wherein the hexacarbonyl is not completely destroyed.

References

1. E. Muetterties and R. Schunn, Quart. Rev. (London), 20, 245 (1966) and references therein.

2. I. Stolz, G. Dobson, R. Sheline, J. Amer. Chem. Soc., 84, 3589 (1962); 85, 1013 (1963).

3. J. R. Preer, Ph.D. Thesis, California Institute of Technology, 1970, pp. 123-124.

4. M. Dartiguenave, Y. Dartiguenave, H. B. Gray, Bull. Chim. Soc. France, 12, 4223 (1969).

5. D. Evans, J. Chem. Soc., 2003 (1959).

Proposition II

It is proposed to investigate the emission of pyrazine and nitrogen bridged decaamminediruthenium dimers and their corresponding monomers. Experiments using sensitizers are suggested for locating the d-d transitions in the N_2 compounds.

Many transition metal compounds with d^6 electronic configurations are known to luminesce.[1] Much work has been done in this area since 1965. Almost all of the complexes investigated have been low spin.[1] Kasha has found that species with d^6 configurations require large crystal fields to render radiationless deactivation improbable.[2] The occurrence of facile radiationless processes has been given as the reason that complexes of Co(III) show little photochemical activity when excited at their d-d band energies.[3]

Among the d^6 systems studied have been complexes of Ru(II), Os(II), Rh(III), Ir(III), and Pt(IV).[1] Except for the hexahalo-platinates(IV), the vast majority of compounds investigated have shown either ligand to metal charge transfer or intraligand emission. This is understandable when one remembers that complexes with heterocyclic organic rings have usually been used. It has been found, in such cases, that the t_{2g} and e_g d orbitals are highly split. The π^* orbitals of the organic ligands are then actually more stable than the upper e_g orbital pair.[1]

We propose that an investigation of the emission from the μ-nitrogen and μ-pyrazinedecaamminediruthenium dimers (as well as their monomers) be undertaken. In the pyrazine case, one could reasonably expect to observe $\pi^*(\text{pyrazine}) \rightarrow d(t_{2g})$ emission analogous to the luminescence reported for dipyridyl and o-phenanthroline Ru(II) compounds.[4] In the II-II dimer, $d(t_{2g}) \rightarrow \pi^*(\text{pyrazine})$ is thought to be the lowest absorption present.[5] In the corresponding monomer, the same $\pi^*(\text{pyrazine}) \rightarrow d(t_{2g})$ emission should be seen. It will, however, be blue shifted slightly.

Upon going to the 5+ dimer, it may be possible that spin-forbidden luminescence will appear in the infrared region of the spectrum, corresponding to the near IR absorption at 1600 nm. From the fine structure (or lack thereof), it may be possible to further justify our assignment of this absorption as $b_{3u}(xy + xy) \rightarrow b_{2g}(xy - xy)$.[6] Emission with vibrational fine structure would imply that the low energy absorption arises from a $\pi^b(\text{pyrazine}) \rightarrow d(t_{2g})$ excitation. Luminescence lacking fine structure should result from a d-d transition.[6] If emission in the IR is observed, and if a d-d band seems the likely assignment, this would only be the third observed case of Ru(II) d-d emission.[7, 8] It must be admitted that a problem with observing luminescence may exist here. The transition leading to the emission is of such low energy that radiationless decay processes may be the preferred method of deactivation.[1]

Upon going to the ruthenium nitrogen dimer (and monomer), more interesting results should be obtainable. The d-d bands in this compound

could not be ascertained definitively via low temperature absorption spectroscopy. Low temperature emission spectroscopy, however, may prove more fruitful. With ruthenium's large spin-orbit coupling constant, phosphorescence could be observable. Because of the large t_{2g}, e_g splitting (~ 70-80 kcal), radiationless deactivation will not be easy.[1] If, as seems most likely, the d-d bands of the monomer and dimer lie to the red of the intense metal to ligand charge transfer transition, a d-d transition should be the source of any observed emission. This emission must appear to the red of 22.7 kK, the $^3T_{1g} \rightarrow {}^1A_{1g}$ d-d emission of hexacyanoruthenate(II).[7]

Although unlikely, these N_2 compounds may fail to show the expected emission at low temperatures. Two possible reasons for this would be poor intersystem crossing from the lowest singlet level to the lowest triplet level, and/or a very high rate of radiationless decay from the lowest singlet excited state.[9] These two conditions are unlikely here because, as mentioned previously, ruthenium possesses a large spin-orbit constant, and a large 10 Dq. To circumvent these improbable complications if they should arise, we propose bypassing the lowest singlet state by using a series of well characterized organic sensitizers to put ruthenium into its emitting triplet level.[9] In this series we will choose sensitizers with different triplet energies. Ru(II)-N_2 compounds analogous to the parent compounds have been made using NH_3 and trien with H_2O, OH^-, Br^-, I^-, etc in equatorial (xy plane) positions.[10] The observed shift in the intense M $\rightarrow$ L charge transfer band with various ligands

have all been minimal ($\lesssim$ 3 kcal). By adding insulated amine groups on the different sensitizers, and then placing these sensitizers on the rutheniums we probably will be able to find donors with known triplet and singlet energies which will bracket the lowest excited singlet and triplet levels of the ruthenium nitrogen compounds.[9] Similarly, other sensitizers may be used in the reverse manner, i.e., to quench possible ruthenium emission. Here, the conditions needed would be E(triplet Ru) > E(triplet sensitizer), while E(singlet Ru) < E(singlet sensitizer).[9] Once the lowest singlet and triplet transitions are bracketed, it will be possible to extract approximate ligand field parameters (Dq, B, and C) for the $Ru-N_2$ compounds.[7]

Before attempting to add sensitizers directly to the ruthenium center, it may be prudent to first add sensitizers to a highly purified glass forming mixture containing the $Ru-N_2$ compound. Depending on the concentration of the sensitizer in solution, it may be possible to see emission directly without the actual coupling of the sensitizer with the metal.

One final experiment in photochemical energy transfer may be tried. $[Ru(NH_3)_5]_2N_2^{4+}$ may be used to precipitate $Ru(CN)_6^{4-}$. We can examine this Ru cation-Ru anion system for energy transfer in the solid state.[11] If needed, an organic sensitizer may be appended to the cation. If we are fortunate, we may possibly end up with tricenter energy transfer, i.e., sensitizer → ruthenium (cation) → ruthenium (anion) transfer,[9] or some variation of this.

One very good candidate for use as a sensitizer in our studies would be substituted benzophenones ($E_T \sim$ 69 kcal, $E_S \sim$ 74 kcal).[12]

Similarly, amine derivatives of pyruvic acid ($E_T \sim$ 65 kcal, $E_S \sim$ 73 kcal) or variants of Michler's ketone ($E_T \sim$ 61 kcal, $E_S \sim$ 69 kcal) could be used.[12] All hydrocarbons can be solubilized as needed by adding hydrophilic groups. Lifetime and quantum yield data should be obtained whenever possible.

References

1. P. D. Fleischauer, P. Fleischauer, Chem. Rev., 70, 199 (1970).

2. F. Zuloaga, M. Kasha, Photochem. Photobiol., 7, 549 (1968).

3. A. Adamson, W. Waltz, E. Zinato, D. Watts, P. Fleischauer, R. Lindholm, Chem. Rev., 68, 541 (1968).

4. D. Klassen, G. Crosby, J. Md. Spect., 26, 72 (1968).

5. P. Ford, D. Rudd, R. Gaunder, H. Taube, J. Amer. Chem. Soc., 90, 1187 (1968).

6. D. Carstons, G. Crosby, J. Mol. Spect., 34, 113 (1970).

7. M. Mingardi, G. B. Porter, Spectrosc. Letts., 1, 293 (1968).

8. D. Klassen, G. Crosby, J. Mol. Spectrosc., 25, 398 (1968).

9. N. J. Turro, "Molecular Photochemistry," Benjamin, New York, 1967.

10. R. Harris, B. Wright, Can. J. Chem., 48, 1815 (1970).

11. H. Gausmann, H. Schlaeffer, J. Chem. Phys., 48, 4056 (1968).

12. Values shown here were obtained from a list of sensitizers circulated in Professor G. S. Hammond's research group.

Proposition III

It is proposed to study similar antiferromagnetic d^1 and d^9 transition metal complexes by magnetic resonance techniques in an effort to determine if the spin pairing mechanism operative in these antiferromagnets differ.

A number of years ago, Ginsburg and coworkers[1] synthesized a series of cupric and oxovanadium(IV) 5-substituted-N-(2-hydroxy' phenol)salicylideneimine complexes.
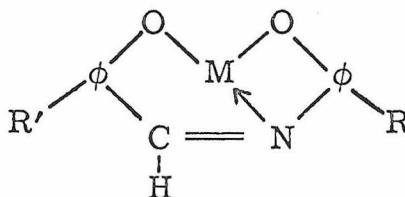
After investigating the magnetic susceptibilities of these complexes as a function of temperature, they concluded that these compounds were magnetically isolated exchange coupled antiferromagnets. Ginsburg, et al. assumed these compounds to have a dimeric structure comparable to other very similar imines whose crystal structures had been determined,[2] and whose susceptibilities also indicated the presence of antiferromagnetism.

In the original work,[1] Ginsburg noted that the exchange integral, J, varied differently in the cupric and vanadyl cases when substituents R and R' were changed on the salicaldehyde rings. To explain this, it was proposed that the coupling mechanism operative in the vanadyl complexes was a direct one. This entails the direct overlap of the

orbital containing the unpaired spin of metal A with the orbital containing the unpaired spin of metal B.[3] On the other hand, it was maintained that spin coupling in the cupric series resulted from a superexchange mechanism via bridging oxygens. This mechanism envisions spin pairing to arise from electron correlation effects transmitted through filled bonding oxygen orbitals.[3]

We believe that both series of compounds should be investigated further to verify the nature of the coupling mechanism(s) present. Considering that relatively few vanadyl antiferromagnets are known,[4] continued investigation of this vanadyl series is desirable. Furthermore, if superexchange is operative in both the cupric and vanadyl series, it will be interesting to see if the superexchange mechanism itself differs. In the d^1 VO^{2+} case, the unpaired electron is located in a t_{2g} orbital, while in the d^9 Cu^{2+} case the unpaired electron is located in an e_g orbital. One might expect to find superexchange via π orbitals in the vanadium complexes, and superexchange predominantly through σ orbitals in the copper compounds. Finally, these experiments would be interesting because, as has been pointed out previously, investigations on the nature of the coupling mechanism in antiferromagnets have been rare.[4]

In order to find out if differences in the coupling mechanism exist, it is proposed that a low-temperature ESR study of the VO^{2+} and Cu^{2+} complexes be undertaken, with ^{17}O labelling in the bridging positions. It is known that phenols with ^{17}O labelling can be synthesized.[5] Measurements could be done on powders, but single

crystals would be preferable. Doping in a diamagnetic lattice is usually desirable, but in cases like ours, it is not obligatory.[6] In this system, with its relatively bulky organic ligands, dilution should already be extensive. Many cases of coupled dimeric metal compounds with less bulky ligands have been looked at successfully without the necessity of further dilution.[6]

If spin pairing is due to superexchange, superhyperfine peaks from the labelled oxygens should be observable. Superexchange in contrast to direct coupling places unpaired spin density on the bridging oxygens in the paramagnetic state. Any appearance of super-hyperfine structure in the vanadyl series would be interesting because of its exceptional rarity in VO^{2+} complexes. If superhyperfine is noted in both complexes, a relationship of the form $A = \rho Q$, $Q \simeq 40$ G [5] can be used to compare unpaired spin density in the two series.

Attempts should also be made to observe a contact shift of the ligand aromatic protons in the NMR. This can be tried both on the solid with a broad-line spectrometer or in solution with a high resolution instrument. Previous workers have been able to extract meaningful contact shifts from solid samples.[7] The meta hydrogens here should move in one direction, while the other aromatic protons should move in the opposite direction. Before looking for solution contact shifts, the Evans method for measuring magnetic susceptibility of solutions[8] should be employed to verify the dimeric nature of these compounds in solution. If the results are positive, we can

proceed to look for a paramagnetic shift. Because of the singlet-triplet equilibrium present, we may very well observe a shift despite the relatively long T_1 of Cu^{2+} and VO^{2+}.[9] It will be interesting in itself to see if such an equilibrium can compensate for a long T_1 and narrow the resulting resonance peaks. Should a shift be observed for cupric and vanadyl here, it will be the first time, or very nearly the first time, that such a shift would be observed for these ions.

If superexchange is operative, unpaired spin density will be present in the 1s H orbitals of the rings, and a large paramagnetic shift will be observed.[7] No unpaired spin density can be transferred to the rings if a direct mechanism is present.

The importance of the pseudocontact term in the total shift can be ascertained.[10] Contact shifts can be obtained from the total paramagnetic shift by putting an upper bound on the pseudocontact contribution.[11] If a shift is observed, the relationship $A = \rho Q$ ($Q = -22.5$ G) may again be used to obtain data about unpaired spin densities ρ. A, the hyperfine coupling constant, is determined experimentally from $\Delta H = -AH \dfrac{\gamma e}{\gamma N} \dfrac{g \beta s (s + 1)}{6 \, S' kT}$.[12] It must be emphasized that whether a paramagnetic shift will be observed or not in the NMR is a priori unpredictable, and each case must be investigated individually (13).

Perhaps the most definitive experiment that can and should be done, would be crystal structure determinations of both complexes. If the Cu–Cu distance is within 0.1–0.2 Å of the metallic copper distance, 2.56Å,[14] it is safe to assume a direct interaction. Similarly, a distance within 0.1–0.2Å of the metallic vanadium

distance 2.64Å $^{(14)}$ will almost always indicate that direct metal-metal interactions are present. In both cases, if superexchange is the mechanism, metal-metal distances should be over 3Å, in all probability well over.

References

1. A. Ginsburg, et al., J. Inorg. Nucl. Chem., 29, 353 (1967), and references therein.

2. G. Barclay, B. Hoskins, J. Chem. Soc., 1979 (1965).

3. M. Kato, Chem. Revs., 64, 99 (1964).

4. P. Ball, Coordin. Chem. Revs., 4, 361 (1969).

5. V. Dimworth, Angw. Chemie, 6, 34 (1967).

6. G. Kokoszka, G. Gordon, Transition Metal Chemistry, 5, 181 (1969).

7. M. Inoue, M. Kubo, Inorg. Chem., 9, 2310 (1970).

8. D. Evans, J. Chem. Soc., 2003 (1959).

9. D. Eaton, W. Phillips, Adv. Mag. Res., 1, 122 (1965).

10. G. LaMer, Inorg. Chem., 6, 1921 (1967).

11. F. Rohrschied, Inorg. Chem., 6, 1607 (1967).

12. D. Eaton, W. Phillips, op. cit., p. 115.

13. Ibid., p. 106.

14. Interatomic Distances, The Chemical Society, London, 1958.

Proposition IV

It is proposed to measure the temperature dependence of the dipole moments of substituted biferrocenes in order to determine their barriers to rotation.

Biferrocene has been known for about a decade. Except for random studies on its ring substitution reactions, relatively few investigations have been undertaken on this compound. This is surprising once one recognizes that biferrocene exhibits hindered internal rotation about the bond connecting the joined $C_5H_5^-$ rings.[1]

Hindered internal rotation has been, and is, a topic of great theoretical and experimental interest to chemists. Much effort has been expended in explaining the nature of the interactions causing this phenomenon. Various different experimental methods have been developed to measure the extent of these interactions. Among these methods have been microwave spectroscopy,[2] nuclear magnetic resonance,[3] and the monitoring of changes in optical activity.[3]

We propose studying the barrier to rotation in biferrocene. Actually, we propose determining the magnitude of the two barriers to rotation in biferrocene. One barrier arises from the pseudo double bond between joined $C_5H_5^-$ rings. The second barrier results from steric repulsions between non-bonding cyclopentadienyl rings when they are brought into a cisoid configuration. In addition to their intrinsic

interest, information on these barriers could be correlated with measured barriers in similar organic systems, e.g., biphenyls.[3]

In studying the barriers to rotation here, the more common techniques mentioned above can not be employed. Microwave spectroscopy can not be used on large polyatomic systems. Monitoring the rate of racemization or using NMR requires making ortho substituted biferrocenes which, by themselves, destroy the planarity of the bonding $C_5H_5^-$ rings. The substituents also would add their own repulsive interaction to the total rotational barrier. We propose, therefore, studying the rotational barrier by monitoring changes in the compound's dipole moment.

Following changes in the dipole moment of a molecule to obtain its rotational barrier is not a new technique. It has been used on halogenated alkanes and a few other compounds.[4] In order to have a moment which is easily and accurately measureable, we propose using the readily obtainable 3,3'-diacetyl substituted biferrocene.[5] When the compound is in its normal symmetric trans form, the dipole moment should be near zero. Substitution at the 3,3' positions would not itself be expected to hinder rotation. The bonded rings are held rigidly with respect to each other, and these substituents can never become ortho to one another.[6] Once rotation or even wagging becomes appreciable, the moment should show an increase. If, like biferrocene, this substituted biferrocene has a high enough vapor pressure, it can be investigated in the vapor phase.[4] If this is impractical, measurements in some non-polar solvent will also suffice.[4]

With increased rotation, the moment will rise dramatically. The final constant value obtained in the free rotation limit should be approximately $\sqrt{2}$ m sin 36°, [7] where m is the moment of acetylferrocene. For 3,3′-diacetyl substituted biferrocene, the limiting moment should be ~ 3.5 D.

To obtain consistent and realistic values for both barriers to rotation, we propose treating the data in three different ways. First, we can make the crudest approximation and assume that the pseudo double bond barrier, V_2, is much smaller than V_1, which arises from steric repulsion when the non-bonded $C_5H_5^-$ rings are cis. A reasonable potential function would then be

$$V(\varphi) = \frac{V_1}{2}(1 + \cos\varphi), \text{ where } \varphi$$

is the azimuthal angle. Now it has been shown that for this case[4]

$$\mu^2(\varphi) = 2m^2 - 2m^2 \cos\theta_1 \cos\theta_2$$
$$+ 2m^2 \sin\theta_1 \sin\theta_2 \, \rho$$

$$\text{where } \rho = \frac{\int_0^\pi \cos\varphi \, \exp[-V(\varphi)/RT] d\varphi}{\int_0^\pi \exp[-V(\varphi)/RT] d\varphi}$$

and θ_1 and θ_2 are the angles between dipole axes and the axis of rotation. In our case, $\theta_1 = \theta_2 = 36°$. ρ has been evaluated and shown to be

$$\rho = \frac{i \, J_1[i(V_1)/2RT]}{J_0[i(V_1)/2RT]} \text{ , where}$$

J_1 and J_0 are Bessel functions.[4] Here, m is just the dipole moment of the substituted ferrocene.

The second method for data treatment that should be used is a refinement of the first. Assume a potential function of the form $V(\varphi) = \dfrac{V_1}{2}(1 + \cos\varphi + k + k\cos 2\varphi)$. V_2 here is a significant fraction, k, of V_1, i.e., $V_2 = kV_1$. In this case, k should be in the 0 to 0.33 range. Using numerical integration, ρ can be evaluated. A best fit for V_1 and k should be obtainable.

A third and final analysis of the data may be undertaken by using[8]

$$\mu^2 = \frac{N_t m_t^2 + N_c m_c^2}{N_t + N_c} = \frac{\dfrac{N_c}{N_t} m_c^2}{1 + \dfrac{N_c}{N_t}} \quad ,$$

where m_c and m_t ($\equiv 0$) are the moments of the cisoid and transoid forms of 3,3'-diacetylbiferrocene, and N_c and N_t are the number of molecules in each configuration. In our case, m_c should be approximately 3.55 D. Effectively, we are assuming only two possible configurations. N_c and N_t can be gotten from the familiar distribution equation

$$\frac{N_c}{N_t} = \frac{f_c}{f_t} e^{-\Delta E/kT} \quad ,$$

where f_c and f_t are the rotational and vibrational partition functions of the two configurations. Only the rotational partion function should be

appreciably different in the cis and trans forms.[7] This is due to differences in moments of inertia. These moments are easily calculable. From all this, $\Delta E(= V_1 - V_2 = V_1 - kV_1)$ is obtainable.

These three treatments should give a relatively consistent value for the magnitude of the barriers in biferrocene. Various other substituted biferrocenes theoretically could also be easily made via Ullman condensations[9] of the properly substituted ferrocenes. Substituent effects on the pseudo double bond may be isolated by varying the groups in the 3, 3′ positions.

References

1. B. Rockett, G. Marr, Tetrahedron, 25, 3477 (1969).

2. C. Townes, A. Schlawlow,"Microwave Spectroscopy," McGraw-Hill, New York, 1955, p. 322.

3. K. Mislow, "Introduction to Stereochemistry," Benjamin, New York, 1965.

4. C. Smyth,"Dielectric Behaviour and Structure," McGraw-Hill, New York, 1955.

5. S. Goldberg, J. Crowell, J. Org. Chem., 29, 996 (1964).

6. A. McDonald, J. Trotter, Acta Cryst., 17, 872 (1964).

7. V. Minkin, O. Osipov. Y. Zhdanov, "Dipole Moments in Organic Chemistry," Plenum Press, New York, 1970.

8. S. Mizushima, "Structure of Molecules and Internal Rotation," Academic Press, New York, 1954.

9. M. Rausch, J. Org. Chem., 26, 1802 (1961).

Proposition V

Spectroscopic investigations of oxidized bridged and
mononuclear dinitrogen metal compounds are proposed.

The study of the ruthenium pyrazine dimer in this thesis was
encumbered with one very major difficulty. The lack of other
binuclear systems which possess similar near IR transitions presented
a handicap in understanding the electronic structure of the pyrazine
complex. An understanding of the bonding in the ruthenium nitrogen
dimer was also hindered by the lack of comparable nitrogen bridged
species.

The only complex which has been found to possess a near IR
band similar to μ-pyrazinedecaamminediruthenium is a biferrocene
picrate compound.[1] A recent report maintaining that a ferrous-
ferric dicyano bridged system has been found which exhibits a tran-
sition in the near IR seems restricted to aqueous solutions.[2]
Within the realm of μ-dinitrogen bimetallic systems, only μ-
dinitrogendecaamminerutheniumosmium^{4+} and μ-dinitrogendeca-
amminediruthenium(II) are well characterized.[3]

Recently, however, a report of the successful oxidation of
$(NH_3)_5RuN_2Ru(NH_3)_5^{4+}$ has appeared.[4] This compound, its corres-
ponding monomer, and the $Os(NH_3)_5N_2^{2+}$ species, were all oxidized.
The osmium complex had a half-life of 15 secs before N_2 was given
off and the aquopentaammineosmium(III) complex formed. Similarly,

the 5+ RuN_2Ru species generated has a $t_{\frac{1}{2}}$ of 3 secs before decomposing to the $Ru(II)$-N_2 monomer, and a monoacidopentaammineruthenium(III) species. It was found that the Ru dimer can withstand the loss of an electron much more readily than its monomer. A $Ru(III)$-N_2 complex was undetectable. It was posited that the dimeric oxidation intermediate was more stable than its monomeric analog because of π back bonding from the remaining Ru(II) center.[4]

We propose investigating the intermediates generated by oxidation of the $(NH_3)_5RuN_2Ru(NH_3)_5^{4+}$, $Os(NH_3)_5N_2^{2+}$, and $(NH_3)_5RuN_2Os(NH_3)_5^{4+}$ species. The infrared, electronic and ESR spectra of these complexes will be obtained using flow system techniques. We suggest attempting to carry out the oxidation of the parent compounds by chemical means first. Preliminary investigations will be needed to determine if the rate of oxidation is compatible with the rate of decomposition of the oxidized intermediate. If, because of the kinetic factor, chemical methods are not feasible, the less desirable but still practical electrolytic methods of oxidation may be used. The actual design of the flow system and electrolysis cell, e.g., diameter of conduit, rate of flow, area of electrode, voltage, etc. are to be determined as needed. It should be remembered that it probably is not imperative to oxidize all the parent molecules in order to get usable spectral information. In carrying out these measurements, cooling the solutions to slow the rates of decomposition may be helpful. At the very least, the osmium monomer oxidation transient with a $t_{\frac{1}{2}} \sim 15$ secs, and, presumably, also the OsN_2Ru^{4+} oxidation

intermediate (which should have an even longer $t_{\frac{1}{2}}$ because of π back bonding from the Ru(II)) will be obtainable in sufficient concentrations to allow spectral work.

Investigating the electronic spectra of these compounds will be instructive. The oxidized ruthenium dimer may exhibit a near IR transition similar to that found in the bridged pyrazine compound. Information concerning the orbital origin of this transition may be obtainable. This could support a d–d intraconfigurational assignment for the bridged pyrazine compound's low energy band. The osmium-ruthenium dimer, when viewed in conjunction with its monomers, may also reveal interesting mixed-valent transitions. Finally, the mixed metal transient should possess ground and excited states which are asymmetrical, thereby slowing the rate of electron "transfer".

Infrared spectra of the N_2 stretch region of the oxidized dimers could show interesting shifts. Evidence for a more azo-like structure in the intermediates may be observed. In the ESR, the RuN_2Ru oxidized dimer may show a room temperature signal, a phenomenon at present observed only in its pyrazine analog.

References

1. D. Cowan, F. Kaufman, J. Amer. Chem. Soc., 92, 219 (1970).

2. G. Emschwiller, C. Jorgensen, Chem. Phys. Letts., 5, 561 (1970).

3. J. Chatt, J. Dilworth, H. Gunz, G. Leigh, J. Sanders,
   J. Chem. Soc. D, 90 (1970).

4. C. Elson, J. Gulens, I. Itzkovich, J. Page, J. Chem. Soc. D,
   875 (1970).